University of São Paulo – USP

São Carlos Institute of Chemistry – IQSC

Amaury Franklin Benvindo Barbosa

Fundamental study of the ethanol electro-oxidation reaction on platinum single-crystal electrodes

Estudo fundamental da reação de eletro-oxidação de etanol sobre eletrodos monocristalinos de platina

São Carlos

2022

Amaury Franklin Benvindo Barbosa

Fundamental study of the ethanol electro-oxidation reaction on platinum single-crystal electrodes

Estudo fundamental da reação de eletro-oxidação de etanol sobre eletrodos monocristalinos de platina

Thesis presented to the Graduate Program in Chemistry at the São Carlos Institute of Chemistry (University of São Paulo) to obtain the degree of Doctor in Science

Concentration area: Physical Chemistry

Supervisor: Prof. Dr. Germano Tremiliosi Filho

São Carlos

2022

Assinatura:
Data:

Ficha Catalográfica elaborada pela Seção de Referência e Atendimento ao Usuário do SBI/IQSC

Barbosa, Amaury Franklin Benvindo
Estudo fundamental da reação de eletro-oxidação de etanol sobre eletrodos monocristalinos de platina / Amaury Franklin Benvindo Barbosa. — São Carlos, 2022.
99 f.

Tese (Doutorado em Físico-Química) — Instituto de Química de São Carlos / Universidade de São Paulo, 2022.

Orientador: Prof. Dr. Germano Tremiliosi Filho

1. Etanol. 2. Platina. 3. Eletroquimica. 4. Eletrocatálise. 5. Catalisadores. I. Título.

Solange Puccinelli - CRB: 1500/8

This thesis is dedicated to my parents: Ana and Gilvan, and my son, Yan.

Acknowledgments

I thank my parents: Ana and Gilvan, my son Yan, my sisters Amanda and Karla for their support throughout my life.

I would like to express my gratitude to my supervisor, Prof. Germano Tremiliosi Filho, for his guidance and support throughout this study, for the opportunity to work at Electrochemistry Group of the São Carlos Institute of Chemistry (IQSC), and especially for his confidence in me.

I would also like to thank Dr. Vinicius Del Colle, for his contribution to the discussion and interpretation of some results.

I also thank for the Coordination for the Improvement of Higher Education Personnel (CAPES) and the São Paulo State Research Foundation (FAPESP – grant number: 2016/13100-1) for the PhD scholarships awarded.

I thank the members of the examining committee for their interest and availability to evaluate this work.

I am very grateful to the professionals of the postgraduate service for their support and patience in answering questions related to academic matters.

I am very thankful for the laboratory professionals of the Electrochemistry Group – IQSC, especially Mauro Fernandes, Jonas Garcia, Valdecir Paganin and Gabriel da Silva, for their important support during the development of this research.

I am very grateful to my co-workers and friends of IQSC: Nelson, Rafael, Rodrigo, Ana, Luiza, Ricardo, Bott, Wanderson, Adriana, Elenice, Pedro, Marcelo, Carlos André, Diego, Carlos, Martin, Gabriel, Nicolas, Amanda, Henrique, James, Vitor, Roberto, Rodrigo Iost, Francisco, Germano, Everton, João, and Lucyano.

Resumo

As células a combustível de álcool direto apresentam algumas limitações devido à dificuldade de oxidar completamente o etanol e formar dióxido de carbono. O controle da seletividade desta reação é de crucial importância para entender como o eletrocatalisador afeta as várias rotas, em um nível molecular. Esta tese apresenta importantes informações de como o mecanismo da reação de eletro-oxidação de etanol é influenciado pelo arranjo atômico superficial de uma série de eletrodos monocristalinos de platina e por ad-átomos de Sn depositados sobre tais superfícies. Inicialmente, a eletro-oxidação de etanol foi investigada em meio ácido sobre uma série de eletrodos monocristalinos com e sem defeitos. Os resultados eletroquímicos mostraram que a eletro-oxidação de etanol é fortemente afetada a medida que os sítios de defeitos-{110} aumentam. A medida que a densidade de defeitos aumenta, a reação de eletro-oxidação de etanol é melhor catalisada. Os resultados de infravermelho *in situ* demostraram que os principais produtos da reação de oxidação de etanol para todas as superfícies investigadas são: CO_2, acetaldeído e ácido acético. Adicionalmente, CO_{linear} é observado. Em seguida, a eletro-oxidação de etanol foi investigada em meio ácido sobre uma série de eletrodos de Pt(111) desordenados, modificados com Sn. Os resultados voltamétricos da oxidação de etanol demostraram que a decoração parcial dos sítios de defeitos-{110} por ad-átomos de Sn levam a um aumento considerável da atividade catalítica desta reação, quando comparados com superfícies de Pt(111) bem ordernadas e Pt(111) desordenadas sem Sn. Os resultados de infravermelho in situ demostraram que os principais produtos da oxidação são CO_2, acetaldeído e ácido acético para as superfícies estudadas, e o principal efeito do Sn é refletido no aumento da produção de ácido acético. Por último, a oxidação de acetaldeído, um importante intermediário da reação de oxidação de etanol, foi investigada sobre superfícies de Pt(111) bem ordenadas e Pt(111) desordenadas, ambas modificadas por ad-átomos de Sn. O eletrodo de Pt(111) é mais ativo para a oxidação de acetaldeído, em comparação com a superfície escalonada de Pt(554) ou com as superfícies de Pt(111) desordenadas. No entanto, quando as superficies de Pt(111) e Pt(111) desordenadas foram modificadas por Sn os resultados melhoraram significativamente. Para ambas as superfícies, há um extraordinário deslocamento do potencial de início da oxidação para valores mais negativos, indicando a oxidação de espécies adsorvidas tais como CO e CHx formadas em baixos potenciais. Esses resultados fornecem informações fundamentais da oxidação de etanol, os quais podem contribuir para um entendimento em nível atômico de catalisadores reais.

Palavras-chave: eletro-oxidação de etanol, superfícies monocristalinas de platina, defeitos cristalinos randômicos, eletrólito ácido.

Abstract

Direct ethanol fuel cells present some limitations due to the difficulty of achieving the complete oxidation of ethanol to carbon dioxide. To control the selectivity of this reaction, it is of crucial importance to understand how the electrocatalyst affects the various pathways on a molecular level. This thesis presents important insights of how the mechanism of the ethanol electro-oxidation reaction is influenced by the atomic superficial arrangement of a series of platinum single crystal electrodes and by the Sn ad-atoms deposited over such surface. Initially, the ethanol electro-oxidation was investigated in acid media on a series of well-ordered and disordered Pt(111) single crystal electrodes. Electrochemical results showed that the ethanol electro-oxidation is strongly affected by the {110}-defect sites electrogenerated on Pt(111) electrodes. It was found that as the density of {110}-defect sites increases, the ethanol electro-oxidation reaction is catalyzed better. *In situ* FTIR results demonstrated that the main products of the ethanol oxidation are CO_2, acetaldehyde and acetic acid for all surfaces investigated. Additionally, adsorbed CO_{linear} is observed. Next, the ethanol electro-oxidation was investigated in acid media on a series of Sn-modified and disordered Pt(111) single crystal electrodes. Voltammetric results of the ethanol electro-oxidation demonstrate that the partial decoration of {110}-defect sites by Sn ad-atoms leads to a considerable increase in the catalytic activity towards ethanol electrooxidation reaction, when compared to the well-ordered Pt(111) surface and disordered Pt(111) surface without Sn. *In situ* FTIR results demonstrate that the main products of the ethanol oxidation are CO_2, acetaldehyde and acetic acid for all surfaces investigated and the main effect of Sn is reflected in the increased production of acetic acid. Finally, acetaldehyde oxidation, an important intermediate of the ethanol oxidation, it was investigated on well-ordered Pt(111) and disordered Pt(111) surfaces, both modified by deposited Sn ad-atoms. Well-ordered Pt(111) is more active than stepped Pt(554) or disordered Pt(111) surfaces for acetaldehyde oxidation. However, the results were significantly improved and pointed out an outstanding performance when Pt(111) and disordered Pt(111) surfaces were modified by Sn. For both modified surfaces, there is an extraordinary displacement of the onset potential for more negative potentials, indicating oxidation of adsorbed species such as CO and CHx, already formed at low potentials. These results provide fundamental information on the ethanol oxidation reaction, which contributes to the atomic-level understanding of real catalysts.

Key-words: ethanol electro-oxidation, platinum single-crystal surfaces, random crystalline defects, acid electrolyte.

Contents

Chapter 1

Introduction

1.1 Motivation

Fuel cells are widely known as devices capable of converting chemical energy from fuel into electricity, in clean and efficient way.[1] Therefore, they have been considered as one of the promising solutions to global problems, such as: (i) damage to the environment, (ii) increased demand for energy, and (iii) increased consumption of non-renewable fossil fuels.[2]

Fuel cells using an acid polymer electrolyte membrane (PEMFC) have been explored extensively, with hydrogen being the fuel that has presented the best electrical efficiency and performance.[2,3] However, hydrogen fuel has some disadvantages such as difficulties in obtaining it free of any impurity, storage, and transport.[4,5] As an alternative to hydrogen, liquid alcohols, mainly methanol and ethanol, appear as potential alternatives to feed a fuel cell, for two main reasons: they are liquids (easy storage) and their theoretical mass energy density is rather high.[1,5] Compared to methanol, ethanol has some advantages due to its lower toxicity, possibility to be produced in large quantities from biomass (green fuel) and higher theoretical mass energy density (8.01 $kWh.Kg^{-1}$ for ethanol and 6.1 $kWh.Kg^{-1}$ for methanol), close to the gasoline.[1,3]

Figure 1.1 illustrates the basic components and reactions that occur in a direct ethanol fuel cell (DEFC). This electrochemical system consists in two electrodes (anode and cathode), which act as electronic conductor, separated by an electrolyte, a proton exchange membrane (PEM), which é an ionic conductor.[3]

At the anodic compartment, the ethanol oxidation takes place, according to the following reaction:

$$\text{Anode: } C_2H_5OH + 3H_2O \rightarrow 2CO_2 + 12H^+ + 12e^- \qquad (1.1)$$

At the cathode occurs the reduction of oxygen from the air, according to reaction:

$$\text{Cathode: } 3O_2 + 12H^+ + 12e^- \rightarrow 6H_2O \qquad (1.2)$$

In theory, at the anode of a DEFC, the complete oxidation of ethanol (in acid medium) would lead to the formation of carbon dioxide and water and would occur the release of a total of 12 electrons per molecule of ethanol (equation 1.3). Nevertheless, DEFCs presents some limitations due to the difficulty of achieving the complete oxidation of ethanol to carbon dioxide.

Overall reaction: $C_2H_5OH + 3O_2 \rightarrow 2CO_2 + 3H_2O$ (1.3)

Figure 1.1. Schematic representation of a DEFC.

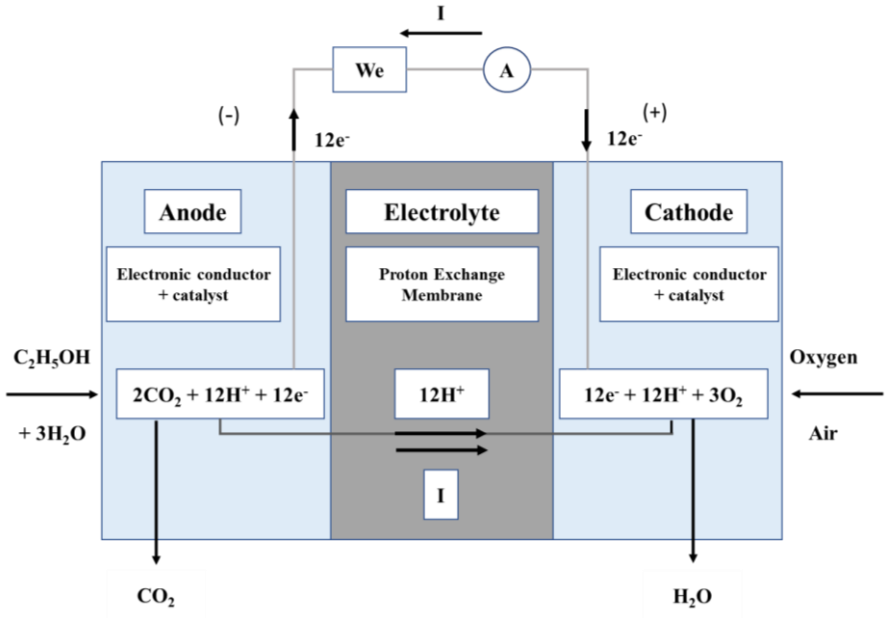

Source: Adapted from LAMY *et al*., 2002.[3]

According to experimental and theoretical studies, the mechanism of the ethanol oxidation reaction (EOR) is very complex, occurring through many successive and parallel paths.[6,7] In addition to CO_2, many adsorbed intermediates (as CO and CH_x) and partial oxidation products (as acetaldehyde and acetic acid), which preserve the integrity of the C-C bond, are produced during this reaction.[6,8] Figure 1.2 shows a well-accepted simplified mechanism for the EOR on Pt and Pt-based electrocatalysts in acid medium.[8,9]

Figure 1.2. Simplified mechanism for the EOR on Pt and Pt-based electrocatalysts in acid medium.

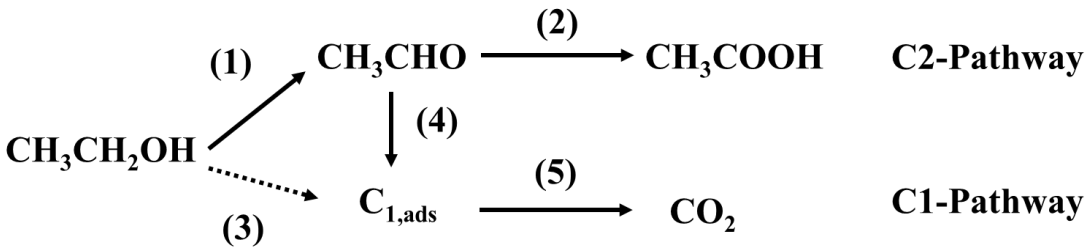

Source: Adapted from LAI and KOPER, 2010.[9]

In the C2-pathway, ethanol is first oxidized to acetaldehyde (reaction 1) and subsequently to acetic acid (reaction 2), liberating two electrons in both steps. Alternatively, in

the C1-pathway, the C-C bond can be cleaved in ethanol or acetaldehyde (reactions 3 and 4), forming CO_{ad} and additional fragments which can be oxidized to CO_2 (reaction 5), liberating 12 electrons per ethanol molecule.[8,9] Although carbon dioxide is the preferred reaction product, it was found that, under fuel cell conditions, the main products are acetaldehyde and acetic acid.[4] The formation of partial oxidation products results in loss of efficiency of the DEFCs.[3] Therefore, the main catalytic challenge in the EOR is to improve the selectivity of the catalyst toward carbon dioxide.[9]

To control the selectivity of the EOR, it is of crucial importance to understand how the electrocatalyst affects the various pathways on a molecular level.[9,10] Electrocatalysts used in practical applications are complex systems, constituted by noble metal nanoparticles anchored to an inert support to minimize the amount of electrocatalyst needed, where its resultant performance (activity, selectivity, and stability) depends on many factors.[10,11] Figure 1.3 shows an illustration of a real-world high surface-area nanoparticulate electrocatalyst. In this figure are highlighted the main factors and parameters that control the electrocatalyst performance such as: different facets, surface defects, interactions with the support material, surface and bulk composition, size effects, specific properties of the electrochemical interface, electrolyte composition, and other parameters.[11] Therefore, in fundamental studies the complex catalytic system is often replaced by a simplified model.[10,11]

Figure 1.3. Real-world high surface-area nanoparticulate electrocatalyst and main factors and parameters that control its electrocatalytic performance.

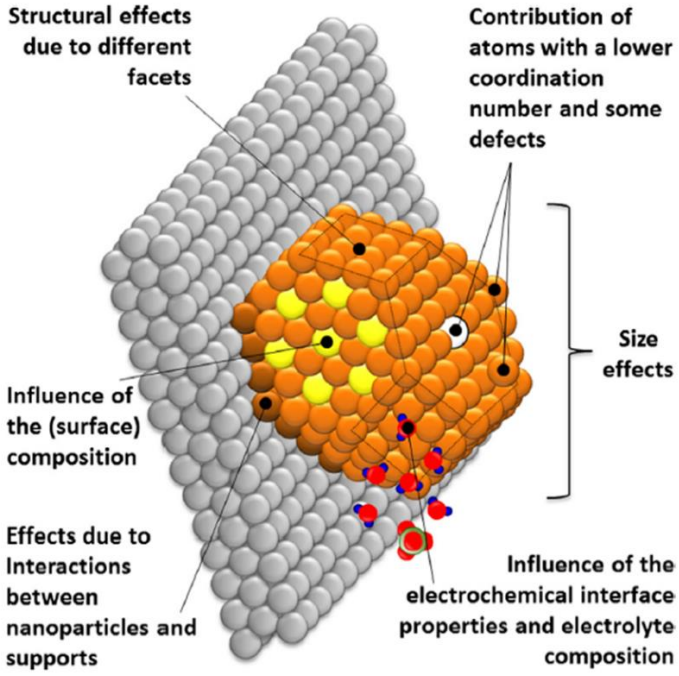

Source: From BANDARENKA and KOPER, 2013.[11]

Single crystal metallic surfaces are a less complex catalytic system, since such surfaces have a well-defined atomic arrangement. For that reason, they serve as models to establish the correlation between their superficial atomic structures and electrocatalytic activity.[10,11]

Figure 1.4 illustrates the various surface structures that can be obtained by cutting and polishing a face-centered cubic (FCC) crystal, such as platinum, along different directions, known as a unit stereographic triangle.[10]

At the vertex of the triangle are the three low-indexes surfaces or basal surfaces: (111), (100), and (110). Among them, the (111) and (100) faces are flat at the atomic scale with high packing density of the surface atoms, whereas the (110) plane is rough with step atoms. Other faces lying in the sidelines and locating of the triangle are high-indexes surfaces. The three sidelines inside the stereographic triangle represent [01$\bar{1}$], [1$\bar{1}$0], and [001] crystallographic zones, in which the planes exhibit terrace-step structure and are thus also called stepped surfaces. They present a common characteristic, their surfaces are formed by different combinations of terraces and steps with (100), (111) or (110) orientations, depending on their direction and angle in relation to the three basal surfaces. Within the stereographic triangle, steps will have two different orientations, leading to kinked surfaces, an example of which is also given in Figure 1.4.

Figure 1.4. Unit stereographic triangle of fcc single-crystal surfaces and their corresponding surface atomic arrangements.

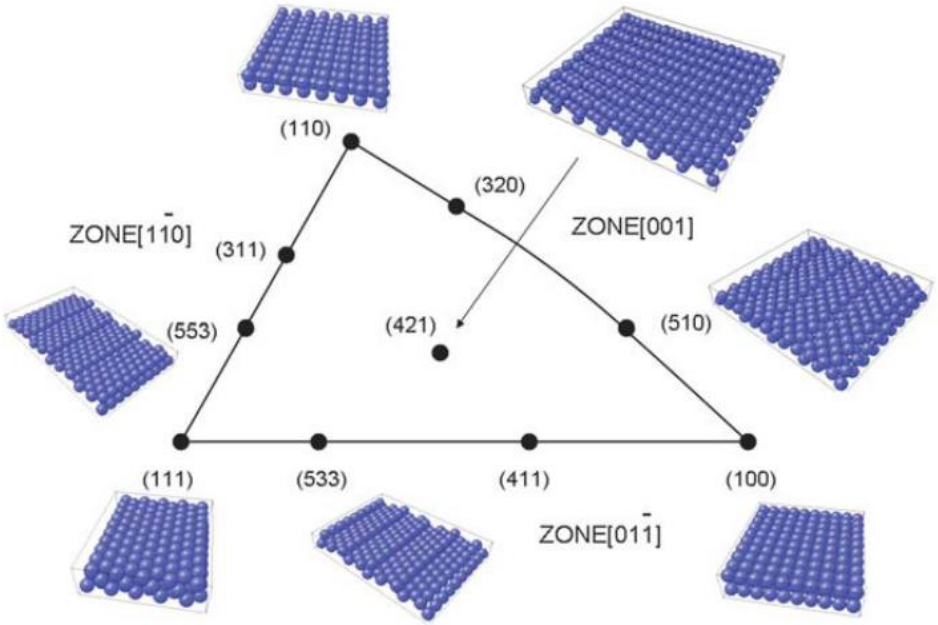

Source: From KOPER, 2011.[10]

Nowadays, it is well-known that the EOR is a highly structure sensitive reaction.[6–10,12,13] Despite all the efforts, the relationship between catalyst structure and catalytic activity and/or selectivity in the EOR is still not completely resolved, and this understanding is a pre-requisite to the rational design of new electrocatalysts for practical applications.

1.2 Scope of this thesis

The research presented in this thesis is focused on understanding the mechanism of the ethanol electro-oxidation on platinum electrodes.

In Chapter 2, the ethanol electro-oxidation in acid media on a series of well-ordered and disordered Pt(111) single crystal electrodes is investigated. Voltammetric and chronoamperometric data show how the density of random defects influences the ethanol electro-oxidation mechanism. *In situ* FTIR data show the product distribution is strongly dependent on the density of random defects present on the electrode surface.

In Chapter 3, the ethanol electro-oxidation in acid media on a series of Sn-modified and disordered Pt(111) single crystal electrodes is investigated. Voltammetric data show the combined effect of the random defects on Pt(111) and Sn deposition at submonolayer levels over the mechanism of the ethanol electro-oxidation. *In situ* FTIR data show the product distribution is strongly dependent on the Sn coverage degree on the electrodes.

In Chapter 4, the acetaldehyde electro-oxidation in acid media using different electrodes was investigated. First the acetaldehyde electro-oxidation on well-ordered Pt(111), stepped Pt(554) and disordered Pt(111) is investigated. Voltammetric and chronoamperometric data show how the mechanism of the acetaldehyde electro-oxidation is severely affected by the surface structure of the electrode. Next, acetaldehyde was also investigated on well-ordered Pt(111) and disordered Pt(111) surfaces, both modified by deposited Sn submonolayers. Electrochemical results show the combined effect of the random defects on Pt(111) and Sn deposition at submonolayer levels in the mechanism of the acetaldehyde electro-oxidation. The study with acetaldehyde complements the understanding of the proposal of this work since it is one of the important intermediates formed and represents an essential species to be considered in the discussion of the alcohol oxidation mechanism.

In the last chapter, the main conclusions and perspectives futures of this research are addressed.

Chapter 2

Effect of the Random Defects Generated in the Surface of Pt(111) on the Electro-oxidation of Ethanol: Electrochemical and FTIR Studies

This chapter has been adapted with permission from the John Wiley and Sons: Amaury F. B. Barbosa, Vinicius Del Colle, Ana M. Gómez-Marín, Camilo A. Angelucci, Germano Tremiliosi-Filho, “Effect of the Random Defects Generated in the Surface of Pt(111) on the Electro-oxidation of Ethanol: An Electrochemical Study,” ChemPhysChem, v. 20, p. 3045-3055, 2019.

2.1 Introduction

Ethanol electro-oxidation reaction (EOR) has been extensively investigated due to its possibility to be used in direct alcohol fuel cells (DAFCs) for electric energy generation.[1,14–16] Ethanol presents a relatively low toxicity; it can be produced in large scale from the biomass fermentation [1], because of that it is considered as a "green compound". Apart of this, its complete oxidation to CO_2 produces 12 electrons, as an efficient way to produce electrons. However, the ethanol electro-oxidation reaction is complex since it involves different steps and difficulties such as, alcohol adsorption, difficulty in breaking the interatomic C-C bond, adsorption of broken alcohol fragments that can poison the surface of the electrode, the slow kinetics of the electronic charge transfer, the difficulty of desorption of some reaction products. All of these steps represent complications that must be solved prior to the practical use of the direct alcohol fuel cell. Additionally, these problems generate large anodic overpotentials that greatly reduce the possibility of use of the ethanol/oxygen fuel cell.[3,17]

Pure platinum (Pt), Pt-alloys and Pt modified by sub-monolayers containing other metals from Pt group, such as Os and Ru, or Sn, are commonly used as electrocatalysts for the EOR.[1,3,4,18–20] In acid solutions, the proposed simplified oxidation mechanism for platinum electrodes has a dual-path, as it can be seen in Figure 2.1.

Figure 2.1. Simplified mechanism of the ethanol oxidation reaction on platinum electrodes in acid media.

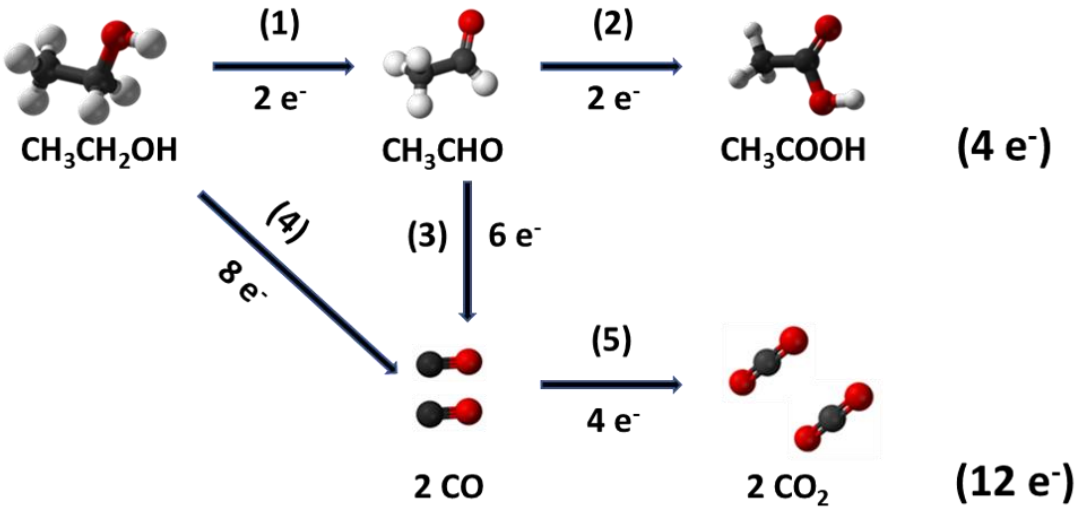

Pathways 1 and 2 show that ethanol can be oxidized to acetaldehyde and subsequently to acetic acid, releasing 4 electrons, which reduces the efficiency of the system since acetic acid

is a final product, thus, interrupting any posterior reaction to CO_2.[6,21] The intended path for the ethanol oxidation leads to the formation of CO_2, which requires the cleavage of the C–C bond. This cleavage can occur either in the ethanol molecule (pathway 4) or in the reaction intermediate acetaldehyde molecule (pathway 3) and leads to the formation of adsorbed species such as carbon monoxide and other fragments of (CH_x) type.[6] Due to the strong adsorption properties of CO on noble metals, it has been considered as a catalytic poison.[6,8,12] However, CO might be also considered as a true active intermediate necessary to complete the oxidation of the ethanol molecule to CO_2 [22] (pathway 5), releasing 12 electrons.

Nowadays, it is well known that the ethanol oxidation is a highly structure sensitive reaction on platinum electrodes.[6,8–10,12,13,23,24] In this sense, research using model electrodes, such as single crystal surface, has provided first rational insights about the relationship between the selectivity/electrocatalytic activity and the atomic arrangement of the electrode surface for the EOR.[6,8,13,24] Fundamental studies of this nature, might be used to understand the electrocatalytic behaviour of extremely complex real catalyst (ex. nanoparticles supported on carbon).

Among the three basal planes, the Pt(111) electrode shows the lowest electrocatalytic activity in acid medium, both in terms of current density and for the splitting of the C–C bond. On Pt(111), the incomplete oxidation of ethanol to acetic acid is the main reaction step observed in acidic media also acetaldehyde is formed as a secondary product (pathways 1 and 2, Figure 2.1), additionally, CO and CO_2 are formed in very small amount. Whereas on Pt(110) and, mainly, on Pt(100), the breakage of the C–C bond and, consequently, CO formation is favoured in the same medium [8], which contributes to the subsequent step forming the final product, CO_2, (pathway 5, Figure 2.1).

One of the alternatives to improve the electrocatalytic activity of Pt(111) is the use of regularly stepped single crystal surfaces with different terrace lengths, allowing the introduction of defects in a controlled approach. Colmati *et al.* [12] studied the ethanol oxidation on two different series of vicinal Pt(111) electrodes: surfaces with terraces of (111) symmetry separated by monoatomic (110) step, Pt(S)[(n-1)(111) x (110)], and surfaces with terraces of (111) symmetry separated by monoatomic (100) steps, Pt(S)[n(111) x (100)]. These authors observed that the ethanol oxidation current increases with increasing (110) step density, whereas for the electrodes with (100) steps the current diminish as the step density increases. They also showed that stepped surfaces with (100) steps appear to be much less active for C–C bond breaking than surfaces with (110) steps. However, the formation of acetic acid also was enhanced with increasing (110) step density.

In contrast to the large number of information with respect to the effect of well-defined defects of the stepped surfaces on the ethanol oxidation reaction, very little is known regarding the effect of non-defined defects (random defects), normally found in practical catalysts, for this reaction.[25]

Generation of random, non-well-defined defects on Pt surfaces can be achieved upon cycling the electrode to high potentials.[26–30] It has been widely reported that by this electrochemically procedure the generation of defects can be followed by the highly regular evolution of the voltammogram, and, after a given number of cycles, depending of the upper potential limit employed, the current-potential profile reaches a limiting shape indicating that a steady-state distribution and coverage of random defects have been reached.[27,28]

Recently, by employing this methodology in a sulphuric acid solution Fernández *et al.* showed that this is a highly reproducible method to generate random defects on initially well-ordered Pt(100) and Pt(111) surfaces, controlling in a careful and systematic way the resulting amount of surface defect.[31,32] They also showed the influence of random superficial defects on the glycerol electrooxidation reaction on the Pt(100) and Pt(111) surfaces.

In the present work, it was used the method reported by Fernández *et al.* [32] to prepare Pt(111) surfaces with different densities of random defects in an acid solution of non-adsorbing electrolyte ($HClO_4$). Next, a quantitative and systematic study of the effect of random superficial defects in the EOR on the disordered Pt(111) surfaces in perchloric acid solution was carried out by using cyclic voltammetry (CV) and chronoamperometry (CA). Their electrocatalytic behaviour was compared with the 'defect-free' Pt(111) surface. In addition, voltammetric experiments of CO stripping both on 'defect-free' Pt(111) and disordered Pt(111) surfaces were performed in order to get a better understand the effect of random defects on the EOR reaction kinetics. Finally, *in situ* FTIR measurements were performed to obtain information on the intermediates and products generated during the ethanol oxidation on the electrodes used in this study.

2.2 Experimental section

2.2.1 Experimental conditions, electrodes and reactants

All experiments were carried out at room temperature (25 ± 1 ºC) in a conventional three-electrode single cell. The chemicals used for solution preparation were perchloric acid (70%, Sigma-Aldrich), ethanol (99,9%, Panreac) and ultra-pure water from a Millipore System

(18.2 MΩ cm^{-1}). Hydrogen (White Martins, 99.99%) was used for flame-annealing treatment and argon (White Martins, 99.998%) to deoxygenate the solution. A reversible hydrogen electrode (RHE) and a Pt platinized foil (1 cm^2) were employed as a reference electrode and as a counter electrode, respectively. A Pt(111) single crystal was used as a working electrode, having geometric area of 0.0452 cm^2, which was prepared according to Clavilier method.[33]

2.2.2 Generation of random crystalline defects on well-ordered Pt(111) surface

Electrochemical measurements were carried out using a computer-controlled Autolab PGSTAT 302 potentiostat equipped with analog potential scan (Scangen). Prior to each experiment, the electrodes were flame-annealed in a hydrogen-oxygen flame and cooled in a reductive Ar:H_2 atmosphere (~3:1), thereafter they were transferred to the electrochemical cell under protection of a drop of deoxygenated ultra-pure water.[34] Prior to transfer the working electrode in contact with the oxygen-free working electrolyte (0.1 M $HClO_4$ solution), a potential of 0.05 V was applied in order to maintain the ordered state induced by the thermic treatment.

All experiments in this work were carried out maintaining the working electrode in the hanging meniscus configuration to ensure that only the mono-oriented surface was in contact with the working solution.[35] Next, voltammetric sweeps were collected in the potential region between 0.05 V and 0.9 V to verify the quality of the surface as well as the cleanliness of the surface and the solution.

In order to generate random defects on a clean and initially well-ordered Pt(111) surface, successive and controlled voltammetric sweeps were performed in the potential region between 0.05 V and 1.3 V at 50 mV s^{-1} in a solution of 0.1 M $HClO_4$. It has been previously reported that repetitively electrode excursions to potentials higher than 1.15 V progressively destroy the initial surface order.[28]

In this work, three disordered Pt(111) surfaces were prepared with different defect densities, by fixing the number of excursions to a high potential region where surface roughening may takes place. Electrodes are denoted here as “Pt(111)-X”, where “X” indicates the number of cycles performed between 0.05 V and 1.30 V. Next, the final electrode surface state was characterized by performing voltammetric sweeps between 0.05 V and 0.9 V at 50 mV s^{-1} in the same electrochemical cell. It is important highlight that this upper potential limit of 0.9 V does not cause additional structural modifications to the freshly-prepared disordered Pt(111)-X electrodes.

The presence of defects on well-ordered Pt(111) electrodes is commonly identified by the appearance of characteristic current signals in the voltammogram at low potentials. These current signatures take place in similar potential region where voltammetric currents classically ascribed to the adsorption/desorption of hydrogen at defect zones of {110}- and {100}-symmetry on Pt(111) vicinal surfaces also appear, around 0.13 and 0.27 V, respectively.

Therefore, similar to previous works [36], integrated charges from these potential regions were employed, as a first approximation, to estimate the defect density of resulting surfaces generated by applying the described electrochemical procedure. From Figure A1.1 in the Supporting Information it is clear the formation of three crystallographic surface zones. The resulting surface is composed of a mixture of {111}, {110} and {100} symmetry zones with a corresponding specific atomic orientation. Each specific atom in the {110} and {100} zones constitutes the denominated defects. Thus, the charge corresponding to the {110} or {100} symmetry zones divided by the electron elementary charge results in each corresponding defect densities, from where surface fractions of each zone were calculated (see Table 2.1).

2.2.3 Voltammetric and chronoamperometric measurements of ethanol electro-oxidation reaction on the disordered Pt(111) electrodes

After preparing the surface with a desired density of defects, the electrode was transferred to an electrochemical cell containing 0.1 M $HClO_4$ and 0.1 M ethanol solution to study the ethanol oxidation reaction by means of cyclic voltammetry and chronoamperometry. During this transfer process, the electrode surface was protected by a drop of electrolyte. Prior to placing the working electrode in contact with the solution, a potential of 0.05 V was applied in all experiments.

The voltammetric sweeps recorded in the electrolyte solution containing the organic molecule were performed at a potential range of 0.05 - 0.95 V at 50 mV s^{-1}. In the chronoamperometric experiments, similar to what it has been reported in other works [8,12], prior to apply the potential of interest on the electrode surface, the electrode was subjected to a pre-treatment, in which two conditioning potentials were applied. The purpose of this protocol was to remove the adsorbates derived from the ethanol electro-oxidation from the surface, so that the initial current recorded at the desired potential would be as close as possible to the current measured on a clean surface. For this, the electrode was kept for 10 s at 1.0 V, to oxidize adsorbed CO, CH_x and/or COH/CHO fragments formed during the oxidation of ethanol [8,12], and then, it was polarized for 0.01 s at 0.1 V to reduce the oxides and to desorb the acetate

formed at the previous potential.[8] Chronoamperometric data were collected for 600 s with a time resolution of 0.1 s in each potential of interest, performing potential steps of 0.1 V from 0.5 V up to 0.9 V.

2.2.4 Voltammetric measurements of CO stripping on the disordered Pt(111) electrodes

In order to perform voltammetric experiments of CO stripping on disordered Pt(111) surfaces in a solution of 0.1 M $HClO_4$, CO (White Martins, 99.5%) was bubbled into the solution for 5 min while the electrode potential was set at 0.1 V. Next, the CO dissolved in the solution was removed by purging the solution with Ar for 20 min in all experiments. Finally, voltammetric CO stripping was performed, starting at 0.1 V and positive-going sweeping until 1.0 V under 20mV s^{-1}.

2.2.5 In situ FTIR measurements

For the FTIR studies of ethanol oxidation, a reference spectrum was acquired at 0.05 V. Thus, other spectra were recorded after applying successive potential steps of 0.05 V in the positive direction from 0.05 to 0.95 V *vs.* RHE. The potential was controlled by an Autolab potentiostat/galvanostat (model AUT85732). The working electrode was a commercial Pt(111) disk (d = 10 mm, from MaTeck) and a trapped H_2 bubble in contact with a Pt wire was used as the reference (RHE), all potentials in this work were referred to this reference system. The Pt(111)-X electrode was disordered using the same conditions described for the electrode bead-type (Section 2.2.2).

The spectra were computed from an average of 256 interferograms, and the spectral resolution was set at 4 cm^{-1}. Reflectance spectra were calculated as the ratio (R/R_0) of the sample (R) and the reference (R_0) spectra. With respect, the bands registered, positive and negative bands represent loss and gain of species at the sampling potentials, respectively. For all the measurements, a CaF_2 window was used. *In situ* FTIR measurements were carried out by using a VERTEX 70v vacuum Bruker spectrometer provided with an LN-MCT Mid detector.

2.3 Results and discussion

2.3.1 Electrochemical characterization of the disordered Pt(111) electrodes in perchloric acid

Before starting to describe the role of defects generated onto the Pt(111) surface towards ethanol electro-oxidation reaction, it is presented the systematic surface modifications produced by potential cycling only in the supporting electrolyte. In this sense, by the simple use of cyclic voltammetry, substantial information can be get about the reaction site orientations as well as the amount of generated random surface defects.

From a well-ordered surface, it is assumed that the Pt(111) freshly annealed electrode is structured, characterized by large, atomically ordered domains, *i.e.*, a surface with a low amount of surface defects.[37] This assumption has been already revealed, quite precisely, from voltammetric measurements and STM images of platinum electrodes with different surface orientations.[29,30,33,38,39] Furthermore, to evaluate the systematic generation of random defects, a Pt(111) was used as a reference of an ideal surface. The CV profile of a well-ordered Pt(111) surface in acidic media electrolyte is presented in Figure 2.2a (black line) and it is in agreement with results reported previously.[37,40]

The overall CV profile of the Pt(111) electrode shows two distinctive potential regions which are ascribed to characteristics adsorption/desorption processes. At low potentials (0.05 - 0.35 V) the broad current plateau feature has been typically identified as a consequence of the hydrogen adsorption/desorption reaction. The current response around 0.6 - 0.8 V, the so-called "butterfly" feature, is usually associated with the adsorption/desorption of hydroxide (O-containing specie formation, OH_{ads}) from electrochemical dissociation of water.[37] Both processes are very useful for probing the nature of the surface crystallographic orientations and can provide a qualitative, as well as quantitative, characterization of Pt surfaces.[41]

After collecting a characteristic voltammetric profile of a well-ordered Pt(111) electrode within a potential window where the atomic superficial structure remains preserved, the upper potential limit (E_{upper}) was increased to 1.3 V. The selection of the value of E_{upper} for the cyclic voltammogram is crucial to destroy local order and generate defects onto the well-ordered surface.[28,42]

Figure 2.2a depicts the current response (red curves) of a repetitive oxidation-reduction potential cycling up to 1.3 V of Pt(111) surface in 0.1 M $HClO_4$. Taking the voltammetric profile of the freshly annealed Pt(111) electrode as a reference, electrode excursions to the potential region where the oxygen adsorption takes place result in irreversible surface structural

changes, as evidenced by the appearance of new features within the hydrogen adsorption/desorption region (E < 0.34 V), and also changes in the voltammetric profile of the O-containing specie (OH_{ads}) adsorption/desorption process (E > 0.6 V).

Figure 2.2. (a) CV profiles corresponding to (black line) well-ordered Pt(111), (red lines) Pt(111) during a repetitive potential cycling between 0.05 V and 1.3 V, and (blue line) Pt(111) in the last sweep up to 1.3 V, both recorded in a solution of 0.1 M $HClO_4$ at 50 mV s^{-1}. Arrows indicate the direction of the changes as the number of cycles increases. (b) CV profiles of Pt(111) electrodes with different densities of random defects collected in 0.1 M $HClO_4$ and scan rate of 50 mV s^{-1}.

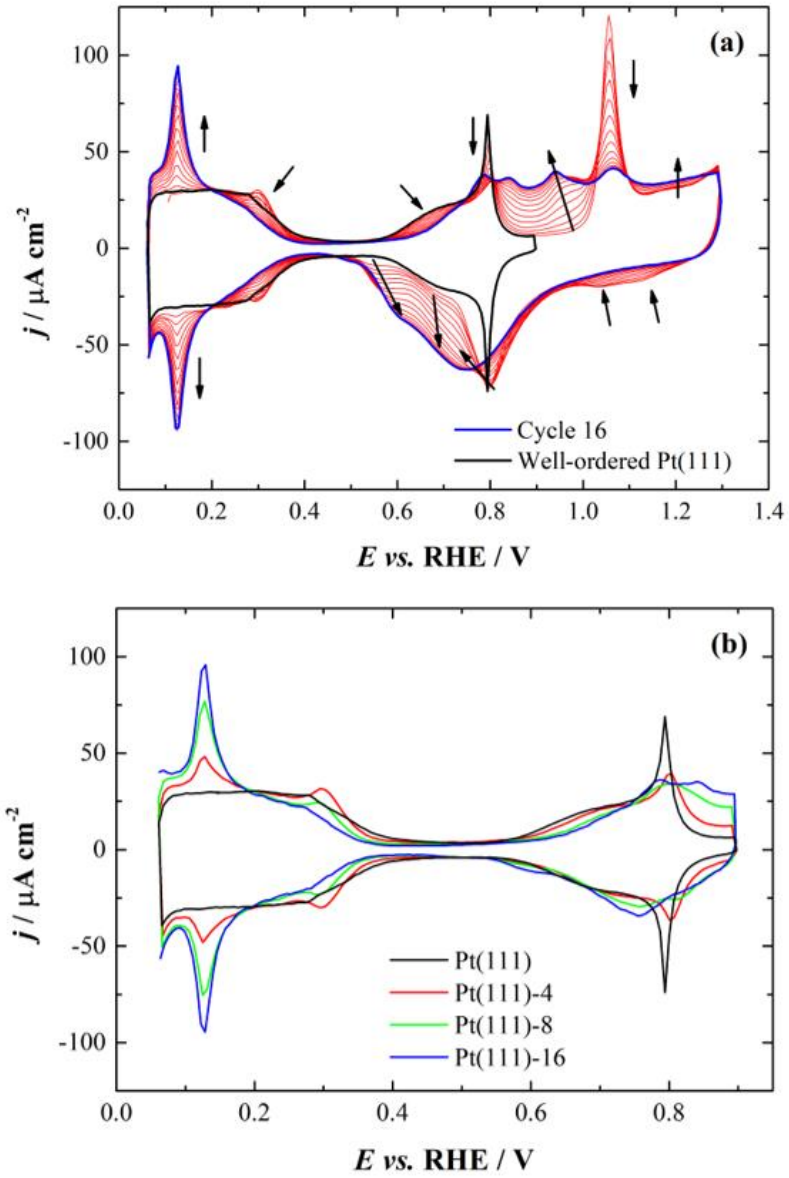

Initially, the creation of surface defects is evidenced by the appearance of two reversible peaks at ~0.13 V and ~0.30 V, typically ascribed to the presence of surface sites with different crystallographic geometries on the ordered Pt(111) vicinal surfaces. From a comparison with the well-established fingerprint profiles of defected single crystal electrode surfaces both

characteristic peaks can be then assigned to surface defects sites on well-ordered Pt(111) vicinal surfaces with {110}- and {100}-defect symmetry, respectively.[33,36,43,44] As the number of cycles to high potentials increases, the current density feature at 0.30 V disappears, while the ones in 0.13 V peak increase, evidencing the majority presence of {110}-type defects on the surface (see Figure 2.2a - CV profile in blue colour). It has been proposed that surface sites represented by the current signal at 0.30 V in the voltammogram slowly transform into {110}-type defects because of the higher stability of these latter surface sites.[42]

It is important to stress that despite the resemblance between CV profiles herein presented (Figure 2.2), and the ones of Pt stepped model surfaces vicinal to (111) pole, both surfaces are structurally different. Well-defined Pt(111) stepped electrodes are characterized by close-packed (111) terraces, separated at regular lengths by steps of either (110) (equivalently denoted (111)), or (100) orientation. In contrast, along the potential cycling, the surface gradually changes by the random formation of both {110}- and {100}-type defects on well-ordered {111} large terrace domains. To substantiate this point, Jacobse *et al.* [29] have demonstrated by using *in situ* electrochemical scanning tunnelling microscopy (EC-STM) that the application of multiple oxidation-reduction cycles, just as the ones employed in this work, destroys the surface order, and gives rise to small monoatomic-high adatom island and vacancy islands.

Following Wakisaka *et al.* [45], the nucleation and growth of Pt defects due to repetitive potential cycling only occurs at the final stage of the surface reduction process, when the electrode reaches 0.5 V in the negative-going sweep back from 1.3 V.

Figure 2.2b shows final CV profiles of selected disordered Pt(111)-X electrodes, generated after performing a different number of cycles up to 1.3 V, in comparison with the well-ordered Pt(111) electrode. From this figure, it is clear that peaks at 0.13 V and 0.30 V, initially absents on the flat Pt(111) electrode, grow as the number of cycles increases, *i.e.* the density of surface defects increases. This observation gives confidence to the assignment of these two features to the voltammetric contribution of defect sites, in agreement to several works. Therefore, the integrated charge determined from current contributions of {110}- and {100}-type of defects in the CV's can be considered to be proportional to the density of random defects of each symmetry type on the surface of disordered Pt(111)-X electrodes.[36,46]

Table 2.1 displays integrated charge of current contributions of {110}- and {100}-type of defects. It can be observed that the charge related to {110}-type defects increases as the number of cycles also increases. Consequently, the density of defects and the fraction of {110}-surface for this symmetry also increase. In contrast, the charge associated to {100}-type defects

show a dual dynamic. Initially, the charge increases during first cycles, reaching a defect density of ~3.9 x 10^{13} defects cm^{-2} and a fraction of {100}-surface of 0.03 in the fourth cycle (Pt(111)-4). Then, upon further potential cycling, it decreases to 2.90 x 10^{13} defects cm^{-2} and the fraction of {100}-surface decreases to 0.02 in the eighth cycle (Pt(111)-8) and, finally, this current contribution disappears from the voltammogram in the sixteenth cycle,(Pt(111)-16). Therefore, it can be considered that {100}-type defects are absent in this latter disordered surface. Moreover, for the two disordered surfaces in Table 2.1, {110}-type defect density is always larger than the one of {100}-type of defects. Charge values in Table 2.1 depict well the gradual increase of surfaces defects upon consecutive cycling, *i.e.* the increasing surface roughening of the initially well-ordered Pt(111) electrode.

Table 2.1. Electric charge corresponding to the peaks at 0.13 V ({110}-type defects) and 0.30 V ({100}-type defects), density of random defects of the disordered Pt(111)-X surfaces and surface fractions of {110}- and {100}-type defects.

Surface	{110}-type defects			{100}-type defects		
	Charge / µC cm^{-2}	Density of random defects / 10^{13} cm^{-2}	Fraction of {110}-surface	Charge / µC cm^{-2}	Density of random defects / 10^{13} cm^{-2}	Fraction of {100}-surface
Pt(111)-4	16.39	10.2	0.11	6.23	3.9	0.03
Pt(111)-8	26.28	16.4	0.18	4.64	2.9	0.02
Pt(111)-16	41.72	26.1	0.28	-	-	

By comparing CV profiles of disordered Pt(111)-X electrodes with different densities of random defects, it can be observed that upon increasing the defect density by going from ordered Pt(111) to disordered Pt(111)-4, the butterfly feature related to OH adsorption/desorption on terraces is still visible in the CV profile of the Pt(111)-4 electrode. This shows that even after four oxidation-reduction cycles up to 1.3 V, the Pt(111)-4 electrode still preserves large well-ordered domains.[36] By increasing the defect density, from Pt(111)-4 to Pt(111)-8 and later to Pt(111)-16, the butterfly feature gradually vanishes, showing that at least eight oxidation-reduction cycles are required to affect largely the surface order.

In overall, from the above discussion, it is seen that all disordered Pt(111) electrodes present a peak at 0.13 V associated to {110}-type defect (Figure 1.2b), and the intensity of this peak is directly linked to the number of performed cycles between 0.05 V and 1.30 V. On the other hand, the peak at 0.30 V related to {100}-type defect is only seen on voltammetric profiles of Pt(111)-4 and Pt(111)-8. This kinetic dynamic of the surface disordering process is in agreement with to the one previously reported in other works, where perchloric acid [28,29] as

well as sulphuric acid [42] were employed as electrolytes. The latter study also suggested that the {100}-type defects are converted into energetically favourable {110}-type defects.

2.3.2 Effect of random defects on the ethanol electro-oxidation reaction. Comparison between ordered and disordered Pt(111) electrodes

In order to assess the role of random defects of Pt(111) electrodes onto the ethanol electro-oxidation reaction, voltammetric experiments were carried out. Figure 2.3 shows the CV profiles corresponding to the first and second scans for the Pt(111) electrodes with different densities of defects recorded at 0.1 M ethanol + 0.1 M $HClO_4$ solution at 50 mV s^{-1}. For the sake of clarity, current profiles of each electrode are presented "unfolded" with respect to the potential axis, since typical CV profiles for ethanol oxidation presents overlapped oxidation currents in the positive and negative scans.[8]

Taking the Pt(111) electrode as a reference surface, the comparison of the CV profiles of the ordered and disordered Pt(111) electrodes, clearly illustrates the surface structure effect on ethanol electro-oxidation reaction, in line with results observed for basal planes of Pt single-crystal electrodes and also oriented nanoparticles.[8,13,47] Differences mainly arise in current densities, peak potentials, and the value of the reaction onset, as it is depicted in Figure 2.4, as well as in the magnitude of the surface deactivation observed between the first and second cycles and represented in Table 2.2 as electrode deactivation percentages. The voltammetric profile of the ethanol electro-oxidation in acid media on ordered Pt(111) electrodes displays very slow oxidation rates at potentials below 0.3 V, due to the formation of adsorbed poisoning intermediates as CO_{ads} and hydrocarbon residues ($CH_{x,ads}$ and $COH_{x,ads}$/$CHO_{x,ads}$) from dissociative ethanol adsorption, which in turn decreases the H_{upd} coverage and, simultaneously, the active surface sites for the reaction. This deactivation process occurs at potentials as low as 0.1 V, and CO_{ads} is continuously accumulated on the surface since it cannot be effectively stripped off at E < 0.6 V from the Pt(111) surface.[48–51] As the potential is made more positive, E > 0.35 V, the faradaic current response starts to increase (0.35-0.5 V), forming a broad peak with a maximum centered at ~0.58 V, denoted as peak 1, followed by a less pronounced small shoulder at ~0.77 V, denoted as peak 2. In the negative-going scan, the current density response increases producing a single anodic peak at 0.6 V. Below this potential, the current density response rapidly decreases and, at potentials below ~0.4 V, the electrode surface is re-poisoned by ethanol decomposition products.

The maximum peak densities in the positive- and negative-going scans, as well as the general CV profile, are roughly similar for the first voltammetric cycle on ordered Pt(111). However, a strong hysteresis in the current–potential profile is seen between the anodic and the cathodic sweep from the second cycle CV (see Figures 2.3 and A1.2). These findings are related to the formation and adsorption of CO and others species like acetaldehyde and/or acetic acid at low potentials, and their posterior oxidation (except acetic acid) only at $E > 0.7$ V, which in turn, during the negative going sweep, the ethanol reaction resumes at potentials where the produced CO is readily oxidized and does not accumulate on the surface.[8]

Figure 2.3. Positive-going and negative-going voltammetric scans corresponding to the (a) first cycle and (b) second cycle of the ethanol electro-oxidation on the ordered and disordered Pt(111) electrodes in a solution of 0.1 M ethanol + 0.1 M $HClO_4$. Scan rate of 50 mV s^{-1}.

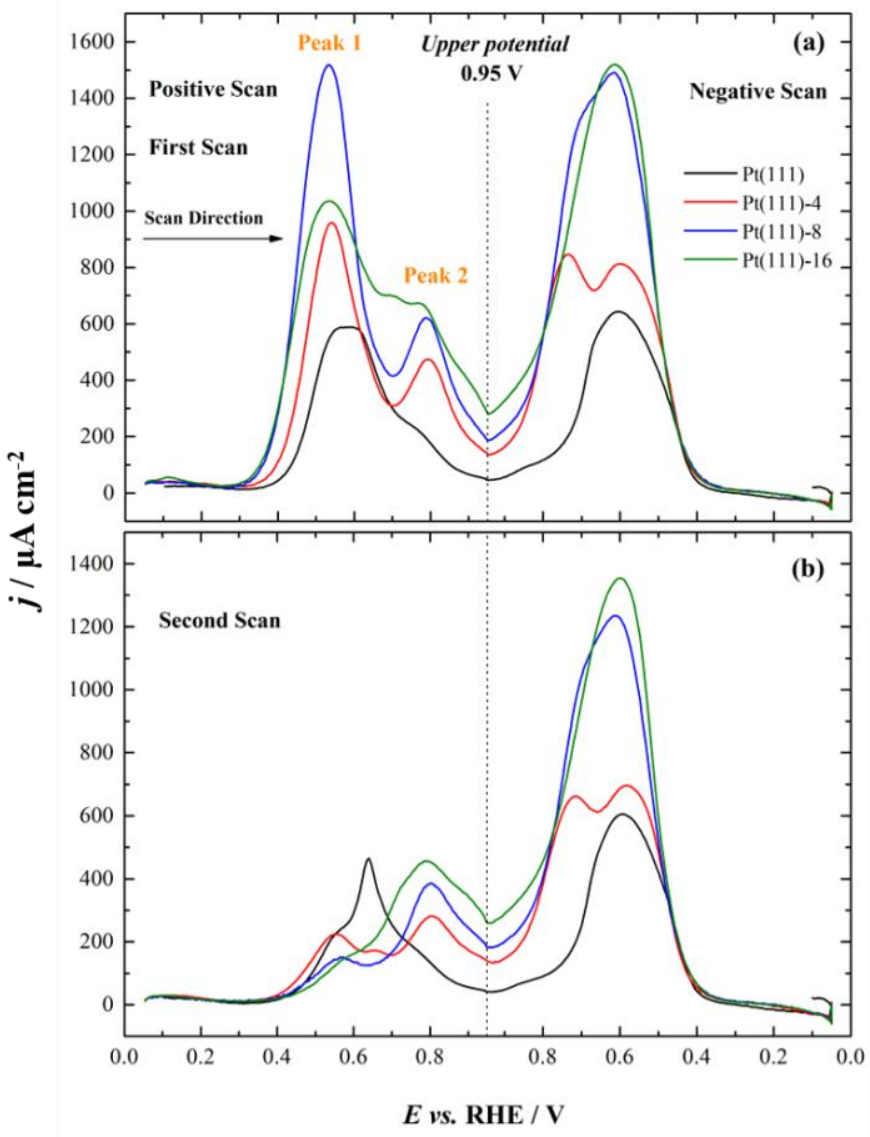

Figure 2.4. Plot of the (a) peak current density, (b) peak potential and (c) onset potential of the ethanol electro-oxidation (first cycle, positive-going scan) as a function of the density of {110}-type random defects. Dotted lines connecting the data are just for visual aid.

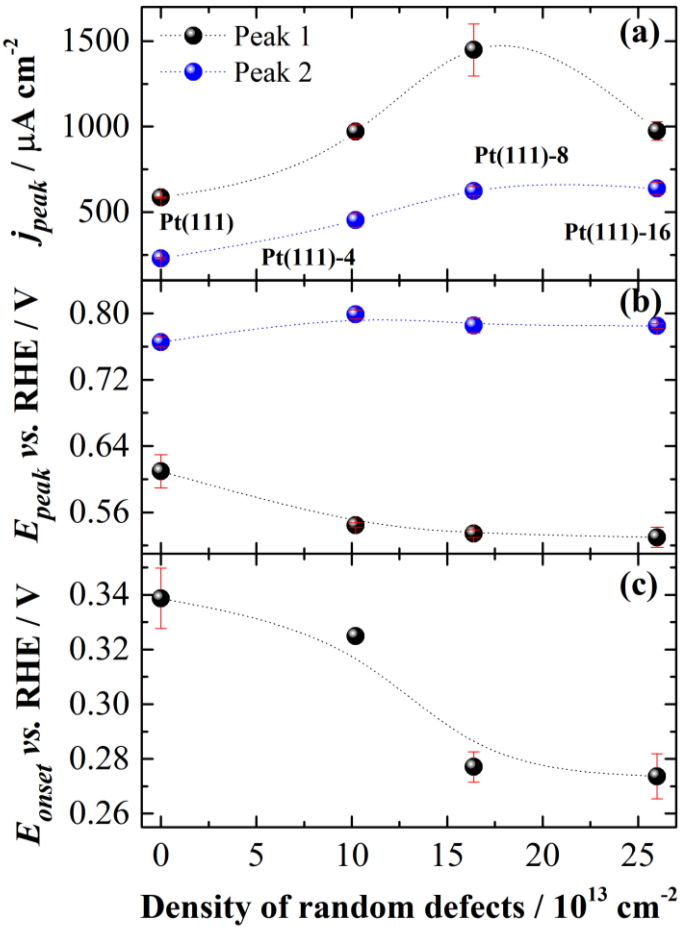

Table 2.2. Percentage of surface deactivation calculated of two different ways: (1) from the J_{peak} values related to the CV profiles and (2) from the current densities values related to the current transients at 0.6 V of the ethanol electro-oxidation on the ordered Pt(111) and disordered Pt(111) electrodes.

Surface	CV profiles		Current transients	
	Peak 1 deactivation (%): J_{peak} of the first and second cycles	Peak 2 deactivation (%): J_{peak} of the first and second cycles	Deactivation (%): current densities at 0.1 s and 0.5 s	Deactivation (%): current densities at 0.1 s and 600 s
Pt(111)	20.78	25.57	24.59	78.11
Pt(111)-4	76.51	40.84	25.35	86.23
Pt(111)-8	89.98	38.10	3.86	82.32
Pt(111)-16	85.53	32.08	29.27	87.15

On disordered surfaces, the presence of random defects promotes the oxidation of ethanol, as it is clearly seen in Figures 2.3a and 2.4a from maximum current values on the first voltammetric cycle. Increasing the density of defects continuously shifts both the potential of the first peak and the reaction onset potential towards less positive values, while keeping the

value of the potential of the second peak practically constant (see Figures 2.4b and 2.4c). However, while current densities for the first peak clearly present a maximum activity for the EOR at the Pt(111)-8 surface, those ones for the second peak slowly approach a limit value for the electrocatalytic activity as the amount of surface defects is increased (see Figure 2.4a).

Similarly, disordered Pt(111) electrodes also are more active in the negative-going scan, with the Pt(111)-8 and Pt(111)-16 electrodes being the ones with the highest maximum current values. Besides, on Pt(111)-4 and Pt(111)-8 electrodes the presence of surface defects not only modifies the value of current maxima but also modifies the electrochemical dynamics. In this case, two oxidation peaks at ~0.6 V and ~0.7 - 0.75 V can be distinguished in the negative scan, instead to the single oxidation peak at ~0.6 V recorded for Pt(111) and Pt(111)-16. Thus, because the main difference between Pt(111)-4 and Pt(111)-8, and Pt(111)-16 is the presence of {100}-type of defects, it is probable that the existence of this type of surfaces defects on those former is responsible for the current peak at ~0.7 - 0.75 V.[47]

When comparing global CV's profiles in Figure 2.3, it is clearly seen that the hysteresis between positive and negative-going scans also depends on the surface structure, and as the density of defects increase the hysteresis becomes higher. It is possible that the formation of CO, and/or other intermediate(s) species, during ethanol oxidation, and strongly adsorbed on the electrode surface, is deeply modified by the presence of surface defects.

On the second CV, systematic differences arise when current profiles are compared with the one recorded during the first scan. The most important difference is on the overall electrode electroactivity, as electrode surfaces becomes severely deactivated during the second positive-going scan. This deactivation process can be observed in terms of the magnitude decrease on the current density of the process at the first peak potential more significantly on disordered Pt(111) electrodes. Examination of Table 2.2 shows the outstanding effect of the presence of defects on Pt(111) towards electrode electroactivity upon the first cycle. Processes responsible for the peak 1 are impressively suppressed, achieving deactivation percentages as high as 90% for the Pt(111)-8 surface, in contrast to a 21% of surface deactivation calculated for the well-ordered Pt(111) surface. However, regardless the density of defects on the different surfaces seen in the second cycle, oxidation rates at 0.58 V reach approximately the same values, *i.e.*, $j_{peak\ 1} \approx 225\ \mu A\ cm^{-2}$. On the other hand, although the surface deactivation also affect peak 2, but in lower extent than that observed in peak 1, it follows a trend in relation to density of defects. From the second cycle onwards, the deactivation is minimized and does not diminish considerably.

In contrast, during the second cycle of the negative-going scan the deactivation is significantly lower than one recorded in the second cycle of the positive-going scan on both ordered and disordered Pt(111) electrodes. This result suggests that the process responsible for the first potential peak during the first positive scan is related to the oxidation of ethanol on a surface which is free from adsorbed species. On the negative scan direction, at the same potential range, are already present on the surface strongly adsorbed intermediates that inhibit the oxidation process at the second positive scan.

Inspection of onset potential values also brings additional information about the adsorbed adlayer structure, composition and its kinetics. The presence of defects sites on disordered Pt(111) electrodes, clearly, shifts the onset potential to lower values in the first cycle (Figure 2.3 and 2.4c), while in the subsequent ones they remain approximately the same (as shown in the Figure A1.2 in the Appendix 1).

Onset potential differences can be associated to the complex balance between several concomitant processes that occur at low potentials. The multitude of processes involve the competitive formation of adsorbed adlayer (CO_{ads}, $CH_{x,ads}$ and $COH_{x,ads}/CHO_{x,ads}$) from dissociative reaction of ethanol on a surface that initially is covered by adsorbed hydrogen (H_{upd}). These processes are strongly sensitive to the surface orientation sites [6], and as systematically increase the surface disordering the adlayer build up as a consequence of the surface structure. Considering only an adlayer built up with CO, although consisted of different structures of that present on EOR, traditional CO stripping measurements show similar trends regarding the onset potential as observed in the EOR as will be discussed in details in the Section 2.3.3.

In fact, for EOR the adsorbed CO is of central interest and its reactivity and extent of formation play a crucial role in the kinetics.[52] Furthermore, the structure and reactivity of this adsorbed layer is also associated to the onset of the O-containing specie formation (generally ascribed as OH_{ads}) necessary for the electro-oxidative removal of the adsorbed species and consequently, to the overall mechanism of ethanol oxidation.[6]

Cyclic voltammograms in Figure 2.3 reflect a transient situation, as a result of the ethanol oxidation on the electrode, and the subsequent, surface deactivation process because of the formation of strong adsorbing intermediate species that block surface active sites. Therefore, these current-potential profiles may only represent an average situation, a snapshot of those different processes occurring, and competing, at the electrode surface, taken at a time ca. 0.5 s (the characteristic time, τ_v, of cyclic voltammetry experiments at 50 mV s^{-1}) *i.e.* the time during which a stable electroactive species can communicate with the electrode.[53] Then, the reasons

why the Pt(111)-8 surface is the most active surface under these conditions cannot be easily understood.

Additional information regarding the ethanol oxidation activity of disordered Pt(111) electrodes, and subsequent surface deactivation, can be also gained by performing chronoamperometric measurements at different times, and at different potentials. Figure 2.5 resumes chronoamperometric parameters at several times and at five different potentials for Pt(111) and disordered Pt(111)-X electrodes. In this figure, three times were chosen: 0.5 s, Figure 2.5a, the characteristic time of CVs in Figure 2.3, 600 s, Figure 2.5b, a time long enough to achieve a "quasi" steady state current, and evaluate the surface deactivation, and 0.1 s, Figure 2.5c, the minimal time inside the resolution employed on chronoamperometric measurements. Here, it is important to mention the necessity to perform an electrochemical pre-treatment before each chronoamperometric experiment, as described in the experimental section, in order to guarantee the cleanliness of the surface before each potentials step, and therefore the reproducibility of results. A typical series of chronoamperometric measurements for the ethanol electro-oxidation on ordered and disordered Pt(111) electrodes recorded at 0.6 V by 600 s are shown in Figure A1.3.

By comparing Figure 2.3 and results in Figure 2.5a, it is found that current densities on all disordered Pt(111)-X electrodes at a fixed potential are higher (significantly at some potentials) than the corresponding currents from CVs in Figure 2.3, especially for the Pt(111)-16 surface. On the other hand, the current densities of the Pt(111) electrode are almost the same in voltammetric as well as in chronoamperometric experiments, a similar study also on Pt(111) has been reported the same behaviour but at a higher ethanol concentration.[8] Besides, in contrast to voltammetric results, the electrode activity of Pt(111)-8 and Pt(111)-16 disordered surfaces toward the ethanol oxidation is practically the same at all five potentials, and for both 0.5 and 600 s times, with a current maximum reached at ~0.6 V.

Figure 2.5. Current densities measured at potentials collected in the chronoamperometric experiments at different times (a) 0.5, (b) 600 s and (c) 0.1 s. Dotted lines connecting the data are just for visual aid.

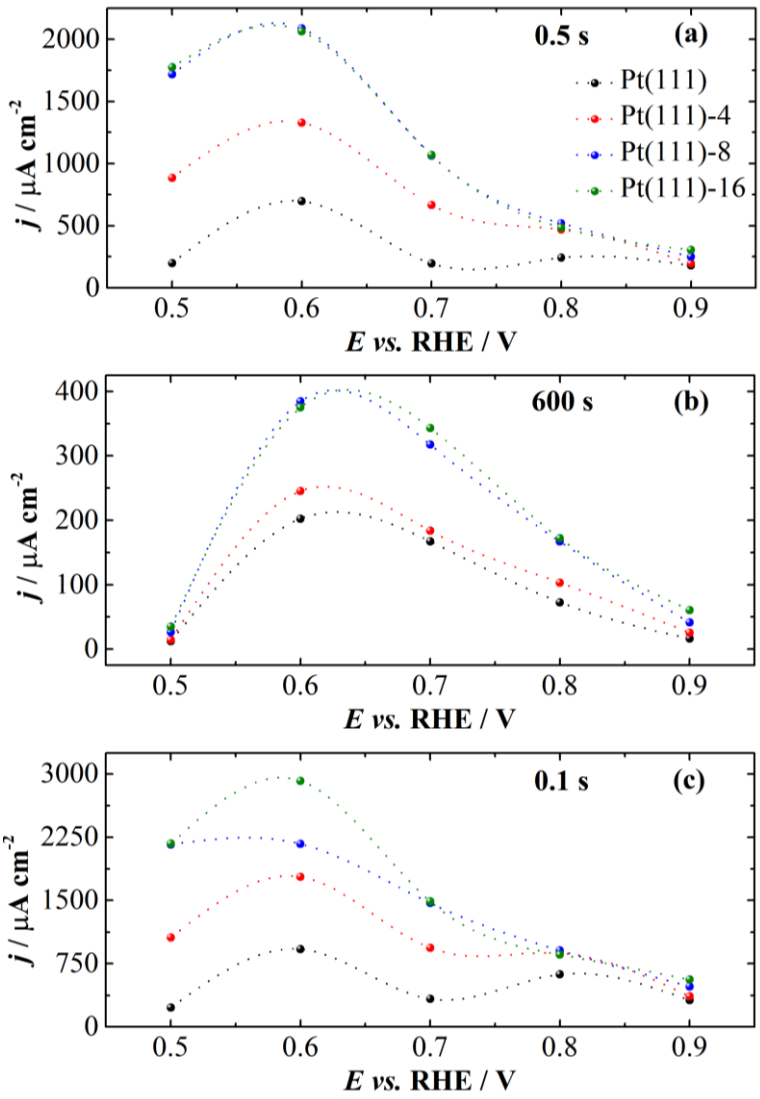

In order to clarify the role of surface defects on the electrode activity toward the ethanol oxidation, *i.e.*, if there is a maximum in the activity at a given defect density value after which the electrode activity decreases, or if the activity increase tends toward a plateau limit, chronoamperometric results at 0.1 s were also analysed, and results are given in Figure 2.5c. It is expected that at shorter times surface deactivation because of strongly adsorbed intermediates on defects sites would take place at a lesser extent, as it can be clearly seen in Figure 2.5 from the higher oxidation currents recorded at 0.1 s, relative to the ones at 0.5 s. Moreover, from data in Figure 2.5c it is seen that it is the Pt(111)-16 surface the one that reaches the highest current density at 0.6 V, becoming now the most active surface at this specific potential.

Therefore, in contrast to results in Figure 2.3, results in Figure 2.5c strongly suggests a continuously increase on the electrode activity toward the ethanol oxidation with the density of

defects, being the Pt(111)-16 surface the most active surface at 0.6 V. Differences on ethanol oxidation activities between results in Figures 2.3a and 2.5a can be explained by considering the surface deactivation process. In this framework, it could be said that Pt(111)-16 surface is not the most active surface from Figures 2.3a and 2.5a because, being the most active surface, it is the one that also deactivates faster. Only at short times, as the ones represented in Figure 2.5c, the highest intrinsic activity of Pt(111)-16 becomes evident. This result would be different from the intrinsic activity decrease toward ethanol oxidation at increasing step densities reported from studies at Pt(111) vicinal surfaces.[13] However, because data on those studies were taken at 0.015 s, our conclusions are preliminary, and more work is still necessary in order to confirm this point.

A faster deactivation of Pt(111)-16 electrode, compared to the Pt(111)-8 surface is clearly seen from calculated percentages for current decays of ~29% and ~3% between data at 0.1 and 0.5 s, respectively, given in Table 2.2. Nevertheless, the fact that measured currents at Pt(111)-16 and Pt(111)-8 are practically the same at all times and other potentials but 0.6 V, reveals the complex reaction mechanism for the ethanol oxidation, and no further conclusions can be extracted from these data. Notice for example that after first seconds at each potential step, chronoamperometric curves, as those given in Figure A1.3, rapidly drop and attain “quasi” steady-state currents significant smaller than expected currents for diffusion-controlled processes, confirming the existence of several competing processes, including the formation of strongly adsorbed intermediates that block surface active sites and slowly deactivate the electrode.

On the other hand, notice that oxidation currents at 0.9 V on all electrodes, both on Pt(111) and disordered Pt(111)-X surfaces, and at all times in Figure 2.5 are significantly smaller, relative to maximum currents recorded from chronoamperometric measurements. Therefore, poisoning species during ethanol oxidation strongly adsorbed on surface defects at 0.9 V can be only stable species at high potentials, *i.e.*, not adsorbed CO. This result is further supported by noticing that it is holding the potential at 1.0 V for 10 s what makes different the initial state of the surface on chronoamperometry and cyclic voltammetry experiments, while holding the potential at 0.1 V for 0.01 s before each potential step is practically equivalent to the "surface cleaning" achieved during the cyclic scan in the low potential region.

2.3.3 CO stripping on the well-ordered and disordered Pt(111) electrodes

As mentioned above, the formation and subsequent oxidation of CO is one of the main processes inside the reaction mechanism of ethanol oxidation on Pt surfaces. Therefore, kinetic details of CO oxidation can shed light regarding the main role of surface defects on the electrode reactivity.[34,52,54] In this sense, CO stripping is considered a typical experiment in electrocatalysis to determine reactivity parameters of different electrocatalyst towards CO oxidation, together with important details regarding the electrode/electrolyte structure.[52] Moreover, CO studies provide critical information for formulating models to understand how its strong adsorption and formation on metal surface plays an important rule over the reaction mechanism of most of organic molecule electro-oxidation and, thus, contributing with new insights in designing more efficient electrocatalyst with practical application.[52]

Figure 2.6 presents the stripping voltammograms of CO oxidation onto ordered and disordered Pt(111) electrodes recorded at 20 mV s^{-1}. Disregarding the pre-oxidation process, all the ordered and disordered Pt(111) electrodes show a single intense oxidation peak. It can be clearly observed that the rate of CO oxidation is affected by the superficial atomic arrangement of the Pt(111) electrodes, revealed by a systematic shift of the reaction onset potential of the main peak to less positive values as the density of random crystalline defects increases, *i.e.*, random crystalline defects enhance the beginning of the CO adlayer oxidation. Therefore, on the ordered and disordered Pt(111) electrodes the beginning of the oxidation increases in the order Pt(111) < Pt(111)-4 < Pt(111)-8 < Pt(111)-16.

The results presented above are in according to the reported in literature.[34,54] From chronoamperometric stripping experiments of a complete CO monolayer at disordered Pt(111) electrodes, Petukhov *et al.* [54] showed that the electrode with the higher defect density is more active, as it oxidizes the CO adlayer in a shorter period of time. Lebedeva *et al.* [34] have showed that the presence of even a low amount of random crystalline defects, introduced via cooling the flame-annealed Pt(111) in air, decreases the overpotential of CO adlayer oxidation compared to the ordered Pt(111) electrode. A similar catalytic effect of regular defects, present in vicinal Pt(111) electrodes with steps of {110} symmetry, on the CO adlayer oxidation has also been observed.[55,56]

Such behaviour has been explained in terms of that both random crystalline defects and steps (*i.e.*, regular defects) act as nucleation centers for the formation of oxygen-containing species, by reducing the overpotential of its formation and as such catalyse CO oxidation.[34,54]

Figure 2.6. CO stripping voltammetry after keeping the electrode at 0.1 V for 5 min in CO saturated electrolyte and 20 min under argon bubbling, for the well-ordered and disordered Pt(111) electrodes in 0.1 M $HClO_4$ at 20 mV s^{-1}.

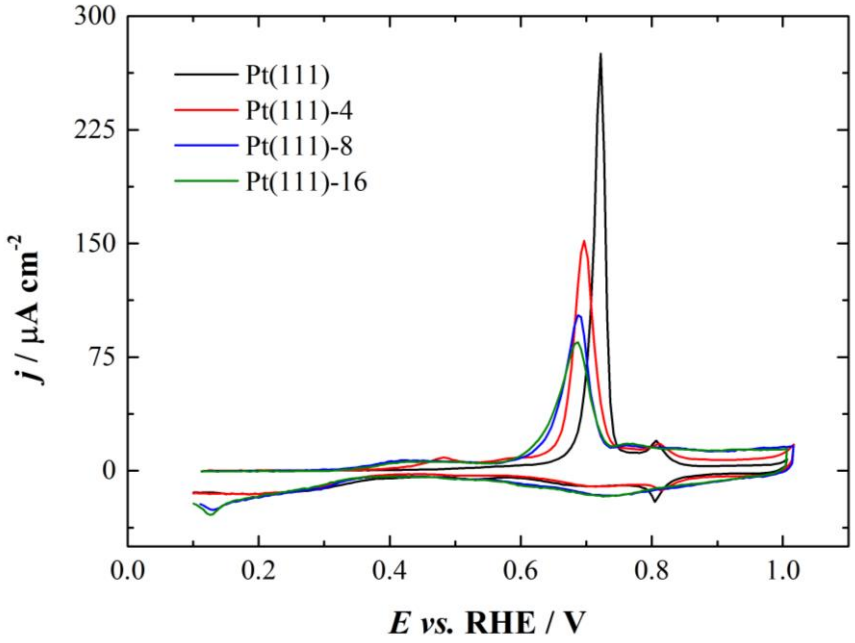

The charges obtained from CO electro-oxidation decrease as the density of random defects increases following the order: Pt(111) > Pt(111)-4 > Pt(111)-8 > Pt(111)-16, indicating that the adlayer packing density is lower on the disordered Pt(111) electrodes, from a comparison with the results observed for stepped Pt(111) electrodes.[56–58] Lebedeva *et al.* [56] have suggested that it is the higher concentration of surface oxygen-containing species on stepped Pt surfaces that primarily determines the higher catalytic activity. The lower CO packing density apparently plays only a secondary role.

In respect to the behaviour observed in the CV profiles of the EOR on the ordered and disordered Pt(111) electrodes shown in the first cycle (Figure 2.3a), namely, the shifting of the reaction onset potential and potential of peak 1 to less positive values as the density of random defects increases, seems be directly linked to beginning of the electro-oxidation of CO on the random defects present in disordered Pt(111) electrodes.

In addition, the results from Figure 2.6 also strongly evidence that poisoning species responsible for the current drops in Table 2.2 from both cyclic voltammetry and chronoamperometric measurements cannot be only assigned to adsorbed CO. This is because the reaction onset for CO oxidation on all disordered Pt(111)-X electrodes, ~E > 0.4 V, takes place at those potentials where the first oxidation peak of the first positive-going scan occurs (0.35 < E < 0.8 V). Then, similar to what has been already suggested from ethanol oxidation studies on Pt stepped surfaces [6,12], adsorbed acetate, acetaldehyde, CO, or oxidable "CH_x"

and COH/CHO fragments [6,12] , formed because of ethanol oxidation at defect sites, should be the main formed species responsible for the surface deactivation described in Table 2.2. Nevertheless, it is the electrode activity toward CO oxidation what may determine the reaction onset potential for ethanol oxidation.

2.3.4 Identification of the reaction intermediates and products by in situ FTIR

The *in situ* FTIR gives us outstanding evidence of the influence of surface structure versus the nature of different adsorbed species and products formed during electrocatalytic reactions. Figure 2.7 presents a set of FTIR spectra for ethanol oxidation reaction obtained on four different electrodes: Pt(111), Pt(111)-4, Pt(111)-8, and Pt(111)-16 at different sampling potentials.

Figure 2.7. *In situ* FTIR spectra obtained for the ethanol oxidation on ordered and disordered Pt(111) surfaces: (a) Pt(111), (b) Pt(111)-4, (c) Pt(111)-8 and Pt(111)-16. Spectra obtained in 0.1 mol L^{-1} $HClO_4$ + 0.1 mol L^{-1} CH_3CH_2OH solution. Reference spectra taken at 0.05 V. Sample spectra collected from 0.05 to 0.95 V at intervals of 50 mV.

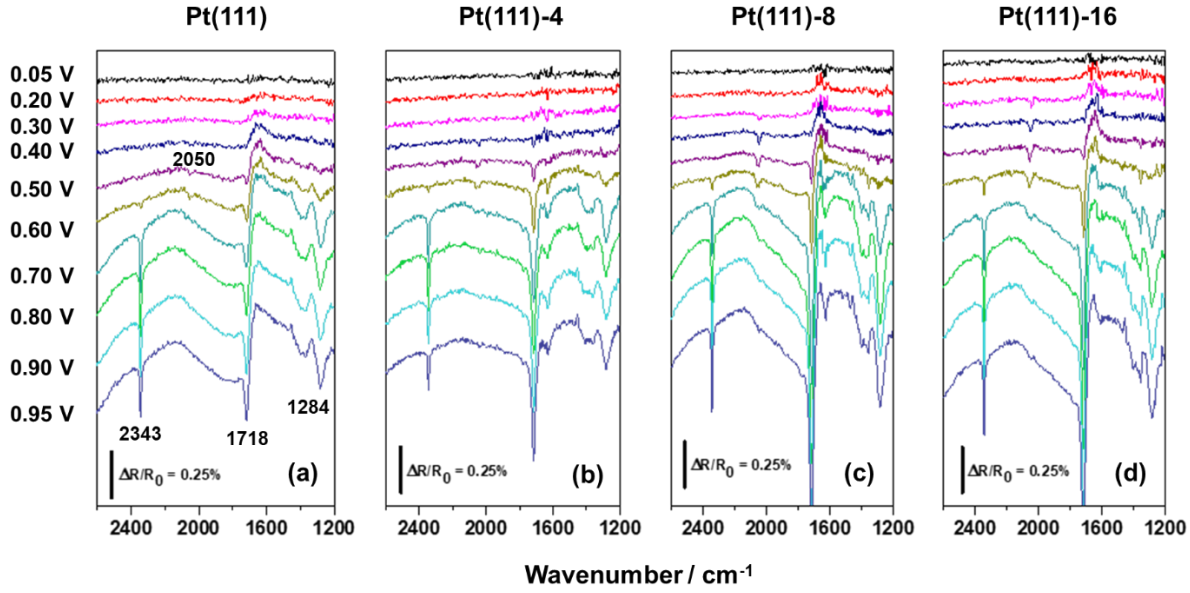

According to FTIR spectra, the wavenumber range between 2600 cm^{-1} and 1200 cm^{-1} includes only the bands associated with CO_2 (2343 cm^{-1}), CO_{linear} (2050 cm^{-1}), acetaldehyde/acetic acid (1718 cm^{-1}) and acetic acid (1284 cm^{-1}). Table 2.3 presents the frequencies of relevant bands that can be found in the spectra.[8]

Table 2.3. Assignment of the IR frequencies in the spectra for ethanol oxidation.

ν_{H_2O}/cm^{-1}	Functional group	Mode
2341	CO_2	O–C–O asymmetric stretching
2030–2070	Adsorbed CO	Linearly bonded
1713	COOH or CHO	C=O stretching
1640	H_2O	H–O–H bending
1280	COOH	Coupling C–O stretching + OH deformation

The FTIR spectra presented in Figure 2.7 give us an overview of the formation of main bands from ethanol electrooxidation, then the CO_{linear} and CO_2 band intensities taken from the series of spectra in Fig. 2.7 were plotted as a function of the potential (Figure 2.8).

Figure 2.8. Band intensities as a function of the potential. (a) CO and (b) CO_2, both obtained from Figure 2.7.

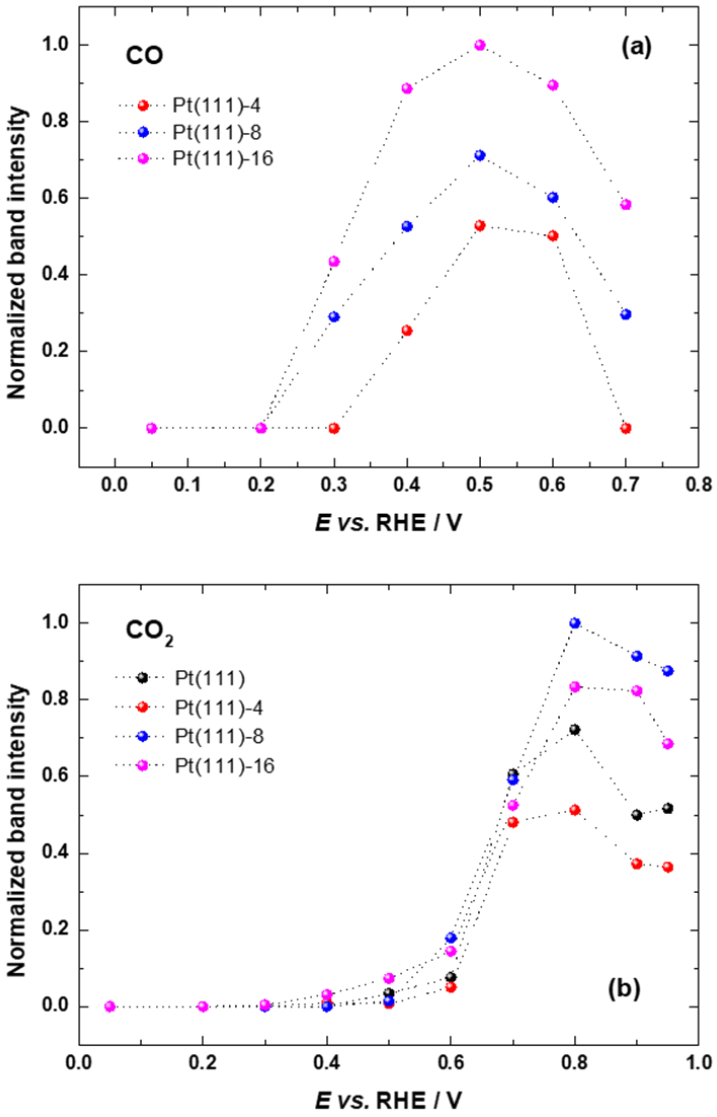

By the results for CO_{linear} production presented in Figure 2.8 a, it is observed that the cleavage of the C–C bond of the ethanol molecule to form adsorbed CO_{linear} occurs preferentially on defected surfaces, while for Pt(111), only a small amount of CO_{linear} is formed above 0.50 V, as can be seen in Figure 2.7. Based on this results we can confirm that (111) terraces address the route of the reaction to form acetic acid and acetaldehyde, being the former produced mostly.[8,59]

An analysis of CO formed onto defected surfaces, Figure 2.8 a, reveals that these surfaces promotes the cleavage of the C-C bond of ethanol more easily than the well-defined surface, Pt(111). As the {110}-defects are formed, more CO is produced, this result explains the electrochemical behavior observed during the cyclic voltammetry (Figure 2.3a), in which the onset potential is displacement to a more negative potential for surfaces having defects. In this case, the enhancement of electroactivity of these surfaces is explained based on the random defects generated, as a consequence, the breaking of ethanol molecule adsorbed on the defects is favored and the CO is promptly formed. The Pt(111)-16 had a fraction of 28% of {110}-defects formed on (111) terraces, although all defected surfaces present the same trend, this surface reached the highest activity to form CO_{linear} at 0.50 V and, thereafter, the amounts of CO decay (Figure 2.8 a).

According to Figure 2.8 b, CO_2 formation starts at 0.60 V for all surfaces studied, and its amount changes according to the applied potential. The Pt(111)-8 presented at 0.80 V the higher value among all surfaces. Curiously, Pt(111) at 0.70 V showed a slight increase over the other ones. The beginning of CO_2 production coincides with decreasing in CO_{linear}, indicating that the CO consumption is linked to CO_2 formation. Therefore, the defected surfaces play a decisive role in the mechanism of the ethanol reaction, in which the pathway is strongly changed and contributes to increasing the reactivity of the surface.

The reaction mechanism of ethanol yields different intermediates according to the surface arrangement. Pt(111) is less selective to form species such as CO and CH_x, so most of the CO_2 produced throughout the reaction comes through a route other than the formation of CO. On the other hand, Pt(111)-X electrodes display the highest catalytic activity for the splitting of the C–C bond, denoting that this type of randomly generated structure promotes the breakdown of the molecule at low potentials, *ca.* 0.3 V.

Also, it is possible to detach the surface with more defects, Pt(111)-16, produces more CO compared to the other ones, however, this species is not quite converted to CO_2 during the positive-going scan, even at 0.70 V, part of CO remain on the surface (Figure 2.7 a). Therefore, a positive effect to converting the ethanol into CO_2 just was observed for a surface having 18%

of {110}-defects and 2% of {100}-defects, in this case, Pt(111)-8 was more selective towards CO_2.

Figure 2.9 presents the band intensities of acetic acid at 1284 cm^{-1} and the contribution of acetic acid and acetaldehyde at 1718 cm^{-1} as a function of the potential. Acetic acid is an undesirable intermediated formed during ethanol oxidation because leads to a low electrons release ($4e^-$). An analysis of band intensity at 1284 cm^{-1} corresponds exclusively to acetic formation band, above 0.60 V this intermediate rises and reaches a maximum at 0.80 V for Pt(111)-8, while for the other surfaces the amounts are lower and similar, except for Pt(111)-16 which at 0.90 V presented a significant value. Curiously, for Pt(111) and Pt(111)-4, the behavior for this band was practically the same, which leads us to believe that a small number of defects does not contribute to the formation of this species.

In principle, the defects electrogenerated seem to cause more impact on acetaldehyde formation as can be seen in Figure 2.9 (b), which presents the band intensities of acetaldehyde + acetic acid. The trend observed here is completely different when compared to the acetic acid band commented previously. Herein the acetaldehyde is formed above 0.40 V and its contribution extends over the whole applied potential well peculiar for each surface studied, while that for the acetic acid band (1284 cm^{-1}) the profile presented was not so different among the surfaces studied.

Therefore, we conclude that acetaldehyde enhances or gives form to the profile of the band at 1718 cm^{-1} instead of acetic acid. Taking into account this fact, the defected surfaces impact strongly on the mechanism of the ethanol oxidation reaction, once {110}-defects formed in higher amounts, as is the case of Pt(111)-8 and Pt(111)-16, the production of acetaldehyde is detached concerning Pt(111) surface. This means that the defects act to form more 2C species, like acetaldehyde and acetic acid, as well as, 1C species such as CO and CH_x. The defects became the Pt sites much more active in breaking the C-C bond of the ethanol molecule and at the same time favor the acetaldehyde formation with the consequent break of this molecule.

Figure 2.9. Band intensities as a function of the potential for the bands at (a) 1284 cm^{-1} and (b) 1718 cm^{-1}, both obtained from Figure 2.7.

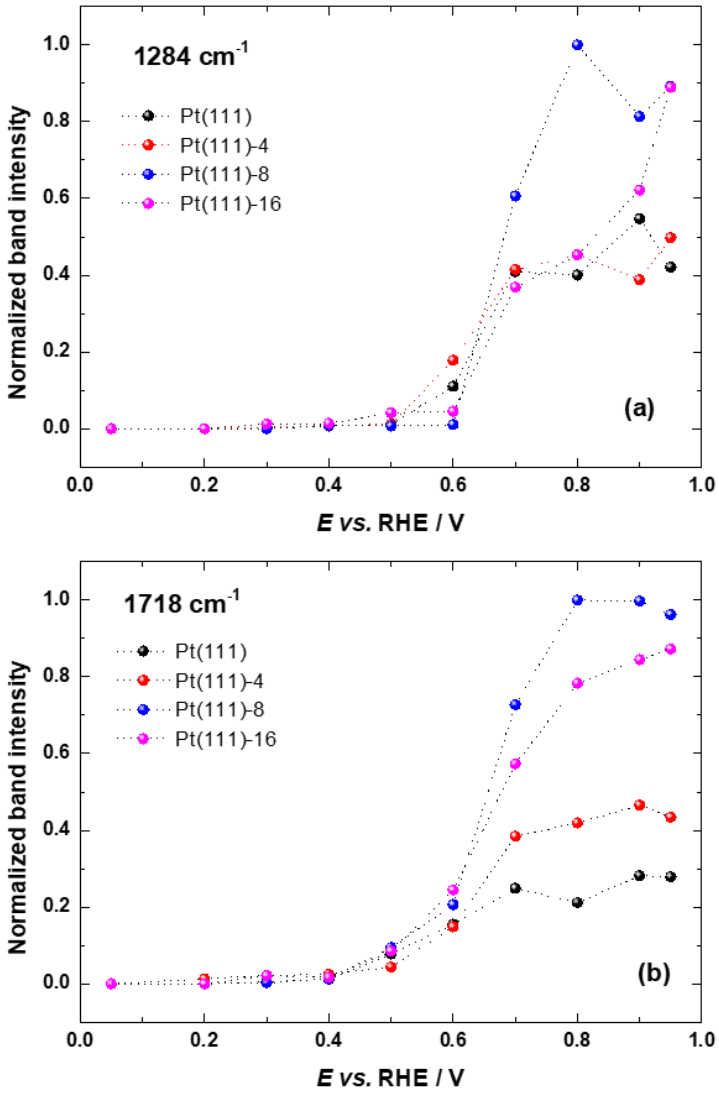

2.4 Conclusions

The ethanol electro-oxidation reaction is very sensitive to ordered and disordered Pt(111) surface, being the Pt(111)-8 and Pt(111)-16 disordered surfaces the most active and tolerant to the ethanol residues poisoning. These ones have a lower onset potential compared to well-ordered Pt(111) and disordered Pt(111)-4, indicating that certain level of disorder influences positively the EOR performance.

The anodic profile observed in the first scan for EOR contains two very well-defined current peaks for disordered Pt(111)-X electrodes. A comparison with Pt(111) shows that the electroactivity for disordered surface is more active, even at low potential, evidencing the

capability of defects in producing great number of active species. In addition, at high potential, a well-defined second peak highlights the performance of these surfaces, being more pronounced than Pt(111).

From the chronoamperometric experiments, the highest intrinsic activity of Pt(111)-16 becomes evident at 0.1 s. It could be said that the Pt(111)-16 surface is the most active in short times as 0.1 s. However, it is the one that also deactivates fastest.

The CO stripping experiments showed that the CO molecule is more strongly bonded to surface of the ordered Pt(111) electrode than on those of the disordered Pt(111) electrodes with {110}- and {100}-type defects, revealed by the shifting in the reaction onset to less positive values as the density of random defects increases. This fact seems to explain the shifting of the reaction onset potential and potential of peak 1 to lower values as the density of random defects increases observed in the first cycle of the CV profiles of the EOR. However, CO cannot be the only poisoning species responsible by the current drop observed during the positive-going scan of second cycle, since the CO electro-oxidation on all disordered Pt(111)-X electrodes already takes place at those potentials where the first oxidation peak of the first positive-going scan occurs.

The *in situ* FTIR studies demonstrated that the main products of the ethanol oxidation are CO_2, acetaldehyde and acetic acid for all surfaces investigated. In addition, adsorbed CO_{linear} is also observed. The plots of integrated band intensity corresponding to the CO_{linear} and CO_2 revealed that the formation of both species is enhanced in the presence of {110}-type defects. Similarly, acetaldehyde production and acetic acid production is also enhanced. Thus, the defects act to form more 2C species, like acetaldehyde and acetic acid, as well as 1C species such as CO and CH_x.

Finally, the results obtained here provide some basic information concerning the EOR that contributes in understanding the effect of the order/disorder in monoatomic level, and so give us insights in rationalizing the choice of nanomaterials with appropriate sizes and shapes.

Chapter 3

Effect of Tin Deposition over Electrogenerated Random Defects on Pt(111) Surfaces onto Ethanol Electrooxidation: Electrochemical and FTIR Studies

This chapter has been adapted with permission from the Elsevier: Amaury F. B. Barbosa, Vinicius Del Colle, Nelson A. Galiote, Germano Tremiliosi-Filho, “Effect of Tin Deposition over Electrogenerated Random Defects on Pt(111) Surfaces onto Ethanol Electrooxidation: Electrochemical and FTIR Studies,” Journal of Electroanalytical Chemistry, v. 857, 113734, 2020.

3.1 Introduction

Direct alcohol fuel cells (DAFCs) have emerged as a promising clean alternative to the use of contaminant fossil fuel systems to fulfill sustainable energy demands.[1,3,15] Ethanol, in particular, is the most interesting molecule to be used in such systems since it is possible to be obtained directly from biomass, it is easy to store, it is less toxic than other alcohols such as methanol, and it has a high energy density in the complete oxidation to CO_2 when compared with methanol.[3,15,60–62]

Pt is, at present, the best-known catalyst for the oxidation of small organic molecules, like methanol and ethanol.[63,64] However, it is generally accepted that Pt alone is not sufficient to oxidize alcohol at a reasonable rate. The main problem associated with oxidation of alcohols on Pt is the self-poisoning by CO molecule and other strongly adsorbed intermediates that are formed during the oxidation reaction.[52] These species remain onto the surface of the electrocatalysts decreasing the performance and its reactivity. Also, Pt exhibits a limited ability for breaking C–C bonds.[61,65] For commercial application in a fuel cell, the ability of C–C cleavage, as well as the oxidation of adsorbed CO, should be increased.

As observed for other fuels, the ethanol oxidation is a structure sensitive reaction on platinum electrodes.[8,10,13,14,23,47,66] Therefore, the reaction route, as well as the final products of the oxidation, will depend on the surface structure of the electrode. Among the low index planes, the Pt(111) electrode shows the lowest electrocatalytic activity for the splitting of the C–C bond in acidic medium. On this electrode, the ethanol oxidation in the acidic medium proceeds incompletely to acetic acid as the main reaction product, and the acetaldehyde is formed as a secondary product, whereas the CO and CO_2 are formed in a very small amount. On the contrary, on Pt(110) and, mainly, on Pt(100), the breakage of the C–C bond and, consequently, CO formation is favored in the same medium, which contributes to the subsequent step to form the final product CO_2.[8] The strategies to improve the electrocatalysis of this reaction seek electrode materials that increase the ability of the C–C bond cleavage and catalyze the CO oxidation at lower potentials.

An alternative to improve the electrocatalytic performance of platinum electrodes in the ethanol oxidation is the use of stepped Pt(111) surfaces with different terrace lengths.[6,12] On stepped surfaces having (111) terraces and (110) steps, it has been shown that the steps play an important role in the ethanol oxidation on these surfaces. The C–C bond cleavage, which is the required step to yield CO_2, takes place only on these types of sites.[12] Another way is to modify the composition of the Pt using a second metal (M) such as Ru [19], Os [18], and Sn [20], that

act synergically through a bifunctional mechanism or modifying the Pt electronic properties. These co-catalysts form, at a low potential, oxygenated species that aid the CO oxidation (a bifunctional mechanism) and releasing active sites for further reaction, or modifying the electronic properties of Pt weakening the binding energy of the carbonaceous intermediates linked to Pt.[67–69] This last effect decreases the electron back-donation from Pt 5d to the $2\pi^*$ orbital of CO and, consequently, suppress the CO–Pt bonding, resulting in a lower CO coverage and bonding strength.[69]

Ethanol oxidation reaction has been investigated at Pt surfaces modified either by Sn alone [20,62–64,70,71] or in combination [61,72,73] with other metals. Rizo *et al.* [62] demonstrated that the modification of low index Pt single crystals with a submonolayer coverage of Sn enhances the activity of the electrode for the ethanol oxidation process in perchloric acid solution in terms of lowering the rection onset potential and a higher oxidation current. They also showed, employing on-line electrochemical mass spectroscopy experiments, that on both, Pt(111) and Pt(110), the presence of Sn enhances the oxidation of ethanol to acetaldehyde. Besides, the further oxidation of acetaldehyde is sensitive to the Pt surface structure: on Pt(110) there are sites able to break the C–C bond in acetaldehyde to form CO_2, whereas on Pt(111) such sites are not available and acetaldehyde is oxidized further to acetic acid.

Del Colle *et al.* examined the effect of tin on step sites. The study has demonstrated that tin deposited on stepped Pt(111) surfaces has a double effect on the ethanol oxidation mechanism. The presence of low tin coverages on the step sites promotes the ethanol oxidation since it facilitates the oxidation of CO formed previously, on the step where occurs the cleavage of the C–C bond in the molecules, by a bifunctional mechanism. This effect only occurs when there are some available sites on the platinum surface to break the C–C bond, as revealed by the catalytic effect found for partially decorated tin on the step sites. However, when the step sites have been completely decorated by tin, the production of acetic acid is significantly enhanced and CO formation has been almost suppressed since tin has blocked all the platinum step sites, which are together with the tin responsible for the C–C bond breaking.

Recently, Barbosa *et al.* [66] showed that the presence of random defects on Pt(111) enhances the electrocatalytic activity of ethanol oxidation, both in terms of current density as in terms of the onset potential of the alcohol oxidation.

Based on that, this paper aims to investigate the combined effect of the presence of random defects on Pt(111) and Sn deposition at submonolayer levels in the mechanism of ethanol oxidation on Pt(111) modified surface. These studies were done using electrochemical

techniques, *in situ* FTIR experiments and for understanding the role of the CO in the ethanol oxidation process was included in the study of CO stripping.

3.2 Experimental Section

3.2.1 Surface Preparation and Characterization

All experiments were carried out at room temperature (25 ± 1 ºC) in a conventional three-electrode single cell. The chemicals used for solution preparation were perchloric acid (70%, Sigma-Aldrich), ethanol (99,9%, Panreac) and ultra-pure water from a Millipore system (18.2 MΩ cm^{-1}). Hydrogen (White Martins, 99.99%) was used for flame-annealing treatment and argon (White Martins, 99.998%) to deoxygenate the solution. A reversible hydrogen electrode (RHE) and a Pt platinized foil (1 cm^2) were employed as a reference electrode and as a counter electrode, respectively. A Pt(111) single crystal was used as a working electrode, having a geometric area of 0.04486 cm^2, which was prepared according to the Clavilier method.[33] The surface was cleaned by flame annealing and cooled down in H_2/Ar and protected with water in equilibrium with this gas mixture to prevent contamination and surface oxidation before immersion in the electrochemical cell, as described elsewhere.[34]

Electrochemical measurements were carried using Autolab PGSTAT 302 potentiostat equipment. To generate random defects on well-ordered Pt(111) surface, successive voltammetric sweeps were carried out in a potential range of 0.05 - 1.3 V at 50 mV s^{-1} in a solution of 0.1 M $HClO_4$. The repetitive swept to potentials higher than 1.15 V progressively destroy the initial surface order.[28,66]

In this work, one partially disordered Pt(111) surface was prepared by fixing the number of excursions to a high potential region to obtain the desired surface roughening. To guarantee a larger number of defects in the surface, the electrode was cycled 32 times between 0.05 V and 1.30 V. Then, hereafter this electrode will be denoted as Pt(111)-32. After the surface disordering, a CV was registered between 0.05 V and 0.7 V at 50 mV s^{-1} in the same electrochemical cell in order to obtain the final electrode surface state.

The explanation about the appearance of characteristic current signals in the voltammogram at low potential for this disordered electrode was already described elsewhere.[66]

3.2.2 Tin deposition over Pt(111)-32 Surfaces

Tin deposition on the Pt(111)-32 surfaces was carried out by cycling the electrode in solutions containing 10^{-6} M $SnSO_4$ + 0.1 M $HClO_4$ at the potential range between 0.05 and 0.70 V at a scan rate of 0.05 V s^{-1}. Under those circumstances, the Sn deposition is a mass-controlled process that takes place in all this potential range.[20] The ethanol oxidation studies were carried out in a different cell with a 0.1 M C_2H_5OH + 0.1 M $HClO_4$ solution. The voltammetric sweeps were performed at a potential range of 0.05 – 0.95 V at 50 mV s^{-1}.

After the Pt(111)-32 modification by Sn, integrated charges were calculated through the peak at 0.13 V to obtain the percentage of {110}-defects covered. In the present study, it was prioritized to analyze the influence of a small, intermediate and complete Sn layer deposited over defects generated onto ethanol electrooxidation reaction.

After finishing each Sn deposition and the respective ethanol oxidation studies by electrochemical techniques or *in situ* FTIR spectroscopy, the electrodes were cycled between 0.05 and 1.65 V at 200 mV s^{-1} in a fresh $HClO_4$ electrolyte. This procedure favors the oxidation and removal of the Sn deposits from the platinum surface, after that, the surface is ready to carry out a flame-annealing and, thus, recovery its atomic arrangement characteristic that can be confirmed through the voltammetric profile of the Pt(111) in the $HClO_4$ solution.

3.2.3 Voltammetric measurements of CO stripping on the disordered Pt(111)-32/Sn electrodes

Voltammetric CO stripping experiments on unmodified Pt(111)-32 and Sn-modified Pt(111)-32 surfaces in 0.1 M $HClO_4$ was carried out by bubbling CO (White Martins, 99.5%) for 5 min while the electrode was set at 0.1 V. Thereafter, the CO dissolved in the solution was removed by purging with Ar for 20 min. Lastly, the remaining adsorbed CO was stripped off by applying a positive-going scan beginning at 0.1 V up to 0.9 V under 50 mV s^{-1}.

3.2.4 In situ FTIR measurements

For the FTIR studies of ethanol oxidation, a reference spectrum was acquired at 0.05 V. Thus, other spectra were recorded after applying successive potential steps of 0.05 V in the positive direction from 0.1 to 0.95 V *vs.* RHE. The potential was controlled by an Autolab potentiostat/galvanostat (model AUT85732). The working electrode was a commercial Pt(111)

disk (d = 10 mm, from MaTeck) and a trapped H_2 bubble in contact with a Pt wire was used as the reference (RHE), all potentials in this work were referred to this reference system. The Pt(111)-32 electrode was modified by tin using the same conditions described for the electrode bead-type (Section 3.2.2).

The spectra were computed from an average of 256 interferograms, and the spectral resolution was set at 4 cm^{-1}. Reflectance spectra were calculated as the ratio (R/R_0) of the sample (R) and the reference (R_0) spectra. With respect, the bands registered, positive and negative bands represent loss and gain of species at the sampling potentials, respectively. For all the measurements, a CaF_2 window was used. *In situ* FTIR measurements were carried out by using a VERTEX 70v vacuum Bruker spectrometer provided with an LN-MCT Mid detector.

3.3 Results and discussion

3.3.1 Pt(111)-32 Characterization and Tin Deposition

The Pt(111)-32 surface was generated by cycling the original Pt(111) surface in 0.1 M $HClO_4$. In that way, the CVs obtained by applying cyclic voltammetry, show substantial information that can be demonstrated concerning the preferential orientation sites as well as the amount of generated random surface defects.[66]

In the present study, a Pt(111) surface with a reasonable degree of disorder in the surface was reached by cycling 32 times in the potential range between 0.05 and 1.30 V. The CV profile of the partially disordered Pt(111)-32 surface can be seen in the Figure 3.1a.

According to Figure 3.1a, the CV presents the profile of a partially destructed Pt(111) surface after generating random defects with preferential orientations on the electrode surface.[28,66] The appearance of the surface defects is evidenced by the anodic and cathodic peaks at ~0.13 V, which are assigned to the hydrogen desorption and adsorption processes, respectively, on surface sites with preferential crystallographic geometry, namely, {110}-defect symmetry. The integrated charge determined from the current contribution of {110}-type defects in the CV profile was considered to be proportional to the random defect density of {110}-symmetry.[66] Consequently, the defect density obtained for the Pt(111)-32 electrode was of ~ 29.5 x 10^{13} defects cm^{-2}.

In this case, as the electrode is cycled at high potentials for several times, just {110}-defect are observed. However, a small peak (shoulder) was observed at 0.30 V and belongs to

{100}-defects (not shown here), this contribution comes as soon as the electrode is cycled at the beginning and disappears when the electrode is continuously cycled, these defects slowly transforms into {110}-type defects due to its high stability.[42]

Figure 3.1. a) Stable CV profile correspondent to disordered Pt(111) surface by cycling it up to 1.3 V (32 times) in 0.1 M $HClO_4$. b) Progressive modification of Pt(111)-32 by Sn deposition in a 10^{-6} M $SnSO_4$ + 0.1 M $HClO_4$ solution. v = 50 mV s^{-1}.

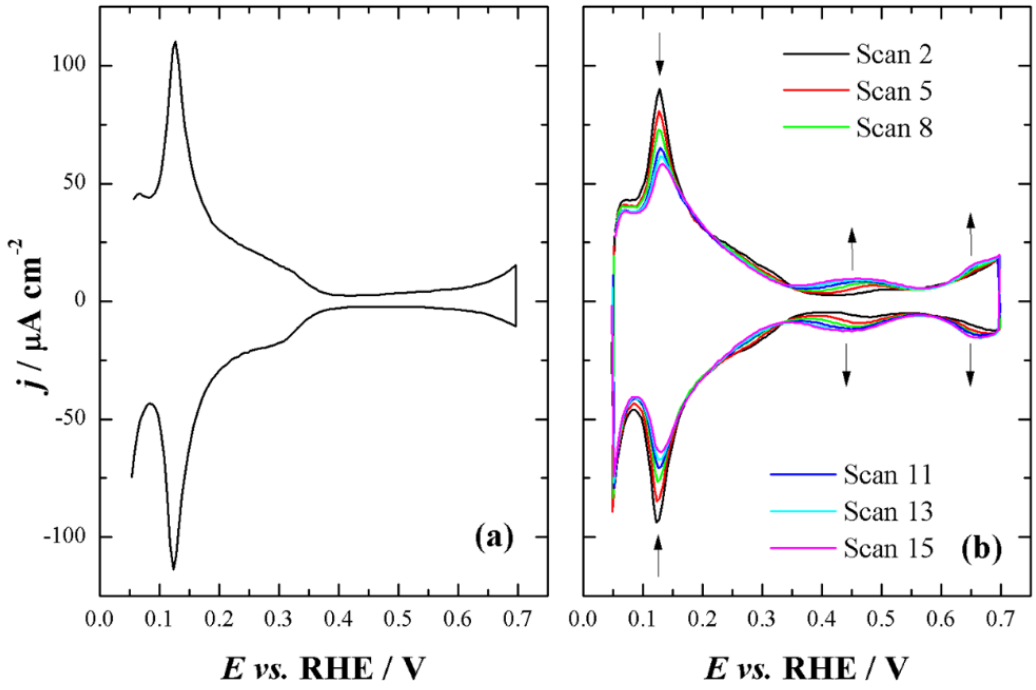

After obtaining the disordered surface, Pt(111)-32, the modification by Sn submonolayers was carried out by cycling this electrode between 0.05 and 0.70 V using a 10^{-6} M $SnSO_4$ + 0.1 M $HClO_4$ solution. According to Figure 3.1 b, is possible to analyze the slowly Sn deposition over the disordered Pt(111)-32, once Sn ions are at low concentration. In this sense, the deposition is governed by mass transfer in all range of potential applied, thus, it is easy to assess the changes in the CV.[20]

According to the CV, two distinct potential regions can be separated and analyzed individually. The first one is assigned to hydrogen adsorption/desorption processes at low potential between 0.06 and 0.35 V. The sharp anodic and cathodic peaks at 0.13 V correspond to the hydrogen adsorption/desorption onto {110}-type defect sites, while the charge difference in the potential region between 0.06 and 0.35 V, after disregarding the peaks at 0.13 V, correspond to the hydrogen adsorption/desorption on the non-affected and remaining Pt(111) terraces. In the potential range of 0.06 and 0.35 V, it can be clearly observed that the current densities of the hydrogen adsorption/desorption processes at 0.13 V slowly decreases as the Sn

is deposited at each potential cycle up to 0.7 V, indicating that Sn was preferentially adsorbed on the {110}-defect sites of the Pt(111)-32 electrode. However, a small decrease of charge is observed between 0.20 – 0.30 V, which might be associated with Sn deposition on (111) terrace atoms near to {110}-defects.

The second potential region, 0.35 – 0.70 V, highlights the double-layer region due to anion adsorption on the terrace sites.[74,75] Looking closely this region, changes in the CV help us to monitor Sn adsorption onto terraces. Two contributions can be mentioned at 0.45 V and 0.65 V. As already evidenced in the literature [70,74–76], these signals are assigned to redox processes of tin ad-atoms. In the first redox process at 0.45 V, the adsorption of hydroxyl species on the adsorbed Sn occurs and the current density increases as the Sn is deposited cycle by cycle. The second process can be assigned to the formation of oxidized Sn(IV) from the Sn(II) species, once the platinum electrodes achieve the high potentials.

It has been revealed that Sn can adsorb irreversibly on Pt single crystals, namely, Pt(100) and Pt(111), in potentials that are dependent on the crystallographic orientation of the surface and on the nature of electrolyte. For Pt(111) and Pt(100) in sulfuric acid, the Sn was kept stable adsorbed on the surface up to the potential of 0.65 V, above this potential, Sn is stripped away from the surface and the hydrogen contribution reappears. On the contrary, over Pt(110) Sn may not be irreversibly adsorbed, because neither the significant inhibition of the current peak from hydrogen adsorption-desorption nor the remarkable Sn_{ad} oxidation current peak is seen.[70]

It is important to mention that the CV features of Sn submonolayers are more evidenced in perchloric than in sulphuric acid solutions. According to Zheng *et al.* [70], adsorbed Sn is stable at potentials lower than 0.69 V (*vs.* RHE) in sulfuric acid solution, but it is more stable in perchloric acid solution up to 0.99 V (*vs.* RHE). Then, in the present study, the E_{upper} was kept at 0.70 V during the deposition stage, in order to avoid Sn dissolution.

In that way, three different Sn coverages were chosen to modify a disordered surface of Pt(111)-32. The Sn coverage degree ($\Theta_{Sn}^{Defects}$) at {110}-defect sites was calculated from the suppression of the hydrogen desorption charge density under the peak at 0.13 V for the unmodified and modified electrodes, according to the following equation 3.1[62]:

$$\Theta_{Sn}^{Defects} = \left(Q_{Pt}^{H} - Q_{Pt,Sn}^{H}\right)/Q_{Pt}^{H} \qquad (3.1)$$

where Q_{Pt}^{H} and $Q_{Pt,Sn}^{H}$ are the charge densities of hydrogen desorption from {110}-defect sites in the absence and presence of deposited Sn, respectively. This analysis of ad-atom coverage did not consider the stoichiometry between heteroatoms attached on the surface and the Pt atoms at defect sites, *i.e.*, the absolute coverage of Sn ad-atoms. However, in the case of Sn at Pt(111), Rizo *et al.* [76] estimated that each Sn ad-atom blocks three Pt(111) sites.

Figure 3.2 shows a series of cyclic voltammograms corresponding to the unmodified and Sn-modified Pt(111)-32 electrodes in 0.1 M $HClO_4$ solution. For the unmodified Pt(111)-32 electrode (black line), the charge density corresponding to the feature at 0.13 V was ~47.2 μC cm^{-2}, equivalent to Q_{Pt}^{H}. After partial blockage of {110}-defect sites by Sn ad-atoms, the charge at this feature decreased to ~31.2 μC cm^{-2} ($Q_{Pt,Sn}^{H}$), corresponding to $\Theta_{Sn}^{Defects}$ equal to 0.34 (red line). For another Sn partial deposition, the charge density was ~21.6 μC cm^{-2}, corresponding to $\Theta_{Sn}^{Defects}$ equal to 0.54 (green line). Figure 3.2 also shows a higher Sn coverage $\Theta_{Sn}^{Defects}$ equal to 1.0 (blue line), which corresponds to the case where the {110}-defect sites were fully occupied, evidenced by the total suppression of the feature at 0.13 V.

Figure 3.2. Cyclic voltammograms at 50 mV s^{-1} of unmodified and Sn-modified Pt(111)-32 electrodes in 0.1 M $HClO_4$ with different Sn coverages. $\Theta_{Sn}^{Defects}$= 0, 0.34, 0.54 and 1.0.

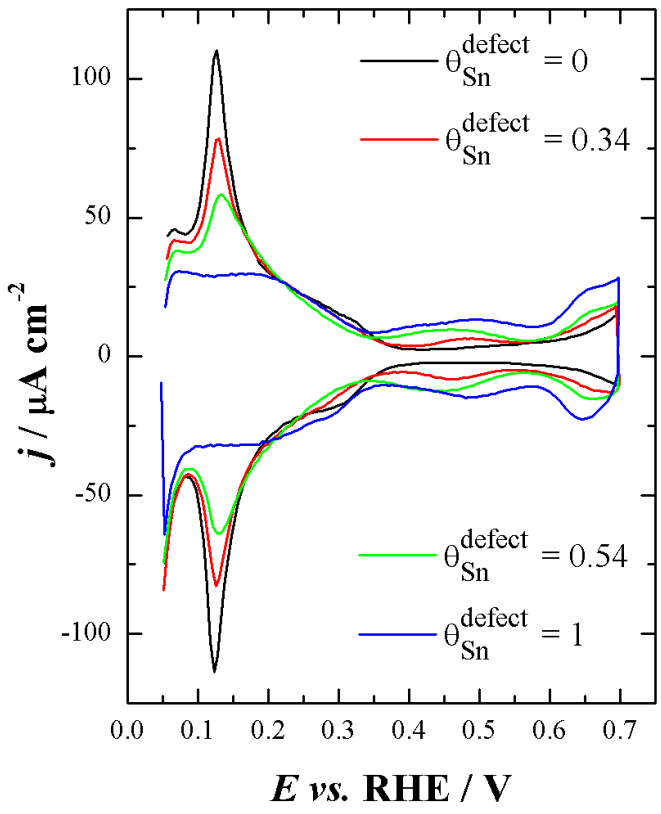

3.3.2 Ethanol electrooxidation over unmodified and Sn-modified Pt(111)-32

After the characterization of the Sn deposits on Pt(111)-32, the electrode was transferred to the cell containing ethanol to investigate the electrocatalytic activity for the different Sn-modified surfaces compared with the unmodified Pt(111)-32 one. The first and second voltammetric cycles for ethanol oxidation are presented in Figures. 3.3a and 3.3b, respectively.

The oxidation on well-ordered Pt(111) surface was carried out for the sake of completeness to compare the performance of this surface with a disordered Pt(111)-32, and with its further modification by Sn deposition. As the Pt(111) was extensively discussed elsewhere [8,13,66], here the intention is giving attention to the influence of {110} defects decorated by Sn towards ethanol electrooxidation.

Analyzing the first scan in Figure 3.3a is easy to observe that during the positive-going scan the current density for the ethanol oxidation on Pt(111)-32 surface was higher than that for the well-ordered Pt(111) surface. Barbosa *et al.* [66] have recently demonstrated that ethanol electrooxidation reaction is extremely sensitive to disordered Pt(111) surface. For example, a Pt(111) surface with a certain degree of disorder ({110}-defect density of 16.4 x 10^{13} defects cm^2), showed better electroactivity than the well-ordered Pt(111) surface, presenting lower onset potential and higher oxidation current density. In that way, the electrochemically generated random defects on initially well-ordered Pt(111) surfaces are capable to improve the performance of the ethanol oxidation reaction.

In the CV profile of Pt(111)-32, during the positive-going scan (Fig. 3a), can be seen two contributions, at 0.58 and 0.80 V, the same behavior is observed for the well-ordered Pt(111) surface, but with lower activity. As it was commented by Barbosa *et al*. [66], the formation of adsorbed poisoning intermediates, as the CO_{ads} and the hydrocarbon residues ($CH_{x,ads}$ and $COH_{x,ads}/CHO_{x,ads}$) produced by dissociative ethanol adsorption at low potential, contribute to the deactivation of the electrode and leads to a lower reaction rate.

In the case of highly disordered surface (Pt(111)-32) compared to well-ordered Pt(111) surface, the reaction onset potential is shifted ca. 0.15 V to lower values. The first peak at 0.58 V is more pronounced than the second one at 0.80 V, showing that the defects favor the kinetic of the reaction at a low potential, while for the second peak situated at 0.80 V the profile is similar for both surfaces.

Besides, the Pt(111)-32 surface showed a relatively strong hysteresis between positive and negative-going scans in the current-potential profile. This behavior is associated with the formation of strongly adsorbed species, mainly CO, that are formed on the electrode surface at

low potentials, during the positive-going scan, and as the potential is scanned to high values, close to the reverse potential, these species are oxidized. As a consequence, the active sites are released for further reaction showing an increase in the current density on the negative-going potential scan when compared with the positive-going potential scan.[8]

To assess the effect of Sn ad-atoms onto disordered Pt(111)-32 surfaces in the ethanol electrooxidation, it was chosen three Sn coverage degrees ($\Theta_{Sn}^{Defects}$ = 0.34, 0.54 and 1.0). In Figure 3.3a, it can be commented that the decoration of the {110}-type defect sites by Sn significantly increases the values of current density, in the positive-going potential scan, and also in smaller degree for the negative-going potential scan (first scan).

Figure 3.3. Positive and negative-going potential scans for the well-ordered Pt(111) and unmodified Pt(111)-32 and Sn-modified Pt(111)-32 electrodes in 0.1 M C_2H_5OH + 0.1 M $HClO_4$ solution with different Sn coverage degrees onto defect sites. v = 50 mV s^{-1}. a) First scan and b) second scan.

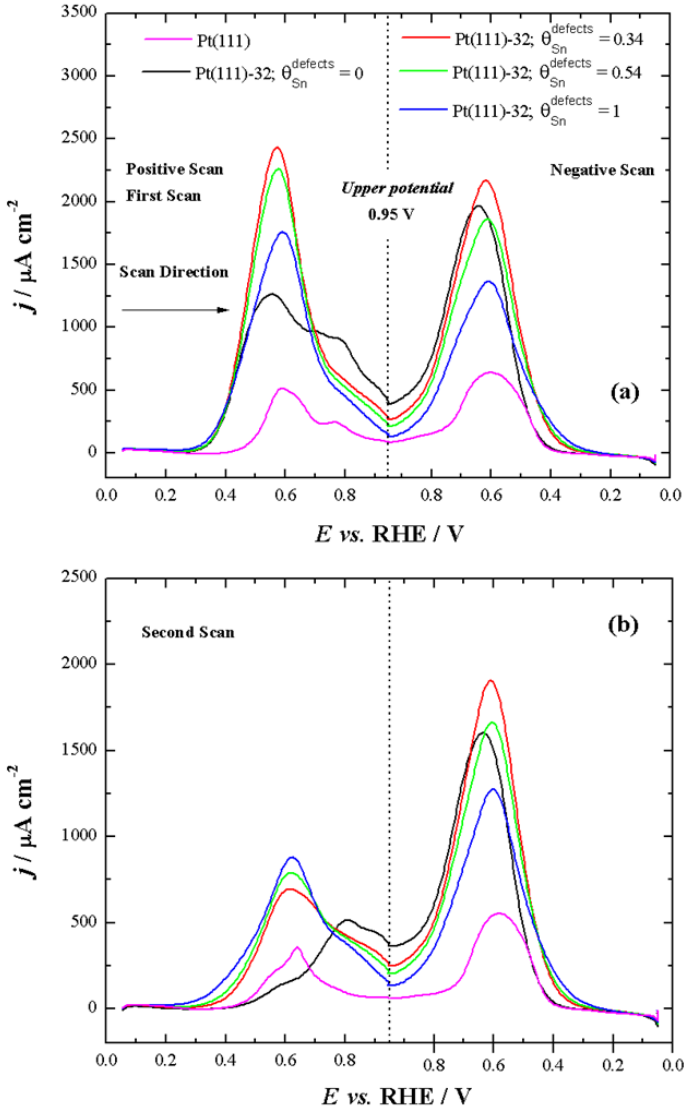

The maximum current densities (positive and negative scans) were obtained when the $\theta_{Sn}^{Defects}$ is 0.34. For the others, Sn coverage the values for the peak current densities diminish, even for the Pt(111)-32 surface with the {110}-defect sites fully occupied by Sn ad-atoms ($\theta_{Sn}^{Defects}$ = 1.0). The surface defects decorated by Sn leads not only to an increase in the currents but also to a significant alteration in the anodic profile. Previously the Sn deposition, the CV profile of the Pt(111)-32 surface displayed two oxidation peaks at ca. 0.58 and 0.80 V, however, after Sn deposition just one intense peak at ca. 0.58 V is observed in the CV profiles for the others three Sn modified surfaces.

The first oxidation peak at 0.58 V is intensified in the Sn-modified Pt(111)-32 surfaces, but the onset potential does not suffer any displacement when compared to the Sn-unmodified Pt(111)-32 surface. This indicates that the beginning of the reaction is, indeed, influenced mainly by {110}-defects sites, but as the Sn ad-atoms are deposited preferentially at {110}-type defect sites, it is suggested that the Sn ad-atoms does not affect the onset potentials and only promote fast reaction kinetics. Summarizing, the Sn-modified Pt(111)-32 surfaces presented higher peak current densities in the positive-going scan than the unmodified Pt(111)-32 surface. In other words, Sn exerts some influence in the ethanol molecules, which in turn might be close adsorbed to defects covered by Sn, or part of the ordered surface that was also modified by Sn ad-islands affecting positively the EOR.

The current-potential profiles in the negative-going scan for the Sn-modified Pt(111)-32 surfaces show only one peak centered at ~0.6 V and the peak current density follows the same trend observed in the positive-going scan. However, considering all surfaces, the trend of peak current density turns out to be different from that observed in the positive-going scans.

An interesting point to be mentioned in Figure 3.3a it is the voltammetric behavior observed in the negative-going scan for the Sn-modified Pt(111)-32 surfaces compared to the unmodified Pt(111)-32 surface. In the negative scan, each surface modified by Sn deposition shows lower peak current magnitudes than the corresponding one registered during the positive scan, while the unmodified surfaces had an opposite behavior. This fact is so positive, once the poisoning tolerance is affected when Sn is presented on the surface, in this case, it contributed considerably forming less poisoning species during the positive scan. Taking into account this remarkable effect, the modification by Sn causes important changes in the CV and this must be linked to the EOR mechanism.

From the CV profiles corresponding to the second cycle (Figure 3.3b), it is possible to observe that well-ordered Pt(111) and the Pt(111)-32 surfaces had significative changes during

the positive-going scan when compared with the first cycle (Figure 3.3a). The current density decreases for both electrodes, which the current peak contributions, previously observed in the first scan, decreased drastically. For the well-ordered Pt(111) surface, the CV profile presents one shoulder at 0.55 V and a peak at 0.64 V, this ordered surface is affected by the intermediary species formed during the first scan, decreasing the current density at ca. 60% for the peak at 0.55 V observed at the first scan. Considering the negative-going scan, observed for well-ordered Pt(111), the loss of the peak current at 0.60 V is 13% lower than that in the first scan. This fact suggests that the surface was already poisoned by strongly adsorbed species from the first scan. In this way, at the begin of the second scan, no Pt sites were available to adsorb ethanol molecule and promote new oxidation reaction, consequently, it is necessary more energy to oxidize these species, which in turn increased the reaction onset potential.

An analysis of the CV profile of the Pt(111)-32 surface in Figure 3.3b showed that the peak observed at 0.58 V, during the first scan, disappeared and remains just the peak current at 0.80 V. Also, it is observed a great deactivation, suffering an 85% loss in peak current density when compared to the first scan. This phenomenon also indicates that the surface is poisoned by species formed in the first scan and remains on the electrode surface when the second sweep starts, thus affecting the onset to more positive potentials by ca. 0.20 V. Another interesting point is that the Pt(111)-32 surface presented levels of deactivation higher than the well-ordered Pt(111), the changes in the voltammetric profile indicates that there was suppression of the main peak at 0.58 V (1st scan) and a better definition of peak at 0.80 V. It is clearly noticed that exist a relationship between electrochemically generated defects and the formation of reaction intermediates, thus, the formation of CO, CH_x, $COH_{x,ads}$/$CHO_{x,ads}$ species may occur in considerably higher quantities during ethanol oxidation on Pt(111)-32 than on well-ordered Pt(111) surface, but also those intermediate species are not easily oxidized in those disordered surfaces.

Based on the above facts, it is easy to mention the contribution towards EOR of Sn deposition onto disordered surfaces. Taking a look at the well-ordered Pt(111) and Pt(111)-32 surfaces, the shape of the CV profiles for both at the first scan (Figure 3.3a) are similar, showing two peaks contribution. However, when Sn is added to Pt(111)-32, the CV for ethanol oxidation changes drastically, in general, the current densities are increased and just one peak at 0.58 V was recorded. The peak current density for Sn-modified Pt(111)-32 ($\Theta_{Sn}^{Defects}$ = 0.34) at 0.58 V are ≈2.0 times higher than those for unmodified Pt(111)-32. This increase of the electroactivity must be linked to changes in the mechanism of the EOR, namely, the intermediates formed on

the Sn-modified surfaces are different and the reaction is selectively changed to generate possibly more acetic acid and the CO formation is suppressed.

The tin decoration of {110}-defect sites provokes an outstanding increase of current densities in the positive-going scan for all the Sn-modified Pt(111)-32 surfaces, even with the surface defects totally covered by Sn ad-atoms ($\Theta_{Sn}^{Defects}$ = 1.0).

Interestingly, the Pt(111)-32 surface with the {110}-defects completely covered by Sn ad-atoms ($\Theta_{Sn}^{Defects}$ = 1.0) is still capable to produce currents higher than the unmodified Pt(111)-32 surface. According to Del Colle *et al.* [20] , stepped surfaces completely decorated by Sn produces highest current densities and acetic acid is produced in great amounts as the major product from the EOR, while CO formation has been almost suppressed, since the step sites which are responsible to the C–C bond breaking are blocked by tin ad-atoms. Nevertheless, in the present study, the opposite behavior has been noted, once the maximum activity for ethanol oxidation for the tin modified electrodes was found for the lower studied coverage degree of 0.34. In this sense, the reaction mechanism is affected deeply by changes in the product distribution for this electrode.

Another interesting point is that tin ad-atoms are promoting the reaction also on the second scan. The disordered electrode without the Sn deposition (Pt(111)-32) showed low current density due to the high poisoning effect as already mentioned. Also, the same happens to the well-ordered Pt(111) surface. Although the currents also decay for the surfaces decorated with tin, the deactivation was considerably lower for those surfaces when compared to the others without Sn. For instance, the Sn-modified Pt(111)-32 ($\Theta_{Sn}^{Defects}$ = 0.34), which presented better electroactivity in the first scan, suffered ca. 70% of deactivation at 0.58 V. The surface with the defects completely blocked by Sn ($\Theta_{Sn}^{Defects}$ = 1.0) showed lower deactivation ca. 49%. For $\Theta_{Sn}^{Defects}$ = 0.54 electrode the deactivation is smaller than that for coverage of 0.34. Another peculiar characteristic is that the peak at 0.58 V stays unshifted for the Sn modified electrodes, which is not observed for the unmodified surfaces. This leads us to believe that the presence of tin continues to favor the oxidation of the strongly adsorbed species at a low potential, on the contrary, the bare electrode is not able to promote these oxidations.

The peak currents measured at the second cycle, in the negative-going scan, follow a different trend when is compared with those at the first scan. In the second scan, the Sn-modified electrodes presented peak current densities higher than ones obtained in the anodic scan for the same cycle. A comparison of current densities obtained from the reverse scan

between the first and second cycles showed that the deactivation is not significant as that observed for the positive scan, which a huge deactivation.

In general, the results showed in Figure 3.3 demonstrated that a disordered surface modified by tin ad-atoms leads to a positive effect over ethanol electrooxidation. The electroactivity of disordered surfaces by itself has already shown great performance when compared to well-ordered Pt(111).[66] However, this surface produces more poisoning species and, thus, it is more susceptible to deactivation at low potential specially for the second cycle onwards. Then, the Sn ad-atoms added onto the {110}-defect sites favors the electrocatalysis of these poisoning species that previously needed greater potential to be oxidized.

3.3.3 CO stripping on unmodified and Sn-modified Pt(111)-32 surfaces

The CO is an important intermediate formed during ethanol oxidation on platinum surfaces, and its formation is an indispensable part of elucidating the ethanol reaction mechanism and understanding how effective the catalyst can oxidize this molecule to CO_2.

The electrocatalytic oxidation of CO onto platinum surfaces is believed to follow a Langmuir–Hinshelwood surface reaction between adsorbed CO molecules and adsorbed oxygen-containing species [55,58,77,78], the latter species is resulting from oxidative water decomposition.

In general, the activity of the platinum electrode for CO oxidation depends on the surface structure and as well as on the number of step density.[52,55,56] The oxidation of CO onto stepped Pt(111) surfaces reveals that the potential of the stripping peak is shifted to lower values as the density of steps increases on the Pt surface.[56] Similar results were observed for the CO oxidation onto Pt(111) surfaces with electrogenerated random defects.[66] Such behavior has been reasoned on both, random crystalline defects and steps (*i.e.*, regular defects), that act as nucleation centers for the formation of oxygen-containing species, by reducing the overpotential of its formation and as such catalyze CO oxidation.[54,56,66]

Given this context, it was investigated the effect of the deposition of Sn onto electrogenerated random defects on Pt(111) surfaces towards oxidation of adsorbed CO, as shown in Figure 3.4. On all investigated surfaces, CO oxidation occurs in two distinct potential regions: i) the region above 0.60 V, which includes the main peak at 0.71 V, and ii) the region below 0.60 V which it is called the pre-peak region, whose position in the voltammogram depends on Sn coverage.

Figure 3.4. CO stripping on unmodified and Sn-modified Pt(111)-32 surfaces with $\Theta_{Sn}^{Defects}$ of 0 (a), 0.34 (b), 0.54 (c) and 1.0 (d). v = 50 mV s^{-1}.

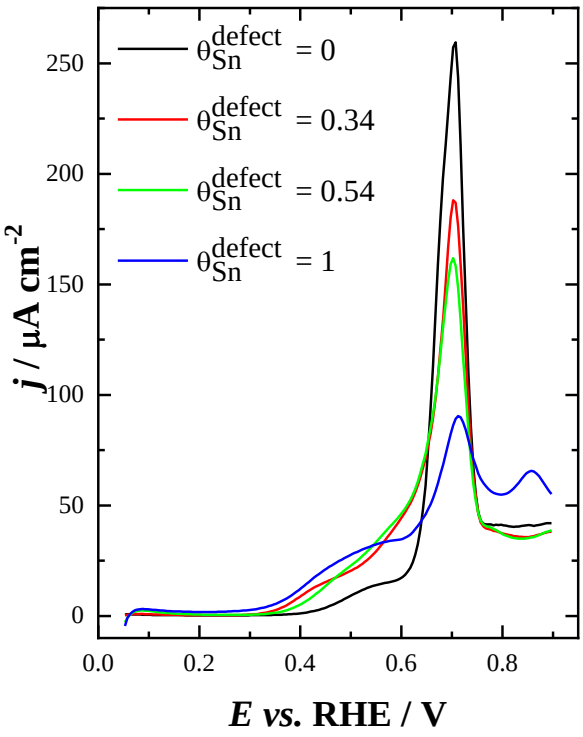

It can be observed that the main peak intensity of the CO oxidation decreases as the {110}-defects sites are being decorated by Sn ad-atoms. This behavior suggests that the decoration of the {110}-defect sites by Sn ad-atoms prevents the CO adsorption on these same sites and, consequently, reduces the charge of CO oxidation on these Pt sites (*i.e.*, CO is oxidized mainly on Sn "free" defect sites).

It is important point out that different from the stepped surfaces modified by tin [79], where there is a clear relationship between tin coverage and the main CO oxidation peak displacement to more negative potentials, herein, no changes were observed in respect to the position of the main CO oxidation peak at 0.71 V, indicating that the CO depletion of Sn-modified Pt(111)-32 surfaces is different from the stepped one after tin deposition.

Another point to highlight is that the pre-peak current densities increase and its potential, progressively, shifts to more negative values with the addition of Sn. This resulted suggests that the CO oxidation at a low potential is favored when Sn ad-atoms are present onto {110}-defect sites of the Pt(111)-32 surfaces. In that way, the CO probably is oxidized by adsorbed OH species formed at low potential through a bifunctional mechanism and, thus, the enhancement in the activity for CO oxidation can be explained by the fact that Sn provides oxygenated species at more negative potentials compared with the unmodified Pt(111)-32 surface, where the water adsorption occurs at higher potentials.[76] As proposed by Farias *et al.* [79], the CO oxidation

observed in the pre-peak occurs at terrace atomic row adjacents to the steps of Sn_{steps}/Pt(hkl) surface, however, this is not clear in the Figure 3.4.

Table 3.1 displays the values of total electrical charge density corresponding to the area of CO desorption (pre-peak + main peak) from CV profiles in Figure 3.4. According to values, the CO oxidation charge decrease as Sn is added onto defect sites on the Pt(111)-32 surface, by going from 338.5 to 250 μC cm^{-2} for the unmodified surface and the surface with highest Sn coverage degree ($\Theta_{Sn}^{Defects}$ = 1.0), respectively. On the other side, the behavior of the pre-peak electrical charge density increases with the addition of Sn. For the unmodified Pt(111)-32 surface the pre-peak charge is ca. 21 μC cm^{-2}, while for Sn-modified Pt(111)-32 surfaces the pre-peak charge is about 120 μC cm^{-2} for all the Sn coverage degrees. This clearly shows that the CO oxidation on the terrace sites occurs catalytically close to the random defect sites on the Sn-modified Pt(111)-32 surface.

Table 3.1. Total electrical charge densities from CO stripping (pre-peak + main peak) of the unmodified and Sn-modified Pt(111)-32 surfaces.

Sn coverage degree	**Charge values (μC cm^{-2})**
0	338.5
0.34	308.0
0.54	283.5
1.0	250.0

Returning to the ethanol oxidation discussed in section 3.3.2, the lowest surface deactivation for the electrode with $\Theta_{Sn}^{Defects}$ = 1.0 (Fig. 3b), should be in part associated with the ability of this electrode to oxidize CO_{ads} at a lower potential than those observed for the other surfaces, as shown in Figure 3.4.

In the CO stripping experiments discussed above, the entire CO adlayer was stripped at once in a single potentiodynamic sweep and, thus, it is not able to get information regarding the surface sites liberated after CO oxidation in the pre-peak. Based on that, experiments changing the upper potential limit of the cyclic voltammogram were done to observe the type of sites released after progressive oxidation of the CO ad-layer by shifting successively the upper potential limit of the voltammetric scan to more positive values.

Figure 3.5a shows the results of the CO stripping on an unmodified Pt(111)-32 surface. Herein the upper potential of the cyclic voltammogram was progressively changed from 0.4 to 0.95 V, in steps of 0.05 V, during each potential excursion the surface adsorbed CO was successively oxidized partially up to full oxidation at higher upper limit potentials. The same

procedure was extended to the Sn-modified Pt(111)-32 surfaces, in this case for convenience was chosen a Sn coverage degree of 0.67 to analyze the behavior of {110}-defect sites partially decorated by tin and at the same time having {110}-defects sites available to CO adsorption.

The CO starts to be oxidized at 0.40 V (see inset in Figure 3.5a), it is possible to see the beginning of a small oxidation current contribution and reaching a maximum at 0.70 V. After this voltammetric potential excursion, still remain some adsorbed CO onto the surface and, finally, it is fully oxidized at 0.75 V. In addition, the CO stripped out at 0.70 V releases Pt active sites that in turns allow the adsorption/desorption of hydrogen onto {110}-defects and at 0.13 V it can be seen in the cathodic region (orange line).

According to these results, firstly, the (111) terrace sites are released cycle by cycle up to 0.70 V and, from this point, the peak assigned to the hydrogen adsorption on {110}-defects appears at the cathodic region. Once the potential is swept up to 0.75 V, a small current contribution remains showing that a small fraction of CO is adsorbed onto {110}-defects, above of this potential, the adsorbed CO is totally eliminated from the surface and the peak at 0.13 V does not change its current value.

An interesting fact also observed in Figure 3.5a it is the appearance of a small peak (shoulder) at 0.28 V after removing off the adsorbed CO at 0.75 V (Figure 3.5a, dark yellow line), which it is not seen in the CV profile of this surface before CO adsorption (Figure 3.5a, grey line). As previously mentioned (section 3.3.1), such peak has been associated with {100}-defect sites at disordered Pt(111) surfaces.[66] In this way, CO oxidation favors the regeneration of {100}-type sites with {110}-type defects already existent. This is assumed, because of the peak current at 0.13 V, assigned to {110}-defects, that does not return to its original peak current value registered before CO adsorption (grey line).

Figure 3.5. Successive CV profiles registered during CO stripping onto (a) unmodified Pt(111)-32 and (b) Sn modified Pt(111)-32 with $\Theta_{Sn}^{Defects}$= 0.67 in 0.1 M $HClO_4$. A blank CV profile is presented before CO adsorption for comparison. v = 50 mV s^{-1}.

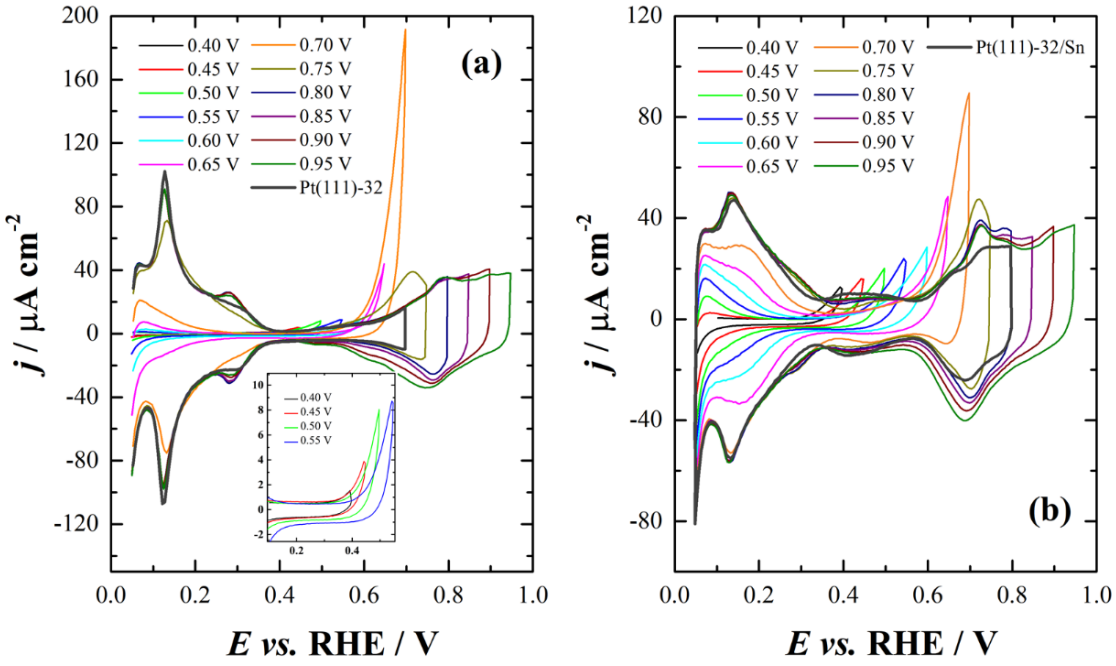

Concerns about CO stripping after the surface modification by Sn can be seen in Figure 3.5b. Herein the CO oxidation starts at 0.40 V with considerable current densities and the small current for hydrogen adsorption rises in the cathodic region as can be observed in the reverse scan (black line). This fact shows that Sn promotes the CO oxidation reaction by activating specific Pt terrace sites at low potential, namely, (111) terrace sites close to {110}-defect sites modified by Sn, once no hydrogen adsorption/desorption processes are observed at 0.13 V. Above 0.70 V (orange line), it is possible to observe in the reverse scan, the peak current for hydrogen adsorption on the terraces and at the {110}-defect sites.

The current densities continue to rise as the potential increases and reaching the apex at 0.70 V, as noted in Figure 3.5b, this current intensity is lower than that for the unmodified Pt(111)-32, since the currents obtained in lower upper potentials were higher than that for surfaces without tin, indicating that more CO was consumed in lower potentials in the presence of tin. Another assumption is that part of the surface is blocked by tin adatoms, which blocks the Pt sites for CO adsorption and posterior oxidation. At 0.72 V the peak current density belongs to CO oxidation onto defects (this peak current is more pronounced than that observed on unmodified Pt(111)-32), thus, the presence of Sn on the defect sites contributes favorably for CO depletion. The small remaining fraction of CO at 0.80 V is finally removed from the surface. Moreover, it was not observed {100}-type defects for Sn-modified electrodes, this

shows that the presence of Sn deposited on the defects contributes unfavorably to this phenomenon.

3.3.4 Identification of the reaction intermediates and products by in situ FTIR spectroscopy

In order to investigate the ethanol oxidation reaction pathways, *in situ* FTIR spectroscopy studies were performed. The assignment of observed IR bands is summarized in Table 3.2. Figure 3.6 shows a collection of IR spectra in the wavenumber region of 1200–2500 during ethanol electrooxidation on unmodified and Sn-modified Pt(111)-32 surfaces, obtained during potential steps from 0.1 to 0.95 V at intervals of 50 mV in 0.1 M $HClO_4$ + 0.1 M ethanol solution. For the purpose of better viewing, only selected spectra are shown.

As seen in Figure 3.6 a-d, bands corresponding to the production of CO_2 (2343 cm^{-1}) and acetic acid (1286 cm^{-1}) are observed for both unmodified and Sn-modified Pt(111)-32 surfaces and their intensities are dependent on surface composition. Several other bands are also observed in Figure 3.6 a-d, which demonstrate the formation of CO and partial electrooxidation products. The bands located around 2030 cm^{-1} and 1716 cm^{-1} are assigned to linearly adsorbed CO (CO_L) and the stretch vibration of the C=O bond, found for both acetaldehyde and acetic acid, while the bands at 1402 cm^{-1} and 1354 cm^{-1} are associated to the formation of adsorbed acetate.

Table 3.2. Identification of different species and their absorption band observed from the IR spectrum.

ν/cm^{-1}	**Functional group**	**Vibrational mode**	**References**
2343	CO_2	O=C=O asymmetric stretching	[13,61]
2030	Linearly adsorbed CO	C–O stretching	[8,61]
1716	COOH or CHO	C=O stretching	[13,61]
1402	Adsorbed $–COO^-$	O–C–O symmetric stretching	[13,80]
1354	$–CH_3$ in acetate	CH_3 in plane bending	[80,81]
1286	COOH	Coupling C–O stretching + OH Deformation	[8,13]

Figure 3.6. *In situ* FTIR spectra obtained for the ethanol oxidation on Sn-modified Pt(111)-32 surfaces with $\Theta_{Sn}^{Defects}$ of 0 (a), 0.34 (b), 0.54 (c) and 1.0 (d). Spectra obtained in 0.1 mol L^{-1} $HClO_4$ + 0.1 mol L^{-1} CH_3CH_2OH solution. Reference spectra taken at 0.05 V. Sample spectra collected from 0.05 to 0.95 V at intervals of 50 mV.

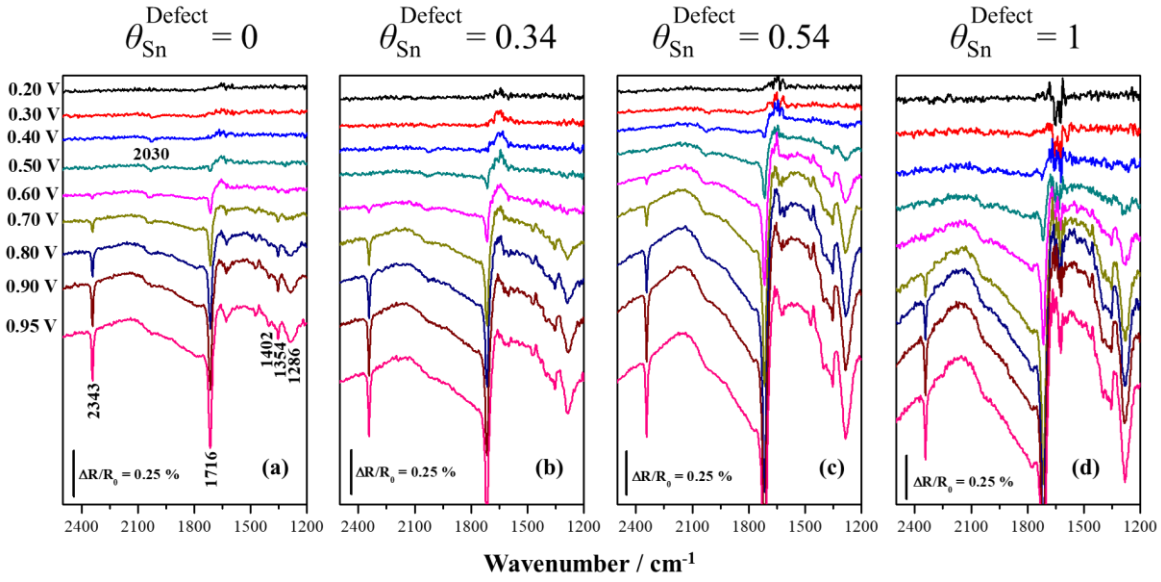

To analyze the final products of the reaction, greater attention was given to bands centered at 2343 (CO_2) and 1286 (acetic acid) cm^{-1}. In that way, the bands associated with CO_2 and acetic acid were integrated (band intensities). In all different Sn coverages the maximum band intensity for both CO_2 and acetic acid occurs at 0.95 V. However, the largest value for the band integration for CO_2 was found for θ_{Sn} = 0.54, while for acetic acid it was for θ_{Sn} = 1.0.

Thus, just for the facility of visualization, a plot of normalized band intensity as a function of potential was constructed where each maximum band intensity values for each Sn coverage value were rationed by the corresponding largest band intensity values for both final reaction products (CO_2 and acetic acid). In such a way the maximum band intensity is assumed as being 1. The resulting plots are shown in Figure 3.7 (a and b).

As can be seen in Figure 3.7a, for the unmodified Pt(111)-32 surface and the Sn-modified Pt(111)-32 surfaces with $\Theta_{Sn}^{Defects}$ equal to 0.34 and 0.54, the formation of CO_2 begins to appear at 0.6 V and its relative band intensity increases with the potential. In contrast, for the Sn-modified Pt(111)-32 surface with the defects completely covered by Sn ad-atoms ($\Theta_{Sn}^{Defects}$ = 1), the production of CO_2 starts at 0.65 V (spectrum is not shown) and, also, can be observed that the relative intensity of theses bands increases as a function of the potential.

According to Figure 3.7a is feasible to affirm that CO_2 production is favored by Sn ad-atoms on the electrode surface, is less pronounced for the Sn-modified surface with the highest

Sn coverage degree ($\Theta_{Sn}^{Defects}$ = 1). However, it is important to point out that even on this surface the amount of CO_2 formed is slightly larger than that observed for the unmodified surface over the complete range of the investigated potential.

Therefore, the highest efficiency showed by Sn-modified surfaces in forming CO_2 can be explained based on the complimentary OH species formed at lower potentials than on Pt sites, once Sn is more oxophilic than Pt. In this sense, CO species linked to (111) terrace sites neighboring to the defect sites are easily oxidized to CO_2.[58]

Figure 3.7. Band intensities as a function of the potential. (a) CO_2 and (b) acetic acid, both obtained from Figure 3.6.

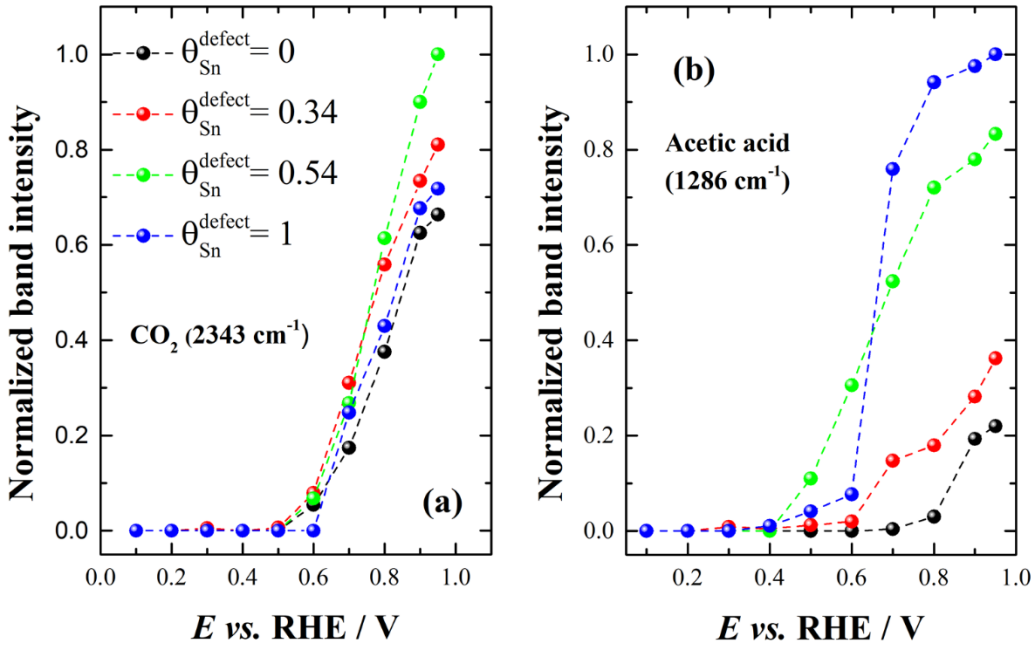

Figure 3.7b shows the integrated band intensities corresponding to the production of acetic acid as a function of the potential. The formation of acetic acid starts at high potential values (0.8 V) for the unmodified Pt(111)-32 surface. For Sn-modified surface ($\Theta_{Sn}^{Defects}$ = 0.34) is slightly anticipated at ca. 0.7 V. In contrast, for the surfaces with coverage degrees of $\Theta_{Sn}^{Defects}$ = 0.54 and 1, the formation of this reaction product is shifted to more negative potential (0.5 V). Also, it can be observed that the band intensities for the unmodified and Sn-modified Pt(111)-32 surfaces increase as the potential becomes more positive.

The comparison of the band intensities shows that the production of acetic acid is favored for the Sn-modified surfaces. Conversely to the behavior observed for CO_2, the acetic acid presents a maximum production for the surface with the higher coverage of Sn ($\Theta_{Sn}^{Defects}$ = 1).

As commented above, the band at 1716 cm^{-1} is associated with the formation of both acetaldehyde and acetic acid, while that the band at 1286 cm^{-1} corresponding to acetic acid, exclusively (Figure 3.6 a-d). Once the band at 1716 cm^{-1} starts to appear first at lower potentials concerning the band at 1286 cm^{-1} this implies that initially correspond to the majority formation of acetaldehyde. It can be observed an increase in the amount of acetaldehyde formed as the Sn coverage degree increases. Also, the onset for the formation of this species changes from 0.50 V on the unmodified electrode to 0.40 V on the Sn-modified electrode with $\Theta_{Sn}^{Defects}$ = 0.54 and 1. Based on the results presented here, as well as previously published studies, the formation of acetic acid comes from the consecutive oxidation of ethanol first to acetaldehyde and then to acetic acid.[6,8,20]

Therefore, the displacement of acetic acid band to lower potentials as well as its bigger production on Sn-modified surfaces (Figure 3.7b) might be explained by the formation of adsorbed $–(OH)_{ads}$ species on Sn ad-atoms at lower potentials, allowing that species as adsorbed acetaldehyde on the platinum catalytic sites also oxidizes to acetic acid at lower potentials, according to the bifunctional mechanism.[20,67,68] Similar behavior of the presence of Sn ad-atoms at regular defects, present in vicinal Pt(111) surfaces with steps of (110)-symmetry, on the ethanol oxidation has also been observed.[20]

To better compare the selectivity of these surfaces, a curve plotting the molar amounts (Q) of CO_2 and acetic acid as a function of the potential was constructed, Figure 3.8. For this, the band intensities (A_i) shown in Figure 3.7 were converted to molar amounts by using the effective absorption coefficients, according to the procedure suggested by Weaver *et al.* [25,82]. The values of the effective absorption coefficient, ε_{eff}, were 3.5 x 10^4 and 5.8 x 10^3 M cm^{-2} for CO_2 and acetic acid, respectively.[25] The amount (Q mol cm^{-2}) of a given species inside the thin layer cavity follows the relationship (equation 3.2):

$$Q = A_i/\varepsilon_{eff} \tag{3.2}$$

As previously described, Sn ad-atoms onto defects improve the production of CO_2 (Figure 3.7a). However, Figure 3.8 shows that CO_2 production is lower compared to acetic acid. Moreover, the production of acetic acid shows a remarkable Sn coverage-dependence compared with that of CO_2. These observations suggest that the main effect of Sn is reflected in the extraordinary increase of acetic acid production, reaching maximum values when the {110}-defect sites are quite covered by Sn.

Figure 3.8. Molar amounts of CO_2 and acetic acid as a function of the potential for each studied surface.

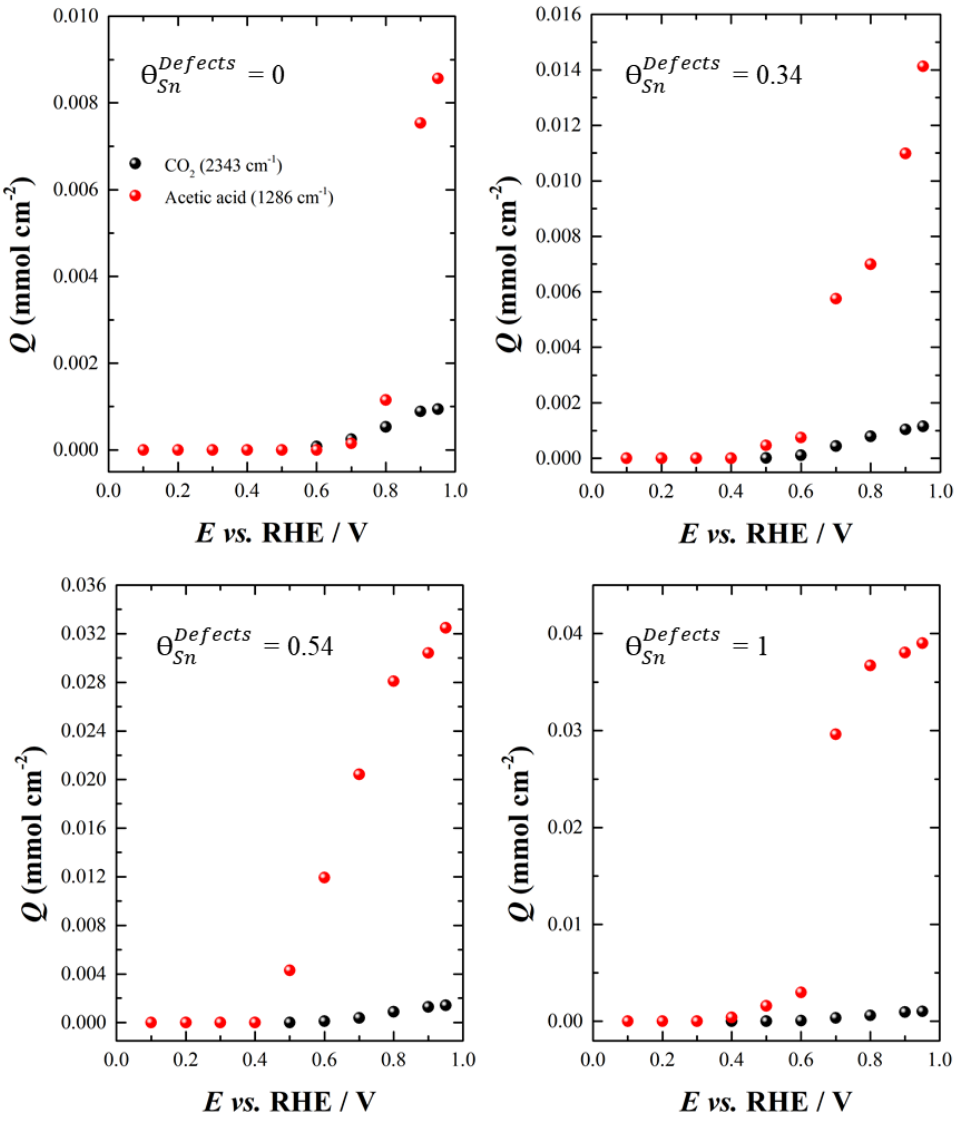

3.4 Conclusions

In this study, it was demonstrated that Sn ad-atoms preferentially deposit on {110}-defect sites electrogenerated over Pt(111) surfaces and, in this way, three different Sn coverage degrees were chosen. Voltammetric experiments of the ethanol electrooxidation demonstrated that the partial decoration by Sn ad-atoms of these defect sites leads to a considerable increase in the catalytic activity towards ethanol electrooxidation reaction, when compared with that observed for the well-ordered Pt(111) surface and disordered Pt(111) surface without tin. Among all investigated surfaces, that one with the Sn coverage degree equal to 0.34 showed

the highest electrocatalytic activity for ethanol electrooxidation, once relatively higher peak current densities (in the positive and negative scans) were achieved for this Sn coverage degree.

CO stripping experiments showed that the presence of Sn ad-atoms on the disordered Pt(111)-32 surfaces shift the onset potential of the CO oxidation to less positive potential values, *i.e.*, Sn improves the CO oxidation at low potentials. Also, defect sites decorated by Sn inhibits the CO adsorption on such sites as accompanied by the decrease of the main peak intensity value of the CO oxidation (~0.71V).

The *in situ* FTIR studies demonstrated that the main products of the ethanol oxidation are CO_2, acetaldehyde and acetic acid for all surfaces investigated. The plots of integrated band intensity corresponding to the CO_2 and acetic acid revealed that both CO_2 formation and acetic acid formation are enhanced in the presence of Sn ad-atoms on {110}-defect sites. On the other hand, CO_2 production compared to that observed for acetic acid still is very low, as revealed by the plots of the molar amount of both species as a function of the potential. Thus, the main effect of Sn is reflected in the increased production of acetic acid.

Chapter 4

Electro-Oxidation of Acetaldehyde on Pt(111) Surface Modified by Random Defects and Tin Decoration

This chapter has been adapted with permission from Springer Nature: Amaury F. B. Barbosa, Vinicius Del Colle, Bruno A. F. Previdello, Germano Tremiliosi-Filho, “Electrooxidation of Acetaldehyde on Pt(111) Surface Modified by Random Defects and Tin Decoration”, Electrocatalysis, v. 12, p. 36-44, 2021.

4.1 Introduction

Several reaction pathways are involved in the complete oxidation of ethanol to carbon dioxide which gives rise to various reaction intermediates such as carbon monoxide, acetaldehyde, and acetic acid.[8] Thus, acetaldehyde is an important reaction intermediates involved in the electro-oxidation of ethanol and represents an essential species to be considered in the discussion of the alcohol oxidation mechanism. Its interaction with metal electrode surfaces is highly relevant for understanding one of the reaction characteristics that occur in direct ethanol fuel cells (DEFCs).[6,83–85] Additionally, acetaldehyde is the smallest oxygenated molecules that contain a carbon chain.[22] Therefore, its electrooxidation can be considered a model to understand how C-C bonds can be broken in small molecules containing a methyl group.[22]

The electro-oxidation of acetaldehyde has been the object of several investigations, including the ones on pristine [86] and modified [87] platinum single crystals, Pt bulk electrodes [88] and thin films [80], Pt-based electrodeposits [89] and Pt-based supported catalysts.[90] However, for this reaction, the studies are scarce on single-crystal surfaces specially if it is considered defected surfaces or defects generated electrochemically (random defects), which normally are found in practical catalysts.

In early studies, a quantitative analysis of the potential dependent FTIR spectra obtained for the acetaldehyde oxidation, in acid medium, on Pt(111) with and without surfaces defects, allowed to infer that the main products are acetic acid and CO_2. On ordered Pt(111), small amounts of acetic acid are formed at high potentials, 0.8 V. This reaction limitation was attributed to the presence of adsorbed species. Also, adsorbed CO ($\theta \approx 0.15$) is presented as reaction intermediate that is completely oxidized at 0.45 V. The observed inhibition of acetic acid formation is less intense on disordered Pt(111) and is absent on polycrystalline platinum.[25] Oxidation of acetaldehyde was studied on Pt(111) and Pt(100) and showed a strong dependence with the surface orientation of platinum. Two parallel reaction steps were proposed, one involving adsorbed CO and species containing C2 adsorbates, all of them leading to CO_2, at potentials higher than 0.5 V. The second pathway involves the adsorbed molecular acetaldehyde being oxidized to acetic acid, probably this pathway occurs via an Eley-Rideal mechanism.[86] To understand the role of surface steps, the oxidation of acetaldehyde, in acid media, was studied on both, basal Pt (111) and Pt (110), and stepped Pt [*n*(111) x (111)] single-crystal electrodes. The electrode activities show a decrease with increasing of step density. The experimental results suggested that occur the break of the C–C bond, indicating that

acetaldehyde is the main species in which the bond is broken in the ethanol reaction mechanism. An acetaldehyde oxidation mechanism has been also proposed, where the formation of carbon dioxide and acetic acid has been included, as well as the formation of adsorbed intermediates detected by spectroscopic methods. The surface step poisoning by CO_{ads} and $CH_{x,ads}$ intermediates is rapid because of the relative facility to break the C–C bond, leading to an unfavorable effect of steps on the oxidation of acetaldehyde.[6]

Recently, Barbosa *et al.* [66] showed that the presence of random defects on Pt(111) enhances the electrocatalytic activity of ethanol oxidation, both in terms of current density as in terms of the onset potential of the alcohol oxidation. These findings are in total agreement with the studies of ethanol oxidation by Weaver *et al*.[25] In another work, Barbosa *et al*. [91] investigated the combined effect of the presence of random defects on Pt(111) and Sn deposition at submonolayer levels in the mechanism of ethanol oxidation on disordered Pt(111) Sn modified surface. In this sense, classical papers published by Shibata and Motoo [92,93] have demonstrated the use of some admetals (Ge, Sn, Sb, As, and Ru) that adsorbs oxygen in order to oxidize and enhances the acetaldehyde reaction. The authors compare the polarization curves for various electrodes at their optimum coverages for Pt electrodes having oxygen adsorbing ad-atoms species. According to the results, the enhancement of acetaldehyde oxidation depends on the number of Pt sites occupied by an ad-atom of the species and oxygen adsorbing ad-atoms. With the aid of oxygen adsorbing ad-atoms, the intermediates are oxidized fastest due to oxygen transference to them.

Considering that acetaldehyde represents an important reaction intermediate model system in the ethanol oxidation, in the present work, it was investigated the effect of random superficial defects in the acetaldehyde electrooxidation reaction on disordered Pt(111) surfaces, in perchloric acid solution. Due to the lack of systematic fundamental studies on acetaldehyde oxidation on platinum single-crystal surfaces modified with random defects, as a first approach, the experimental information obtained here were based only on traditional electrochemical techniques as cyclic voltammetry (CV) and chronoamperometry (CA). Additionally, this reaction was also investigated on disordered Pt(111) surfaces modified by tin sub-monolayer deposited over the electro-generated random defects.

4.2 Experimental section

All experiments were carried out at room temperature (25 ± 1 ºC) in a conventional three-electrode glass cell. The chemicals for solution preparation were perchloric acid (70%,

Sigma-Aldrich), acetaldehyde (99.99%, Sigma-Aldrich), and ultra-pure water from a Millipore system (18.2 MΩ cm). Hydrogen (99.999%) was used for flame-annealing treatment and nitrogen (99.999%) to deoxygenate the solution.

A reversible hydrogen electrode (RHE) and a Pt platinized foil (1 cm^2) were employed as a reference electrode and as a counter electrode, respectively. Well-defined low and high Miller index platinum single crystal planes, Pt(111), Pt(110), and Pt(554), were used as working electrodes, having geometric areas of 0.04486, 0.0511, and 0.0452 cm^2, respectively, which were prepared according to the method developed by Clavilier.[33] The experimental procedure using single crystal, thermic and cooling treatment is described elsewhere.[66]

To generate random crystalline defects on initially well-ordered Pt(111) surfaces was used the protocol presented elsewhere.[66] Briefly, well–ordered Pt(111) surface was submitted to successive voltammetric sweeps in a potential range of 0.05 – 1.3 V at 0.05 V s^{-1} in a solution of 0.1 M $HClO_4$. These repetitive sweeps, to potentials higher than 1.15 V, progressively, random superficial defects are electro-generated.[28,29,66,94] Disordered Pt(111) surfaces are denoted as "Pt(111)-X", where "X" is an indication of the number of potential cycles between 0.05 and 1.30 V.

Tin deposition on well-ordered and disordered platinum surfaces was carried out by cycling the electrode in solutions containing 10^{-6} M $SnSO_4$ + 0.1 M $HClO_4$ at the potential range between 0.05 and 0.70 V at a scan rate of 0.05 V s^{-1}, as described elsewhere.[91] After the modification of Pt(111)-X surface by Sn, integrated charges were calculated through the peak at 0.13 V to obtain the percentage of {110}-defects covered.

Voltammetric and chronoamperometric curves were recorded with an Autolab Pgstat 302 potentiostat. The voltammetric sweeps were recorded in the electrolyte solution containing the acetaldehyde in a potential range of 0.05–0.95 V at 0.05 V s^{-1}. The chronoamperometric experiments were done similarly as described elsewhere.[8,12,66] , preceding the application of the potential of interest on the electrode, it was subordinated to a pre-treatment, in which two conditioning potentials were applied. The intension of this protocol was to clean the surface from adsorbates that come from the acetaldehyde electro-oxidation. The potential program for the chronoamperometric experiments is presented in reference.[66] Chronoamperometric data were collected for 600 s with a time resolution of 0.1 s in each potential of interest, performing potential steps of 0.1 V from 0.5 V up to 0.9 V. Before each experiment the electrodes were polarized at 0.050 V for 20 s, this procedure was necessary in order to reach a constant value of current.

4.3 Results and Discussion

4.3.1 Voltammetric studies

Figure 4.1 (a) and (c) present the anodic voltammetric profiles (1st and 5th scans at 50 mV s^{-1}) of acetaldehyde electrooxidation in acid media for well-defined and defected surfaces. At low potential, the increase of current density, due to the hydrogen adsorption/desorption process, is almost identical when compared to the acetaldehyde free electrolyte solution, with the exception for Pt(554) and Pt(111)-16 surfaces, where this region is a bit uncharacterized.

Remembering that acetaldehyde already at low potential competes for platinum sites with concomitant displacement of adsorbed hydrogen. Thereafter between 0.3 – 0.5 V the current is constant for all surfaces, herein acetaldehyde forms strongly adsorbed species onto the surface and, which, remain strongly linked to surface until being oxidized at higher potentials.

For Pt(111), during the positive-going scan, is observed a significant peak current at *ca*. 0.70 V assigned to the oxidation of species strongly adsorbed at lower potentials. The Pt(554) surface is a combination of 10 atom-wide (111) terraces and (110) monoatomic steps. In this case, the electroactivity decreases compared to Pt(111), and a similar oxidation effect is observed. An analysis of other surfaces has demonstrated a peculiar behavior dependent on the specific surface crystallographic arrangement. For example, the disordered surfaces only show some limited activity at high potentials and do not present a clear peak current. It is observed only a current increase at potentials over 0.6 V. Pt(111)-16, among all defected surfaces studied (Pt(111)-4, Pt(111)-8 and Pt(111)-32), presented the better electroactivity, as can be seen in the CVs (Figures 4.1 and A2.1). The disordered Pt(111)-16 surface has 28% of {110}-defects. For Pt(110), the performance observed, at the 1st scan, was very close to the observed for Pt(111)-16 surface. Therefore, the results obtained for the 1st scan suggest that the presence of step density or {110}-defects sites impacts negatively in acetaldehyde oxidation currents. A careful analysis of the 5th scan (Figures 4.1 (c) and (d)) has demonstrated the surface deactivation for all studied surfaces.

Table 4.1 shows the maxima current density measured at the anodic peak potential, for Pt(111) and Pt(554), or at a potential of 0.9 V for defeted surfaces (where no peak current is observed) registered during the first and the fifth voltammetric cycles, results obtained from the voltammetric profiles of the Figures 1 and A2.1. The percentage of deactivation, calculated from the percentual diminution of the peak current density between the one for the first and the

one for fifth cycles. The values obtained demonstrate the following order of deactivation: Pt(111) > Pt(554) > Pt(110) and Pt(111)-16.

Figure 4.1. CVs of acetaldehyde electrooxidation (0.1 M + 0.1 M $HClO_4$) onto Pt(111), Pt(111)-16, Pt(554) and Pt(110), (a);(b) and (c);(d) represent the 1st and 5th Scan, respectively. ν = 50 mV s^{-1}.

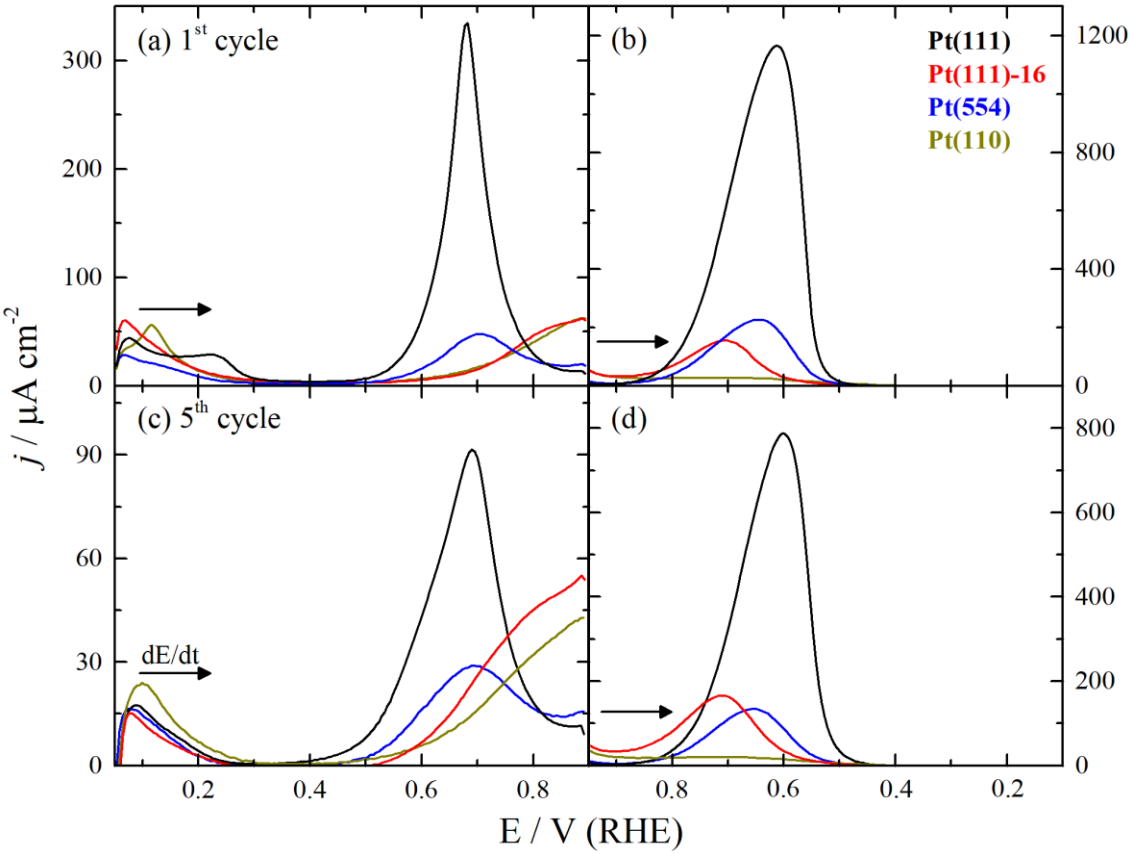

Table 4.1. Maximum current densities, j_p^1 and j_p^5, for the first and fifth cycles and deactivation obtained from the CV profiles of the acetaldehyde electrooxidation on the platinum electrodes.

Surface	**CV profiles**		
	j_p^1 (µA cm^{-2})	j_p^5 (µA cm^{-2})	% Deactivation
Pt(111)	334	91	73
Pt(111)-4	22	19	13.5
Pt(111)-8	29	23	20.5
Pt(111)-16	62	55	11
Pt(111)-32	57	44	23
Pt(110)	63	42	33
Pt(554)	47	29	38

Although Pt(111) showed considerable reactivity in the CV, its deactivation is relevant, indicating the progressive formation of adsorbed species that poison the surface, while, a disordered surface having low performance for acetaldehyde oxidation presents only ca. 11% of deactivation, as can be seen in Table 4.1.

Another interesting characteristic is that Pt(111)-16 showed an increase of current density at 0.70 V throughout the cycles, at the same potential where it is observed the highest current for Pt(111). At a first glance, a well-defined surface as Pt(111) exerts positive influence over the reaction mechanism of acetaldehyde oxidation promoting the split of C–C bond at potentials between 0.3 – 0.5 V where it is formed strongly adsorbed species. Nevertheless, at potential over 0.5 V Pt(111) favors the CO_2 pathway by oxidizing the adsorbed intermediates at the first cycle. Progressively, this surface loses partially this capacity to oxidize the adsorbed poisoner, and consequently, the peak current at 0.7 V diminishes by cycling the potential. On the other hand, a disordered surface as Pt(111)-16 is completely blocked at low potential by species strongly adsorbed, such as CO and CH_x, that are only partially oxidized above of 0.50 V. By cycling the electrode potential, slowly the activity of the disordered surface increases. The Pt(554) single crystal was added in this study just to observe the influence of regular stepped surface over acetaldehyde electrooxidation and at the same time establish a relationship with {110}-defects.

The addition of monoatomic (110) steps on (111) terraces, decreases the current of the main peak at 0.70 V when compared with the basal Pt(111) electrode. This is an indication that (111) terrace sites are more active than the (110) step sites. The charge separation between the top and the bottom of steps governs the CO adsorption strength, where the CO adsorbed on steps, is considered a poison, while on the terrace sites function as an active intermediate. Therefore, there is a clear balance between species suffering reactions on (111) terrace sites, favoring the oxidation kinetics of adsorbed intermediates, and those over (110) strongly bonded, deactivating the surface. Pt(110) exhibits the smallest activity among all studied surfaces.[59]

The reverse scan for the 1st and 5th cycles (Figures 4.1 (b) and (d)) reveals that the currents are much higher than those observed for the positive scans (compare with Figures 4.1 (a) and (c)), the current density values can be seen on the right-hand axis. As was observed for ethanol electrooxidation reaction, the hysteresis effect is linked to acetaldehyde decomposition.[66] The hysteresis between positive and negative-going scans depends on the surface structure, for ethanol electrooxidation it was observed [66] as the density of defects increases the hysteresis becomes higher for defected electrodes. However, for the acetaldehyde

reaction, the effect is quite the opposite, in which random defects produce a lower current density when compared to the well-defined surface Pt(111). Possibly, the {110}-defects promote the pathway in which favors a great number of intermediates strongly adsorbed such as CO and CH_x onto the surface. Although the Pt(111)-16 presented the lowest peak current density in the first negative scan, as can be observed in Figure 4.1b, in the subsequent cycles (Figure 4.1d), the onset potential is slightly displaced for less positive values and the peak current increases. This phenomenon is interesting because show us that a certain amount of defects (28 % of {110}-defects on {111}) is capable to oxidize species strongly linked to the surface at low potential. This could be the reason that the surface seems to be activated along the cycles. The same effect in not observed for well-defined surfaces as Pt(111) and Pt(554), where the reactivity decrease progressively with the voltammetric cycles and, for Pt(110) is not observed electroactivity (see Figure 4.1d).[66]

4.3.2 Chronoamperometric studies

The chronoamperometric experiments were carried out in order to analyze the electrochemical behavior of acetaldehyde reaction in short and long times. Short times give us a picture of intrinsic current at "zero time" as a way to obtain the activity of the electrodes in the absence of intermediates strongly adsorbed as well as comparing the characteristic time of CVs, long time transients is enough to achieve a "quasi" steady-state current, and evaluate the surface deactivation. Figure 4.2 shows the current density, where the last point was collected, from each chronoamperometric curve for five potentials at different times.

The results obtained at 0.1 s reveals that at 0.5 V, Pt(111) has the highest current density among all surfaces, this behavior might be assigned to the capacity of this surface in producing species in which release more electrons during its oxidation. Rodríguez *et al*. [86] have reported that at 0.60 V, CO_2 is the major product formed, and acetic acid is irrelevant up to 0.80 V, then the high current for Pt(111) might be attributed to the oxidation of adsorbed CO or CHx. From Figure 4.2, at 0.6 V, the electroactivities are close to each other, showing a different effect of that observed at 0.5 V. Above this potential, the Pt(111)-16 showed better values of current densities, in this case, it seems that a certain degree of {110}-defects contribute to promote the acetaldehyde oxidation reaction.

Analyzing the curves at 0.5 s, the profile is practically similar to 0.1 s, but the currents are smaller than those observed at 0.1 s, once the surface has already been partially blocked by the strongly adsorbed intermediates and close to the situation reached in the negative-going

scan of the CV. Above 0.50 V, Pt(554) and Pt(111)-16 presented better responses at 0.60 and 0.70 V, respectively. For both times, there is a maximum at 0.60 V and then a decay up to 0.90 V. Curiously this event coincides with the studies carried out by our group [66], which it was observed a similar trend oxidizing ethanol using well-defined and defected surface. Moreover, differently of CVs, the transients measurements in short times have revealed that disordered surface, although showed low performance during CVs, has demonstrated to be more active, from 0.70 V, surface than Pt(111) and Pt(554).

For long term experiments (600 s) the profiles are different concerning the maxima current density. Herein, the results depict, somehow, the voltammetric behavior (Figure 4.1 (a)), in which the prominent current density is located at 0.70 V, while for short times measurements the values were at 0.60 V. A stepped surface, Pt(554) reached better current density followed by Pt(111)-16 and Pt(111), respectively.

Figure 4.2. Current densities measured at potentials collected in the chronoamperometric experiments at different times (a) 0.1; (b) 0.5 and (c) 600 seconds for the following surfaces: Pt(111), Pt(111)-16, Pt(554) and Pt(110). Dotted lines connecting the data are just for visual aid.

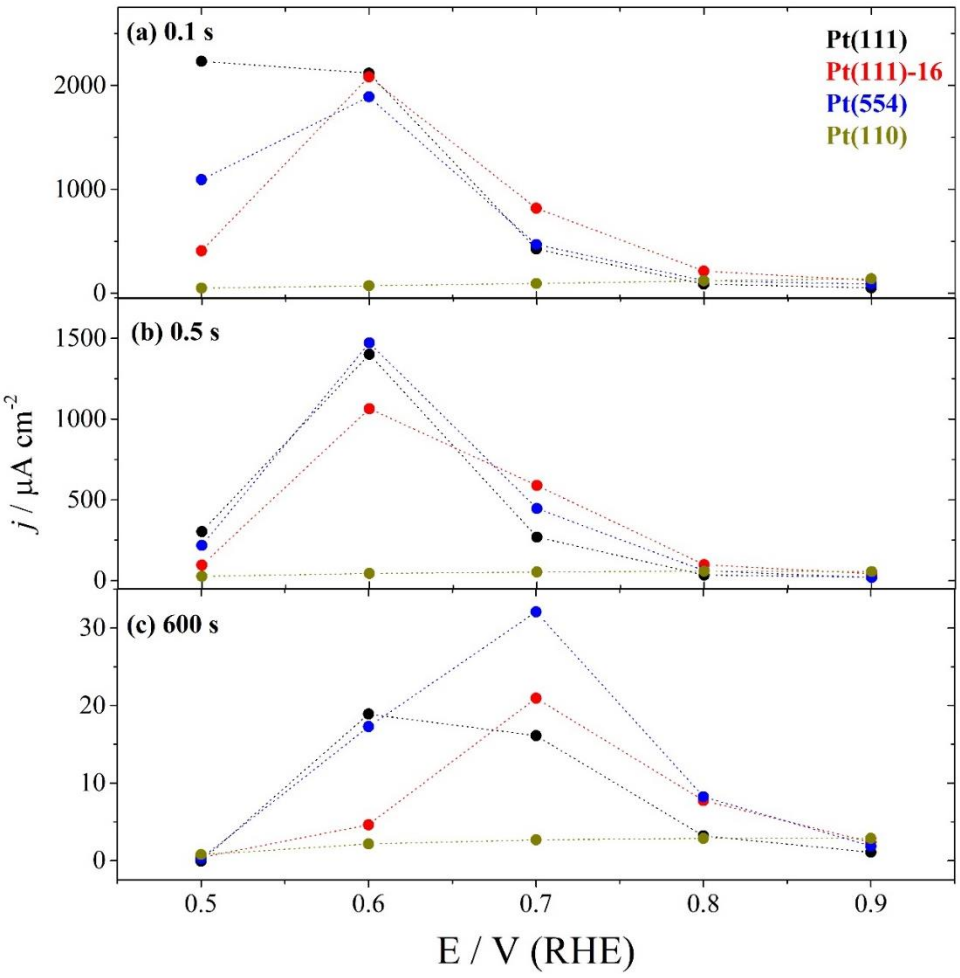

The difference between the currents obtained in short times is reflected by the poisoning rate of the surface because of fast drop and attain "quasi" steady-state currents since many competing processes including the formation of strongly adsorbed intermediates block the surface and slowly deactivate the electrode. Taking into account the CVs (Figure 4.1 (a)), the (110) step density suggests a quantitative and cumulative effect of steps in the deactivation of the oxidation of acetaldehyde. It is important to remember that anion effect causes interferences over the electrode performance, for ethanol electrooxidation the addition of (110) steps improves the activity, since the monoatomic steps disfavor the anion adsorption and its existence changes the chemical properties of the (111) terraces favoring activation of the reaction pathway for CO_2 formation.[6,19,20] Interestingly, acetaldehyde has an opposite trend, some results using sulfuric acid suggest that increasing (110) steps, the surface presented a smaller effect on oxidation currents than is the case for ethanol. The effect of the anion adsorption is preferential on large terraces rather than steps as is the case of (bi)sulfate, then acetaldehyde molecules compete at the same time for the adsorption process. If a poorly adsorbed anion like perchlorate is present, the acetaldehyde will be adsorbed preferentially on the (111) terraces than on surfaces with narrow terraces and, as consequence, the reaction is favored.[6] However, transients measurements have demonstrated a better activity for Pt(554) when compared to Pt(111) above of 0.60 V. For 0.5 and 600 s which it would represent a situation where the surface has already been partially or completely blocked by the strongly adsorbed intermediates the stepped and defected surfaces seem to be more active in oxidizing these species than a surface composed by long (111) terraces. Lai *et al.* [6] have observed similar effects for Pt(15 15 14) and Pt(554), which these surfaces have 30- and 10-atom-wide terraces, respectively. However, the authors noted different behavior for sulfuric acid, indicating that mechanism is altered by anion adsorption and maybe a combined step density versus anion adsorption, favoring a route more efficient for these surfaces. Finally, the Pt(110) for all times and potentials studied showed to be very inactive for acetaldehyde oxidation.

4.3.3 Voltammetric studies of Pt(111)-Sn

After studying the contributions of bare platinum towards the acetaldehyde electrooxidation reaction, we have analyzed the influence of tin (Sn) submonolayers over Pt(111) and Pt(111)-16. The Figure 4.3 presents the modification of Pt(111) by Sn adatoms in three coverages degree: 0.33, 0.40 and 0.75 ML.

Figure 4.3. CVs ((a);(b), 1st and (c);(d), 5th Scan) of acetaldehyde electrooxidation (0.1 M + 0.1 M $HClO_4$) on unmodified and Sn-modified Pt(111): $\theta_{Sn}^{(111)}$= 0.33; $\theta_{Sn}^{(111)}$= 0.40; $\theta_{Sn}^{(111)}$= 0.75. v = 50 mV s^{-1}.

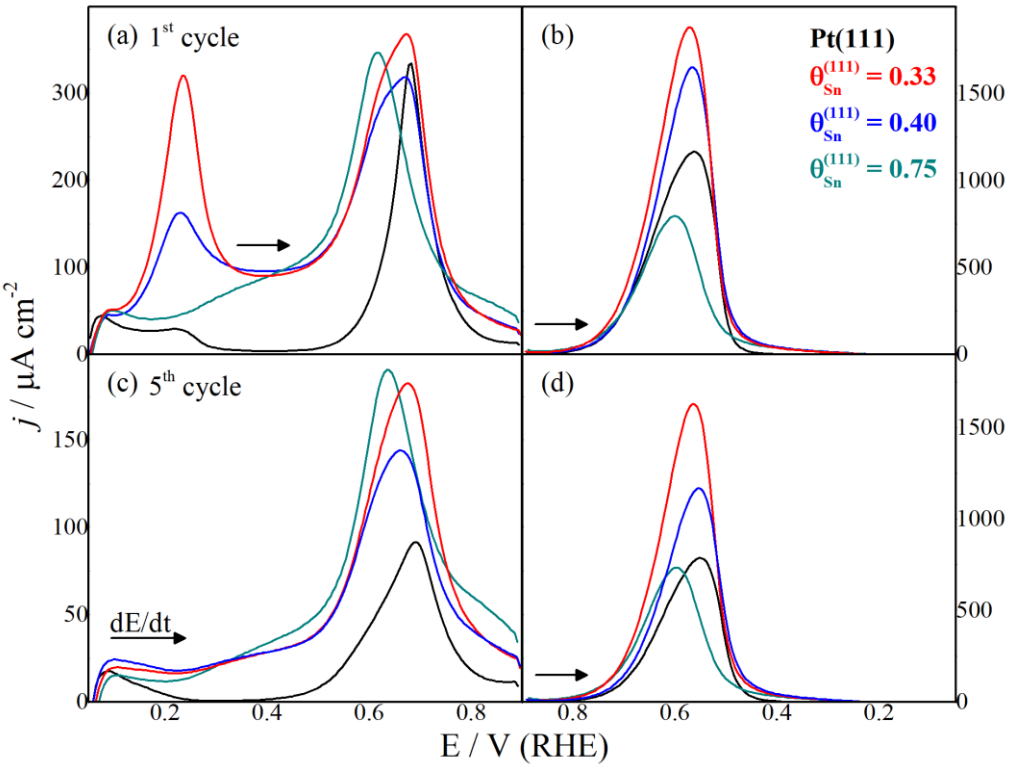

From an analysis of anodic profiles (Figure 4.3 (a)), it is possible to note how the behavior of acetaldehyde oxidation is affected by the presence of Sn on (111). Tin coverage degree of 0.33 ML presents at lower potential an intense peak, at 0.23 V, where normally no contribution is observed for bare Pt(111) (black line). Remembering that in this region the hydrogen competes with acetaldehyde oxidation process, however, the hydrogen desorption prevails, since no peak is observed for acetaldehyde oxidation. Interestingly the Sn addition can oxidize species formed at low potential where Pt is not able to promote the reaction. But this peak diminishes as the amount of Sn increases and is practically negligible for 0.75 ML. This effect must be associated with weakening the interaction property between Sn-Pt, since the expected Sn deposition follows a Volmer–Weber growth mode due to the used protocol.[95] The only peak observed for Pt(111) at 0.68 V is enlarged and displaced to more negative potentials with the Sn presence, the hysteresis effect during negative-going scan (Figure 4.3 (b)) is more pronounced than for Pt(111), with the exception for 0.75 ML. Commenting on the existence of the first peak, its oxidation might be associated with species other than carbon monoxide, once CO formation starts at *ca.* 0.35 V.[86] Also, the fact that its appearance occurs only in the first cycle, observe the (Fig. 3(c)), leads us to believe that it is associated with partial

poisoning of the surface that is generated at the initial potential (0.050 V), this procedure takes some time (20 s).

It is known that Sn promotes a better performance for small organic molecules, for instance, ethanol has more reactivity onto Pt(*hkl*)/Sn than Pt(*hkl*), in this case, the coverage degree of Sn depends on the crystallographic arrangement. According to Rizo *et al*. [62], Sn promoted better performance, for ethanol electrooxidation, when deposited over Pt(111) surface. The authors showed through OLEMS experiments that Pt(111)/Sn enhances the oxidation of ethanol to acetaldehyde, since the gain at onset potential, *ca*. 0.20 V, is assigned to acetaldehyde formation, while the signal for acetic acid shifts from 0.55 to 0.40 V. The CO2 signal (m/z=22) is practically absent indicating that ethanol reaction is addressed to acetaldehyde and acetic acid formation. A careful analysis of the acetaldehyde reaction on Pt(111)/Sn brings outstanding information, since bare Pt(111), belatedly, produces CO2 above 0.60 V [86] and acetic acid at to a greater extent during the reverse scan, because of this the reverse current is high as seen in the Figures 4.3 (b) and (d). The addition of Sn on Pt(111) promotes the acetaldehyde reaction, once the current densities obtained for the five cycles studied, Figure 4.3 (c) and (d), were higher, even at a low potential, than the unmodified surface. Also, the main peak at ca. 0.70 V (Fig. 1 (a)) assigned to CO_2 production is increased due to the enlargement of this peak to more negative potentials.

4.3.4 Voltammetric studies of Pt(111)-16/Sn

As observed through the cyclic voltammograms (Figure 4.1), Pt(111)-16 among all defected surfaces showed a better electrochemical response (see Figure A2.1 and Table 4.1). Recently we have studied the effect of Sn deposition over these surfaces [91] towards ethanol electrooxidation and there was a considerable increase in the electroactivity when compared with that observed for the well-ordered Pt(111) surface and disordered Pt(111) surface without Sn.

The results obtained herein demonstrated the outstanding ability of Sn enhances the acetaldehyde reaction. Figures 4.4 (a) and (b) present the first cyclic voltammogram for acetaldehyde electrooxidation on Pt(111)-16/Sn (0.73 and 0.92 ML). Just as was observed for Pt(111)/Sn, the defected surface also presented notable enhancement when modified by Sn submonolayer. The onset potential was shifted from approximately 0.53 to 0.24 V and 0.53 from 0.11 V for θ_{Sn} = 0.78 and θ_{Sn} = 0.93, respectively. Besides, another interesting point concerns to the maxima current densities attained during anodic profile (Figure 4.4 (a)), for

Pt(111)-16 the higher current is recorded at the end of the applied potential, 0.90 V, while for modified electrode, Pt(111)-16/Sn, two peaks at 0.47 and 0.68 V were observed for θ_{Sn} = 0.78 and, at 0.43 and 0.63 V for θ_{Sn} = 0.93. A comparison between the current density peaks of Pt(111)-16/Sn (θ_{Sn} = 0.93) and Pt(111)-16 show an increase of 4 times, taking into account that this value is attained at 0.43 V (first peak, green curve), i.e. with a potential difference of *ca.* 0.50 V concerning the maximum obtained for Pt (111)-16. Considering the cathodic profile (Figure 4.4 (b)), the high current densities indicate that the direct process produces strongly adsorbed species and are only oxidized at high potentials.

Figure 4.4. CVs ((a);(b), 1st and (c);(d), 5th Scan) of acetaldehyde electrooxidation (0.1 M + 0.1 M $HClO_4$) on unmodified and Sn-modified Pt(111)-16: A) $\theta_{Sn}^{defects}$= 0.73; $\theta_{Sn}^{defects}$= 0.92. *v* = 50 mV s^{-1}.

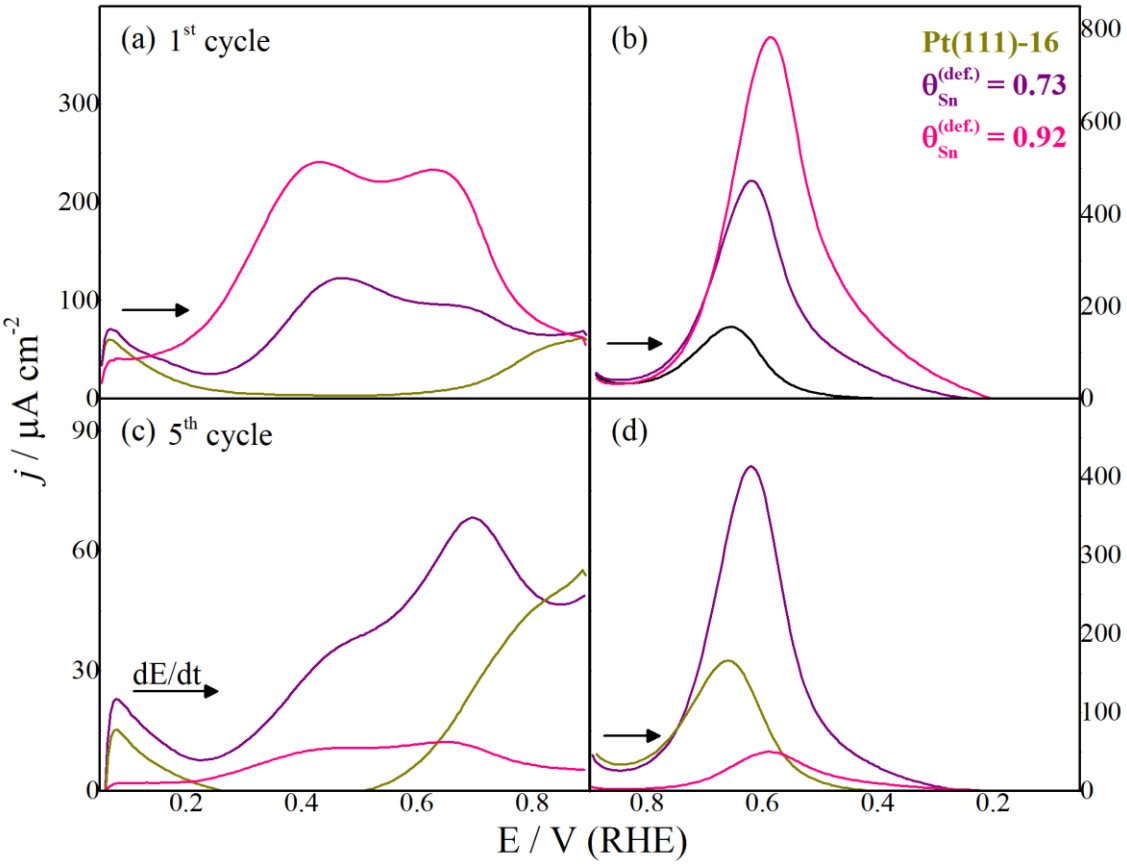

Contrary to earlier reports for ethanol [91], where an Sn coverage degree equal to 0.34 showed the highest electrocatalytic activity, a different effect is observed for acetaldehyde, where more deposited Sn over {110}-defects presents a greater performance of the electrocatalyst. An analysis of 5th scan sheds light on this issue, a huge Sn amount covering the {110}-defects seems to be effective in oxidizing vicinal species already adsorbed at low

potential and thereafter the performance of the surface falls drastically as can be seen in the 5th cycle (Figure 4.4 (c)). The last recorded cycle reveals that the second peak at 0.68 V for Pt(111)-16/Sn (qSn = 0.78) became more prominent, indicating that a probable mechanism is favored at this potential, at the expense of the first peak that is diminished.

A careful analysis of the activity of these surfaces goes through the electrochemical contribution that Pt(110) can provide us. According to Del Colle *et al.* [87], sites (110) can break the C-C bond of the acetaldehyde molecule more easily, even at potentials as low as 0.05 V. In this potential, *in situ* Fourier transform infrared spectroscopic experiments showed already related band from the COlinear. In this way, these species remain adsorbed until the platinum provides the oxygenated species (OH_{ads}) to react and remove them from the surface, although the onset of oxidation currents starts at around 0.55 V. Assuming that the random surfaces are composed by {110}-defects and, in turn, they are modified by Sn adatoms, the species formed due to C–C bond break at low potential are easily oxidized by the Sn presence. In this sense, these two contributions in the CV, at ~0.40 and ~0.65V, can be assigned to different pathways occurring on the surface, which the first peak causes the adsorbed CO oxidation and, the second one might be due to acetaldehyde forming acetic acid, respectively.[87]

Therefore, the presence of Sn onto {110}-defects acts as a promotor to enhance the surface performance at low potentials, oxidizing adsorbed species such as CO and CH_x to CO_2 as well as promote oxidation of acetaldehyde to acetic acid at high potentials. Remembering that acetaldehyde is highly sensitive to the Pt surface structure and its modification by Sn submonolayer, varying Sn amounts, automatically the mechanism of the reaction is quite affected, as can be seen through the 1st and 5th cycle (Figures 4.4 (a) and (c)).

However, some points need to be detached, taking into account ethanol reaction, Sn promotes fast reaction kinetics for defected surfaces, once the onset potential is not affected by Sn presence. Nevertheless, for Pt(111)-Sn the reaction is influenced positively by changing the onset potential to more negative potentials followed by increasing the first current peak located at 0.53 V.[62,70] Now, for acetaldehyde, the currents increase significantly at low potentials *ca.* 0.20 V, compared to ethanol, then is evident that Sn contributes not only through the bifunctional mechanism, since Sn has oxophilic character above 0.40 V, another synergistic effect, ligand effect, between Sn and Pt atoms might be the main reason for the great electroactivity. Finally, the use of Sn towards oxidation of small organic molecules, have displayed a strategy to promote the acetaldehyde oxidation reaction since bare Pt is not able to oxidize species at lowers overpotentials.

Figure 4.5 includes the CVs of the well-ordered and disordered Pt(111) Sn-modified and unmodified surfaces (an overlay of Figures 4.3 and 4.4). As can be observed, the Pt(111)-16/Sn surface does not improve the electrocatalysis of acetaldehyde oxidation as the Pt(111)/Sn does. This effect is clearly observed in Figure 4.5, especially for Pt(111)/$Sn_{0.33}$ and Pt(111)/$Sn_{0.44}$.

Figure 4.5. CVs of acetaldehyde electrooxidation (0.1 M + 0.1 M $HClO_4$) on Pt(111), Pt(111)-16 and Sn decoration surfaces; (a);(b) and (c);(d) represent the 1st and 5th Scan, respectively. ν = 50 mV s^{-1}.

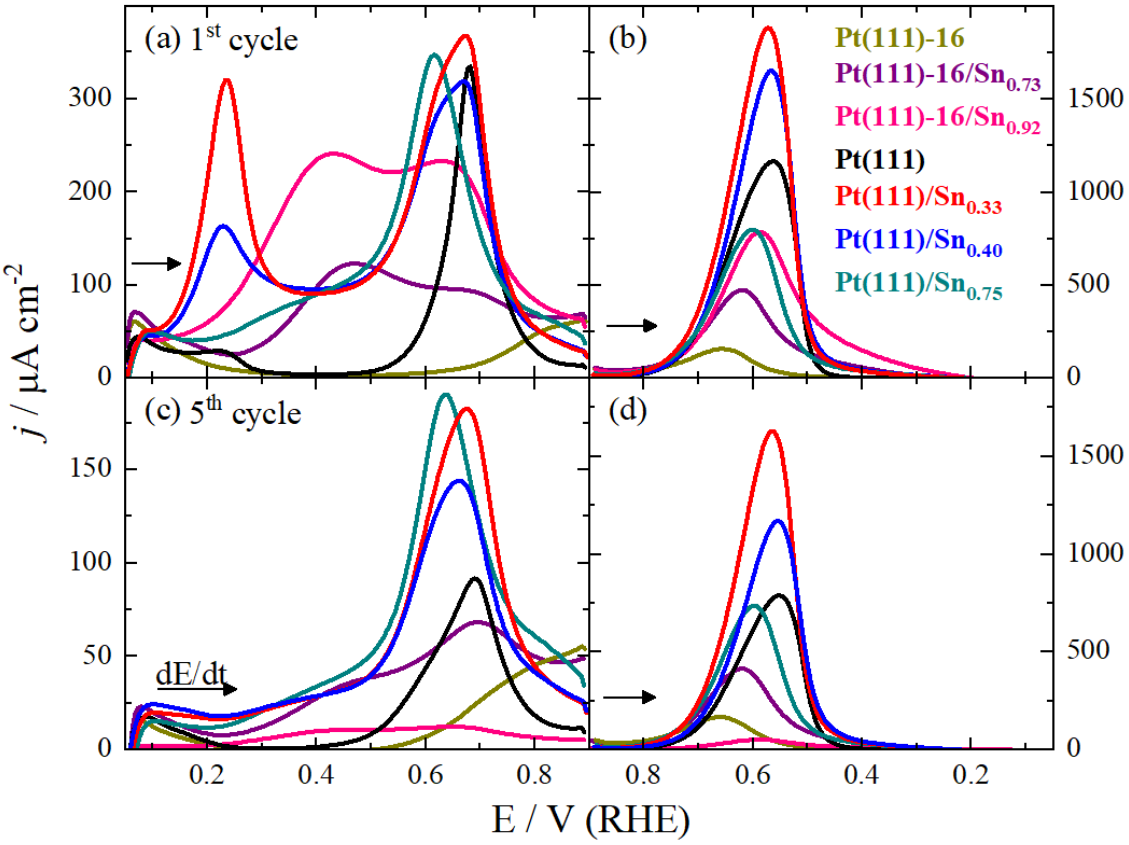

4.4 Conclusions

The present study related the acetaldehyde electrooxidation reaction using different substrates, namely, well-defined and disordered surfaces and their modification by Sn submonolayer. Well-ordered Pt(111) is more active than stepped or disordered platinum surfaces for acetaldehyde oxidation. However, the results were significantly improved and pointed out an outstanding performance when Pt(111) and Pt(111)-16 surfaces were modified by Sn. For both modified surfaces, there is an extraordinary displacement of the onset potential for more negative potentials, indicating oxidation of adsorbed species such as CO and CHx, already formed at low potentials. However, the reaction mechanism differs according to

crystallographic arrangement, (111) terraces modified by Sn adatoms are characterized by promoting the formation of species that release few electrons, namely, acetic acid. While modified surface having {110}-defects addresses the pathway to form mainly CO2 at low potentials, once that defects are capable to break the C–C bond easier than Pt(111). A second electrochemical contribution that governs the formation of acetic acid at high potentials also occurs. Therefore, Sn acts as an interesting promoter to complete the oxidation of species from the breaking of the C-C bond and mainly formed near and inside defects electrogenerated as well as to oxidize adsorbed acetaldehyde preferentially on the terraces to acetic acid.

Chapter 5

Conclusion and Perspectives

This thesis presents important insights into the mechanism of the ethanol electro-oxidation reaction on well-ordered and disordered platinum single crystal electrodes.

In Chapter 2, the ethanol electro-oxidation in acid media on a series of well-ordered and disordered Pt(111) single crystal electrodes is investigated. Electrochemical results showed that the ethanol electro-oxidation is very sensitive to the random defects electrogenerated on Pt(111) electrodes. It is found that as the {110}-type random superficial defects increase, the ethanol electro-oxidation reaction is catalyzed better, resulting at less positive onset and peak potentials values and higher oxidation peak current on disordered surfaces. FTIR results demonstrate that the main products of the ethanol oxidation are CO_2, acetaldehyde and acetic acid for all surfaces investigated. Additionally, adsorbed CO_{linear} is observed. Based on the FTIR results it is concluded that defects act to form more 2C species, like acetaldehyde and acetic acid, as well as 1C species such as CO and CH_x.

In Chapter 3, the ethanol electro-oxidation in acid media on a series of Sn-modified and disordered Pt(111) single crystal electrodes is investigated. Electrochemical and FTIR results show the combined effect of the random defects on Pt(111) and Sn deposition at submonolayer levels in the mechanism of the ethanol electro-oxidation. Voltammetric results of the ethanol electro-oxidation demonstrate that the partial decoration of {110}-type random defects by Sn ad-atoms leads to a considerable increase in the catalytic activity towards ethanol electrooxidation reaction, when compared to the well-ordered Pt(111) surface and disordered Pt(111) surface without Sn. FTIR results demonstrate that the main products of the ethanol oxidation are CO_2, acetaldehyde and acetic acid for all surfaces investigated. It is found that both CO_2 formation and acetic acid formation are enhanced in the presence of Sn ad-atoms on {110}-type random defects, but the CO_2 production compared to that observed for acetic acid still is very low. Thus, the main effect of Sn is reflected in the increased production of acetic acid.

In Chapter 4, first the acetaldehyde electro-oxidation on well-ordered Pt(111), stepped Pt(554) and disordered Pt(111) was investigated. Next, acetaldehyde was investigated on well-ordered Pt(111) and disordered Pt(111) surfaces, both modified by deposited Sn ad-atoms. Well-ordered Pt(111) is more active than stepped or disordered platinum surfaces for acetaldehyde oxidation. However, the results were significantly improved and pointed out an outstanding performance when Pt(111) and Pt(111)-16 surfaces were modified by Sn. For both modified surfaces, there is an extraordinary displacement of the onset potential for more negative potentials, indicating oxidation of adsorbed species such as CO and CHx, already formed at low potentials.

This collection of results contributes to understanding the effect of the order/disorder in monoatomic level, and so give us insights in rationalizing the choice of nanomaterials with appropriate sizes and shapes.

References

1 VIGIER, F.; COUTANCEAU, C.; PERRARD, A.; BELGSIR, E. M.; LAMY, C. Development of anode catalyst for a direct ethanol fuel cell. **Journal of Applied Electrochemistry**, Dordrecht, v. 34, p. 439–446, 2004.

2 GOSSELINK, J. W. Pathways to a more sustainable production of energy: sustainable hydrogen – a research objective for Shell. **International Journal of Hydrogen Energy**, Oxford, v. 27, p. 1125-1129, 2002.

3 LAMY, C.; LIMA, A.; LERHUN, V.; DELIME, F.; COUNTANCEAU, C.; LÉGER, J. M. Recent advances in the development of direct alcohol fuel cells. **Journal of Power Sources**, Amsterdam, v. 105, p. 283–296, 2002.

4 LAMY, C.; ROUSSEAU, S.; BELGSIR, E. M.; COUTANCEAU, C.; LÉGER, J. M. Recent progress in the direct ethanol fuel cell: development of new platinum–tin electrocatalysts. **Electrochimica Acta**, Oxford, v. 49, p. 3901–3908, 2004.

5 VIGIER, F.; ROUSSEAU, S.; COUTANCEAU, C.; LEGER, J. M.; LAMY, C. Electrocatalysis for the direct alcohol fuel cell. **Topics in Catalysis**, New York, v. 40, p. 111-121, 2006.

6 LAI, S. C. S.; KOPER, M. T. M. Electro-oxidation of ethanol and acetaldehyde on platinum single-crystal electrodes. **Faraday Discussions**, Cambridge, v. 140, p. 399–416, 2008.

7 FIERRE-VILAPLANA, A.; BUSO-ROGERO, C.; FELIU, J. M.; HERRERO, E. Cleavage of the C–C Bond in the Ethanol Oxidation Reaction on Platinum. Insight from Experiments and Calculations. **Journal of Physical Chemical C**, Washington, v. 120, p. 11590-11597, 2016.

8 COLMATI, F.; TREMILIOSI-FILHO, G.; GONZALEZ, E. R.; BERNÁ, A.; HERRERO, E.; FELIU, J. M. Surface structure effects on the electrochemical oxidation of ethanol on platinum single crystal electrodes. **Faraday Discussions**, Cambridge, v. 140, p. 379–397, 2009.

9 LAI, S. C. S.; KOPER, M. T. M. The influence of surface structure on selectivity in the ethanol electro-oxidation reaction on platinum. **Journal of Physical Chemistry A**, Washington, v. 1, p. 1122–1125, 2010.

10 KOPER, M. T. M. Structure sensitivity and nanoscale effects in electrocatalysis. **Nanoscale**, Cambridge, v. 3, p. 2054–2073, 2011.

11 BANDARENKA, A. S.; KOPER, M. T. M. Structural and electronic effects in heterogeneous electrocatalysis: toward a rational design of electrocatalysts. Journal of Catalysis, San Diego, v. 308, p. 11-24, 2013.

12 COLMATI, F.; TREMILIOSI-FILHO, G.; GONZALEZ, E. R.; BERNÁ, A.; HERRERO, E.; FELIU, J. M. The role of the steps in the cleavage of the C-C bond during ethanol oxidation on platinum electrodes. **Physical Chemistry Chemical Physics**, Cambridge, v. 11, p. 9114–9123, 2009.

13 XIA, X. H.; LIESS, H. D.; IWASITA, T. Early stages in the oxidation of ethanol at low index single crystal platinum electrodes. **Journal of Electroanalytical Chemistry**, Lausanne, v. 437, p. 233–240, 1997.

14 SHIN, J.; TORNQUIST, J. W.; KORZENIEWSKI, C.; HOAGLUND, C. S. Elementary steps in the oxidation and dissociative chemisorption of ethanol on smooth and stepped surface planes of platinum electrodes. **Surface Science**, Amsterdam, v. 364, p. 122–130, 1996.

15 WANG, J.; WASMUS, S.; SAVINELL, R. F. Evaluation of ethanol, 1-propanol, and 2-propanol in a direct oxidation polymer-electrolyte fuel cell: a real-time mass spectroscopy study. **Journal of the Electrochemical Society**, Pennington, v. 142, p. 4218-4224, 1995.

16 IWASITA, T.; PASTOR, E. A DEMS and FTIR spectroscopic investigation of adsorbed ethanol on polycrystalline platinum. **Electrochimica Acta**, Oxford, v. 39, p. 531–537, 1994.

17 LAMY, C.; COUNTANCEAU, C. Electrocatalysis of alcohol oxidation reactions at platinum group metals. *In*: Liang, Z. X.; Zhao, T. S. **Catalysts for alcohol-fuelled direct oxidation fuel cells**, RSC Energy and Environment Series, Cambridge, 2012, cap. 1, p. 1–70. https://doi.org/10.1595/147106713x671871.

18 COLLE, V. D.; SANTOS, V. P.; TREMILIOSI-FILHO, G. Comparative electrochemical and spectroscopic studies of ethanol oxidation on Pt(h, k, l) modified by osmium nanoislands. **Electrocatalysis**, New York, v. 1, p. 144–158, 2010.

19 COLLE, V.D; BERNÁ, A.; TREMILIOSI-FILHO, G.; HERRERO, E.; FELIU, J. M. Ethanol electrooxidation onto stepped surfaces modified by Ru deposition: electrochemical and spectroscopic studies. **Physical Chemistry Chemical Physics**, Cambridge, v. 10, p. 3766–3773, 2008.

20 COLLE, V. D.; SOUZA-GARCIA, J.; TREMILIOSI-FILHO, G.; HERRERO, E.; FELIU, J. M. Electrochemical and spectroscopic studies of ethanol oxidation on Pt stepped surfaces modified by tin adatoms. **Physical Chemistry Chemical Physics**, Cambridge, v. 13, p. 12163–12172, 2011.

21 WIECKOWSKI, A.; SOBKOWSKI, J.; ZELENAY, P.; FRANASZCZUK, K. Adsorption of acetic acid on platinum, gold and rhodium electrodes. **Electrochimica Acta**, Oxford, v. 26, p. 1111–1119, 1981.

22 LAI, S. C. S.; KLEYN, S. E. F.; ROSCA, V.; KOPER, M. T. M. Mechanism of the dissociation and electrooxidation of ethanol and acetaldehyde on platinum as studied by SERS. **Journal of Physical Chemistry C**, Washington, v. 112, p. 19080–19087, 2008.

23 TARNOWSKI, D. J.; KORZENIEWSKI, C. Effects of surface step density on the electrochemical oxidation of ethanol to acetic acid. **Journal of Physical Chemistry B**, Washington, v. 101, p. 253–258, 1997.

24 LAI, S. C. S.; KOPER, M. T. M. Ethanol electro-oxidation on platinum in alkaline media. **Physical Chemistry Chemical Physics**, Cambridge, v. 11, p. 10446–10456, 2009.

25 LEUNG, L. W. H.; CHANG, S. C.; WEAVER, M. J. Real-time FTIR spectroscopy as an electrochemical mechanistic probe: electrooxidation of ethanol and related species on well-defined Pt(111) surfaces. **Journal of Electroanalytical Chemistry and Interfacial Electrochemistry**, Lausanne, v. 266, p. 317–336, 1989.

26 ITAYA, K.; SUGAWARA, S.; SASHIKATA, K.; FURUYA, N. In situ scanning tunneling microscopy of platinum (111) surface with the observation of monatomic steps. **Journal of Vacuum Science & Technology A**, Melville, v. 8 p. 515–519, 1990.

27 BJÖRLING, A.; AHLBERG, E.; FELIU, J. M. Kinetics of surface modification induced by submonolayer electrochemical oxygen adsorption on Pt(1 1 1). **Electrochemistry Communications**, New York, v. 12, p. 359–361, 2010.

28 GÓMEZ-MARÍN, A. M.; FELIU, J. M. Pt(1 1 1) surface disorder kinetics in perchloric acid solutions and the influence of specific anion adsorption. **Electrochimica Acta**, Oxford, v. 82, p. 558–569, 2012.

29 JACOBSE, L.; HUANG, Y. F.; KOPER, M. T. M.; ROST, M. J. Correlation of surface site formation to nanoisland growth in the electrochemical roughening of Pt(111). **Nature Materials**, Berlin, v. 17, p. 277–282, 2018.

30 RUGE, M.; DRNEC, J.; RAHN, B.; REIKOWSKI, F.; HARRINGTON, D. A.; CARLÀ, F.; FELICI, R.; STETTNER, J. MAGNUSSEN, O. M. Structural reorganization of Pt(111) electrodes by electrochemical oxidation and reduction. **Journal of the American Chemical Society**, Washington, v. 139, p. 4532–4539, 2017.

31 FERNÁNDEZ, P. S.; GOMES, J. F.; ANGELUCCI, C.A.; TERESHCHUK, P.; MARTINS, C. A.; CAMARA, G. A.; MARTINS, M. E.; DA SILVA, J. L. F.; TREMILIOSI-FILHO, G. Establishing a Link between well-ordered Pt(100) surfaces and real systems: how do random superficial defects influence the electro-oxidation of glycerol?. **ACS Catalysis**, Washington, v. 5, p. 4227–4236, 2015.

32 FERNÁNDEZ, P. S.; TERESHCHUK, P.; ANGELUCCI, C. A.; GOMES, J. F.; GARCIA, A. C.; MARTINS, C. A.; CAMARA, G. A.; MARTINS, M. E.; DA SILVA, J. L. F.; TREMILIOSI-FILHO, G. How do random superficial defects influence the electro-oxidation of glycerol on Pt(111) surfaces?. **Physical Chemistry Chemical Physics**, Cambridge, v. 18, p. 25582–25591, 2016.

33 CLAVILIER, J.; ARMAND, D.; SUN, S. G.; PETIT, M. Electrochemical adsorption behaviour of platinum stepped surfaces in sulphuric acid solutions. **Journal of Electroanalytical Chemistry and Interfacial Electrochemistry**, Lausanne, v. 205, p. 267–277, 1986.

34 LEBEDEVA, N. P.; KOPER, M. T. M.; FELIU, J. M.; VAN SANTEN, R. A. The effect of the cooling atmosphere in the preparation of flame-annealed Pt(111) electrodes on CO adlayer oxidation. **Electrochemistry Communications**, New York, v. 2, p. 487–490, 2000.

35 HERRERO, E.; CLAVILIER, J.; FELIU, J. M.; ALDAZ, A. Influence of the geometry of the hanging meniscus contact on the hydrogen oxidation reaction on a Pt(111) electrode in

sulphuric acid. **Journal of Electroanalytical Chemistry**, Lausanne, v. 410, p. 125–127, 1996.

36 CLIMENT, V.; FELIU, J. M. Surface electrochemistry with Pt single-crystal electrodes. *In*: Alkire, R. C.; Bartlett, P. N.; Lipkowski, J. **Advances in electrochemical science and engineering: nanopatterned and nanoparticle-modified electrodes**, Wiley-VCH, Weinheim, 2017, v. 17, cap. 1, p. 1–57. https://doi.org/10.1002/9783527340934.ch1.

37 WAKISAKA, M.; ASIZAWA, S.; YONEYAMA, T.; UCHIDA, H.; WATANABE, M. In situ STM observation of the CO adlayer on a Pt(110) electrode in 0.1 M $HClO_4$ solution. **Langmuir**, Washington, v. 26, p. 9191–9194, 2010.

38 GÓMEZ, R.; CLIMENT, V.; FELIU, J. M.; WEAVER, M. J. Dependence of the potential of zero charge of stepped platinum (111) electrodes on the oriented step-edge density: electrochemical implications and comparison with work function behavior. **Journal of Physical Chemistry B**, Washington, v. 104, p. 597–605, 2000.

39 BREUER, N.; FUNTIKOV, A. M.; STIMMING, U.; VOGEL, R. In situ electrochemical STM imaging of roughened gold and platinum electrode surfaces. **Surface Science**, Amsterdam, v. 335, p, 145–154, 1995.

40 GÓMEZ-MARÍN, A. M.; FELIU, J. M. Oxide growth dynamics at Pt(1 1 1) in absence of specific adsorption: a mechanistic study. **Electrochimica Acta**, Oxford, v. 104, p. 367–377, 2013.

41 RODES, A.; EL ACHI, K.; ZAMAKHCHARI, M. A.; CLAVILIER, J. Hydrogen probing of step and terrace sites on Pt(S)-[n(111) × (100)]. **Journal of Electroanalytical Chemistry and Interfacial Electrochemistry**, Lausanne, v. 284, p. 245–253, 1990.

42 BJÖRLING, A.; FELIU, J. M. Electrochemical surface reordering of Pt(1 1 1): a quantification of the place-exchange process. **Journal of Electroanalytical Chemistry**, Lausanne, v. 662, p. 17–24, 2011.

43 SOUZA-GARCIA, J.; ANGELUCCI, C. A.; CLIMENT, V.; FELIU, J. M. Electrochemical features of Pt(S)[n(110) × (100)] surfaces in acidic media. **Electrochemistry Communications**, New York, v. 34, p. 291–294, 2013.

44 MOSTANY, J.; HERRERO, E.; FELIU, J. M.; LIPKOWSKI, J. Thermodynamic studies of anion adsorption at stepped platinum(hkl) electrode surfaces in sulfuric acid solutions. **Journal of Physical Chemistry B**, Washington, v. 106, p. 12787–12796, 2002.

45 WAKISAKA, M.; ASIZAWA, S.; UCHIDA, H.; WATANABE, M. In situ STM observation of morphological changes of the Pt(111)electrode surface during potential cycling in 10 mM HF solution. **Physical Chemistry Chemical Physics**, Cambridge, v. 12, p. 4184–4190, 2010.

46 CLIMENT, V.; FELIU, J. M. Thirty years of platinum single crystal electrochemistry. **Journal of Solid State Electrochemistry**, New York, v. 15, p. 1297–1315, 2011.

47 BUSÓ-ROGERO, C.; GROZOVSKI, V.; VIDAL-IGLESIAS, F. J.; SOLLA-GULLÓN, J.; HERRERO, E.; FELIU, J. M. Surface structure and anion effects in the oxidation of ethanol on platinum nanoparticles. **Journal of Materials Chemistry A**, Washington, v. 1, p. 7068–7076, 2013.

48 ANGELUCCI, C. A.; HERRERO, E.; FELIU, J. M. Bulk CO oxidation on platinum electrodes vicinal to the Pt(111) surface. **Journal of Solid State Electrochemistry**, New York, v. 11, p. 1531–1539, 2007.

49 GOMES, J. F.; BERGAMASKI, K.; PINTO, M. F. S.; MIRANDA, P. B. Reaction intermediates of ethanol electro-oxidation on platinum investigated by SFG spectroscopy. **Journal of Catalysis**, San Diego, v. 302, p. 67–82, 2013.

50 LAI, S. C. S.; KLEIJN, S. E. F.; ÖZTÜRK, F. T. Z.; VAN REES VELLINGA, V. C.; KONING, J.; RODRIGUEZ, P.; KOPER, M. T. M. Effects of electrolyte pH and composition on the ethanol electro-oxidation reaction. **Catalysis Today**, Amsterdam, v. 154, p. 92–104, 2010.

51 SOUZA-GARCIA, J.; HERRERO, E.; FELIU, J. M. Breaking the C—C Bond in the Ethanol Oxidation Reaction on Platinum Electrodes: Effect of Steps and Ruthenium Adatoms. **ChemPhysChem**, Weinheim, v. 11, p. 1391–1394, 2010.

52 KOPER, M. T. M.; LAI, S. C. S.; HERRERO, E. Mechanisms of the oxidation of carbon monoxide and small organic molecules at metal electrodes. *In:* Koper, M T. M.; Wieckoviski, A. **Fuel cell catalysis: a surface science approach**. John Wiley & Sons, Nova Jersey, 2009, cap. 6, p. 159–207.

53 BARD, A. J.; FAULKNER, L. R. Electrode reactions with coupled homogeneous chemical reactions. *In:* Bard, A. J.; Faulkner, L. R. **Electrochemical methods: fundamentals and applications**. John Wiley & Sons, Nova Jersey, 2000, 2nd ed., cap. 12, p. 379–397.

54 PETUKHOV, A. V.; AKEMANN, W.; FRIEDRICH, K. A.; STIMMING, U. Kinetics of electrooxidation of a CO monolayer at the platinum/electrolyte interface. **Surface Science**, Amsterdam, v. 402–404, p. 182–186, 1998.

55 FARIAS, M. J. S.; FELIU, J. M. Determination of specific eletrochemistry sites in the oxidation of small molecules on crystalline metal surfaces. **Topics in Current Chemistry**, Cham, 377:5, 2019. https://doi.org/10.1007/s41061-018-0228-x.

56 LEBEDEVA, N. P.; KOPER, M. T. M.; HERRERO, E.; FELIU, J. M.; VAN SANTEN, R. A. Cooxidation on stepped Pt[n(111)×(111)] electrodes. **Journal of Electroanalytical Chemistry**, Lausanne, v. 487, p. 37–44, 2000.

57 LEBEDEVA, N. P.; RODES, A.; FELIU, J. M.; KOPER, M. T. M.; VAN SANTEN, R. A. Role of crystalline defects in electrocatalysis: CO adsorption and oxidation on stepped platinum electrodes as studied by in situ infrared spectroscopy. **Journal of Physical Chemistry B**, Washington, v. 106, p. 9863–9872, 2002.

58 LEBEDEVA, N. P.; KOPER, M. T. M.; FELIU, J. M.; VAN SANTEN, R. A. Role of crystalline defects in electrocatalysis: mechanism and kinetics of CO adlayer oxidation on

stepped platinum electrodes. **Journal of Physical Chemistry B**, Washington, v. 106, p. 12938–12947, 2002.

59 FARIAS, M. J. S.; CHEUQUEPÁN, W.; TANAKA, A. A.; FELIU, J. M. Identity of the most and least active sites for activation of the pathways for CO_2 formation from the electro-oxidation of methanol and ethanol on platinum. **ACS Catalysis**, Washington, v. 10, p. 543–555, 2020.

60 WANG, H.; JUSYS, Z.; BEHM, R. J. Ethanol electrooxidation on a carbon-supported Pt catalyst: reaction kinetics and product yields. **Journal of Physical Chemistry B**, Washington, v. 108, p. 19413-19424, 2004.

61 KOWAL, A.; LI, M.; SHAO, M.; SASAKI, K.; VUKMIROVIC, M. B.; ZHANG, J.; MARINKOVIC, N. S.; LIU, P.; FRENKEL, A. I.; ADZIC, R. R. Ternary Pt/Rh/SnO_2 electrocatalysts for oxidizing ethanol to CO_2. **Nature Materials**, Berlin, v. 8, p. 325-330, 2009.

62 RIZO, R.; LÁZARO, M. J.; PASTOR, E.; KOPER, M. T. M. Ethanol oxidation on Sn-modified Pt single-crystal electrodes: new mechanistic insights from on-line electrochemical mass spectrometry. **ChemElectroChem**, Weinheim, v. 3, p. 2196-2201, 2016.

63 DELIME, F.; LÉGER, J. -M.; LAMY, C. Enhancement of the electrooxidation of ethanol on a Pt-PEM electrode modified by tin. Part I: half cell study. **Journal of Applied Electrochemistry**, Dorcrecht, v. 29, p. 1249-1254, 1999.

64 EL-SHAFEI, A. A.; EISWIRTH, M. Electrochemical activity of Sn-modified Pt single crystal electrodes for ethanol oxidation. **Surface Science**, Amsterdam, v. 604, p. 862-867, 2010.

65 DE SOUZA, J. P. I.; QUEIROZ, S. L.; BERGAMASKI, K.; GONZALEZ, E. R.; NART, F. C. Electro-oxidation of ethanol on Pt, Rh, and PtRh electrodes. A study using DEMS and in-situ FTIR techniques. **Journal of Physical Chemistry B**, Washington, v. 106, p. 9825-9830, 2002.

66 BARBOSA, A. F. B.; DEL COLLE, V.; GÓMEZ-MARÍN, A. M.; ANGELUCCI, C. A.; TREMILIOSI-FILHO, G. Effect of the random defects generated in the surface of Pt(111) on the electro-oxidation of ethanol: an electrochemical study. **ChemPhysChem**, Weinheim, v. 20, p. 3045-3055, 2019.

67 WATANABE, M.; MOTOO, S. Electrocatalysis by ad-atoms. Part III. Enhancement of the oxidation of carbon monoxide on platinum by ruthenium ad-atoms. **Journal of Electroanalytical Chemistry**, Lausanne, v. 60, p. 275-283, 1975.

68 WATANABE, M.; MOTOO, S. Electrocatalysis by ad-atoms. Part II. Enhancement of the oxidation of methanol on platinum by ruthenium ad-atoms. **Journal of Electroanalytical Chemistry**, Lausanne, v. 60, p. 267-273, 1975.

69 IGARASHI, H.; FUJINO, T.; ZHU, Y.; UCHIDA, H.; WATANABE, M. CO tolerance of Pt alloy electrocatalysts for polymer electrolyte fuel cells and the detoxification mechanism. **Physical Chemistry Chemical Physics**, Cambridge, v. 3, p. 306-314, 2001.

70 ZHENG, Q. W.; FAN, C. J.; ZHEN, C. H.; ZHOU, Z. Y.; SUN, S. G. Irreversible adsorption of Sn adatoms on basal planes of Pt single crystal and its impact on electrooxidation of ethanol. **Electrochimica Acta**, Oxford, v. 53, p. 6081-6088, 2008.

71 LI, G.; PICKUP, P. G. Decoration of carbon-supported Pt catalysts with Sn to promote electro-oxidation of ethanol. **Journal of Power Sources**, Amsterdam, v. 173, p. 121-129, 2007.

72 PAULINO, M. E.; NUNES, L. M. S.; GONZALEZ, E. R.; TREMILIOSI-FILHO, G. In situ FTIR spectroscopic study of ethanol oxidation on Pt(111)/Rh/Sn surface. The anion effect. **Electrochemistry Communications**, New York, v. 52, p. 85-88, 2015.

73 DOS ANJOS, D. M.; HAHN, F.; LÉGER, J. -M.; KOKOH, K. B.; TREMILIOSI-FILHO, G. Ethanol electrooxidation on Pt-Sn and Pt-Sn-W bulk alloys. **Journal of the Brazilian Chemical Society**, São Paulo, v. 19, p. 795-802, 2008.

74 MASSONG, H.; TILLMANN, S.; LANGKAU, T.; ABD EL MEGUID, E. A.; BALTRUSCHAT, H. On the influence of tin and bismuth UPD on Pt(111) and Pt(332) on the oxidation of CO. **Electrochimica Acta**, Oxford, v. 44, p. 1379-1388, 1998.

75 XIAO, X. Y.; TILLMANN, S.; BALTRUSCHAT, H. Scanning tunneling microscopy of Sn coadsorbed with Cu and CO on Pt(111) electrodes. **Physical Chemistry Chemical Physics**, Cambridge, v. 4, p. 4044-4050, 2002.

76 RIZO, R.; PASTOR, E.; KOPER, M. T. M. CO electrooxidation on Sn-modified Pt single crystals in acid media. **Journal of Electroanalytical Chemistry**, Lausanne, v. 800, p. 32-38, 2017.

77 LEBEDEVA, N. P.; KOPER, M. T. M.; FELIU, J. M.; VAN SANTEN, R. A. Mechanism and kinetics of the electrochemical CO adlayer oxidation on Pt(111). **Journal of Electroanalytical Chemistry**, Lausanne, v. 524, p. 242-251, 2002.

78 GILMAN, S. The mechanism of electrochemical oxidation of carbon monoxide and methanol on platinum. II. The “reactant-pair” mechanism for electrochemical oxidation of carbon monoxide and methanol. **Journal of Physical Chemistry**, Washington, v. 68, p. 70-80, 1964.

79 FARIAS, M. J. S.; CHEUQUEPÁN, W.; TANAKA, A. A.; FELIU, J. M.; Nonuniform synergistic effect of Sn and Ru in site-specific catalytic activity of Pt at bimetallic surfaces toward CO Electro-oxidation. **ACS Catalysis**, Washington, v. 7, p. 3434-3445, 2017.

80 HEINEN, M.; JUSYS, Z.; BEHM, R. J. Ethanol, acetaldehyde and acetic acid adsorption/electrooxidation on a Pt thin film electrode under continuous electrolyte flow: an in situ ATR-FTIRS flow cell study. **Journal of Physical Chemistry C**, Washington, v. 114, p. 9850-9864, 2010.

81 SHAO, M. H.; ADZIC, R. R. Electrooxidation of ethanol on a Pt electrode in acid solutions: in situ ATR-SEIRAS study. **Electrochimica Acta**, Oxford, v. 50, p. 2415-2422, 2005.

82 GAO, P.; CHANG, S. C.; ZHOU, Z.; WEAVER, M. J. Electrooxidation pathways of simple alcohols at platinum in pure nonaqueous and concentrated aqueous environments as studied by real-time ftir spectroscopy. **Journal of Electroanalytical Chemistry**, Lausanne, v. 272, p.161-178, 1989.

83 SUN, S.; HEINEN, M.; JUSYS, Z.; BEHM, R. J. Electrooxidation of acetaldehyde on a carbon supported Pt catalyst at elevated temperature/pressure: An on-line differential electrochemical mass spectrometry study. **Journal of Power Sources**, Amsterdam, v. 204, p. 1–13, 2012.

84 KOKOH, K. B.; HAHN, F.; BELGSIR, E. M.; LAMY, C.; DE ANDRADE, A. R.; OLIVI, P.; MOTHEO, A. J.; TREMILIOSI-FILHO, G. Electrocatalytic oxidation of acetaldehyde on Pt alloy electrodes. **Electrochimica Acta**, Oxford, v. 49, p. 2077–2083, 2004.

85 ANTOLINI, E. Catalysts for direct ethanol fuel cells. **Journal of Power Sources**, Amsterdam, v. 170, p. 1–12, 2007.

86 RODRÍGUEZ, J. L.; PASTOR, E.; XIA, X. H.; IWASITA, T. Reaction intermediates of acetaldehyde oxidation on Pt(111) and Pt(100). An in situ FTIR study. **Langmuir**, Washington, v. 16, p. 5479–5486, 2000.

87 COLLE, V. D.; TREMILIOSI-FILHO, G. Electrochemical and spectroscopic studies of ethanol and acetaldehyde oxidation onto Pt(110) modified by osmium. **Electrocatalysis**, New York, v. 2, p. 285–296, 2011.

88 FARIAS, M. J. S.; CAMARA, G. A.; TANAKA, A. A.; IWASITA, T. Acetaldehyde electrooxidation: the influence of concentration on the yields of parallel pathways. **Journal of Electroanalytical Chemistry**, Lausanne, v. 600, p. 236–242, 2007.

89 MELLO, G. A. B.; GIZ, M. J.; CAMARA, G. A.; CRISCI, A.; CHATENET, M. Search for multi-functional catalysts: The electrooxidation of acetaldehyde on platinum-ruthenium-rhodium electrodeposits. **Journal of Electroanalytical Chemistry**, Lausanne, v. 660, p. 85–90, 2011.

90 WU, G.; SWAIDAN, R.; CUI, G. Electrooxidations of ethanol, acetaldehyde and acetic acid using PtRuSn/C catalysts prepared by modified alcohol-reduction process. **Journal of Power Sources**, Amsterdam, v. 172, p. 180–188, 2007.

91 BARBOSA, A. F. B.; DEL COLLE, V.; GALIOTE, N. A.; TREMILIOSI-FILHO, G. Effect of tin deposition over electrogenerated random defects on Pt(111) surfaces onto ethanol electrooxidation: electrochemical and FTIR studies. **Journal of Electroanalytical Chemistry**, Lausanne, v. 857, p. 113734, 2020.

92 SHIBATA, M.; MOTOO, S. Electrocatalysis by ad-atoms: Part XI. Enhancement of acetaldehyde oxidation by S_{hole} control and oxygen adsorbing ad-atoms. **Journal of**

Electroanalytical Chemistry and Interfacial Electrochemistry, Lausanne, v. 187, p. 151-159, 1985.

93 SHIBATA, M. MOTOO, S. Electrocatalysis by ad-atoms: Part XVII. Electronegativity effect on oxygen donation by oxygen-adsorbing ad-atoms and steric hindrance by alkyl groups in S_{hole} control in aldehyde oxidation. **Journal of Electroanalytical Chemistry and Interfacial Electrochemistry**, Lausanne, v. 201, p. 23-32, 1986.

94 BJÖRLING, A.; HERRERO, E.; FELIU, J. M. Electrochemical oxidation of Pt(1 1 1) vicinal surfaces: effects of surface structure and specific anion adsorption. **Journal of Physical Chemistry C**, Washington, v. 115, p. 15509-15515, 2011.

95 SACHTLER, J. W. A.; VAN HOVE, M. A.; BIBÉRIAN, J. P.; SOMORJAI, G. A. The structure of epitaxially grown metal films on single crystal surfaces of other metals: Gold on Pt(100) and platinum on Au(100). **Surface Science**, Amsterdam, v. 110, p. 19–42, 1981.

Appendix 1

Figure A1.1. Example of the separation of three contributions corresponding to the {110} and {100} defect contributions and the terrace contribution for the Pt(111)-4 electrode.

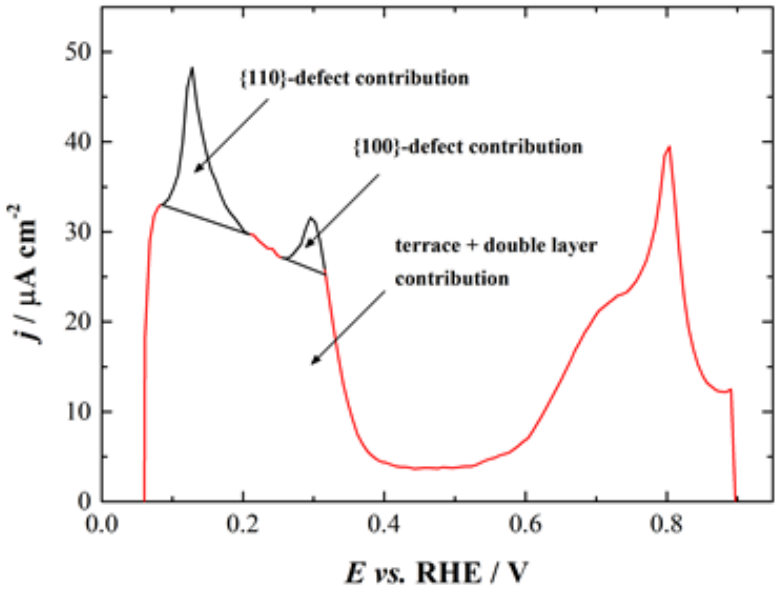

Figure A1.2. First five CV profiles of the ethanol electro-oxidation on the (a) well-ordered Pt(111) and (b, c, d) disordered Pt(111) electrodes in a solution of 0.1 M ethanol + 0.1 M $HClO_4$. Scan rate of 50 mV s^{-1}. Arrows indicate the scan direction.

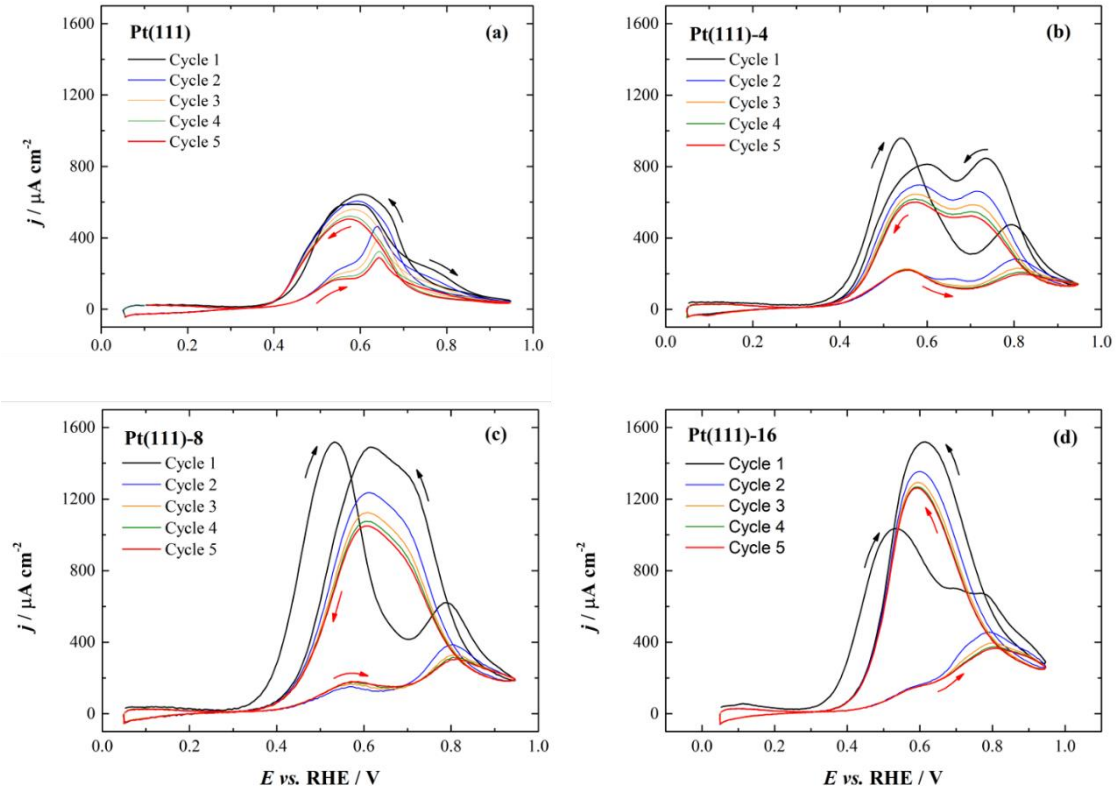

Figure A1.3. Current transients of the ethanol electro-oxidation on ordered and disordered Pt(111) electrodes recorded at 0.6 V by 600 s in a solution of 0.1 M ethanol + 0.1 M $HClO_4$.

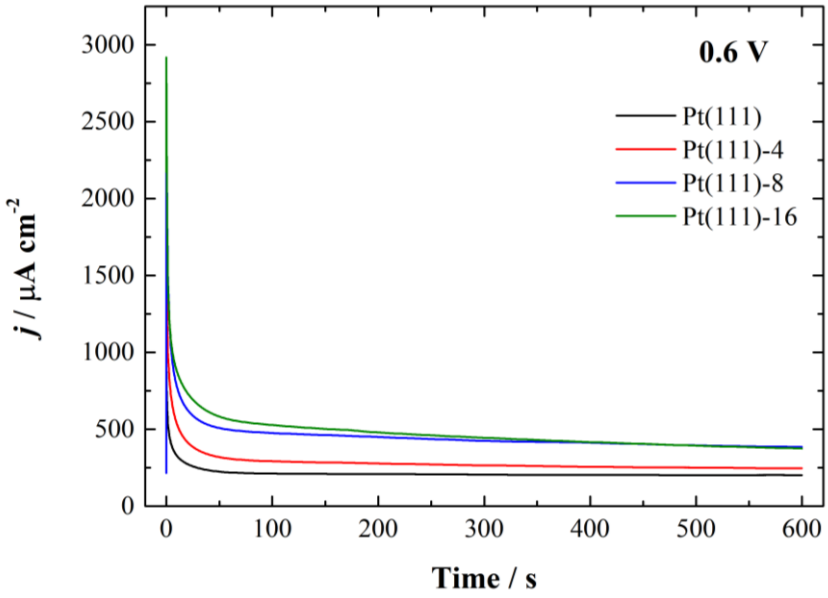

Appendix 2

Figure A2.1. CVs of acetaldehyde electrooxidation (0.1 M + 0.1 M $HClO_4$) onto Pt(111)-4, Pt(111)-8, Pt(111)-16, Pt(111)-32; (a);(b) and (c);(d) represent the 1st and 5th Scan, respectively. v = 50 mV s^{-1}.

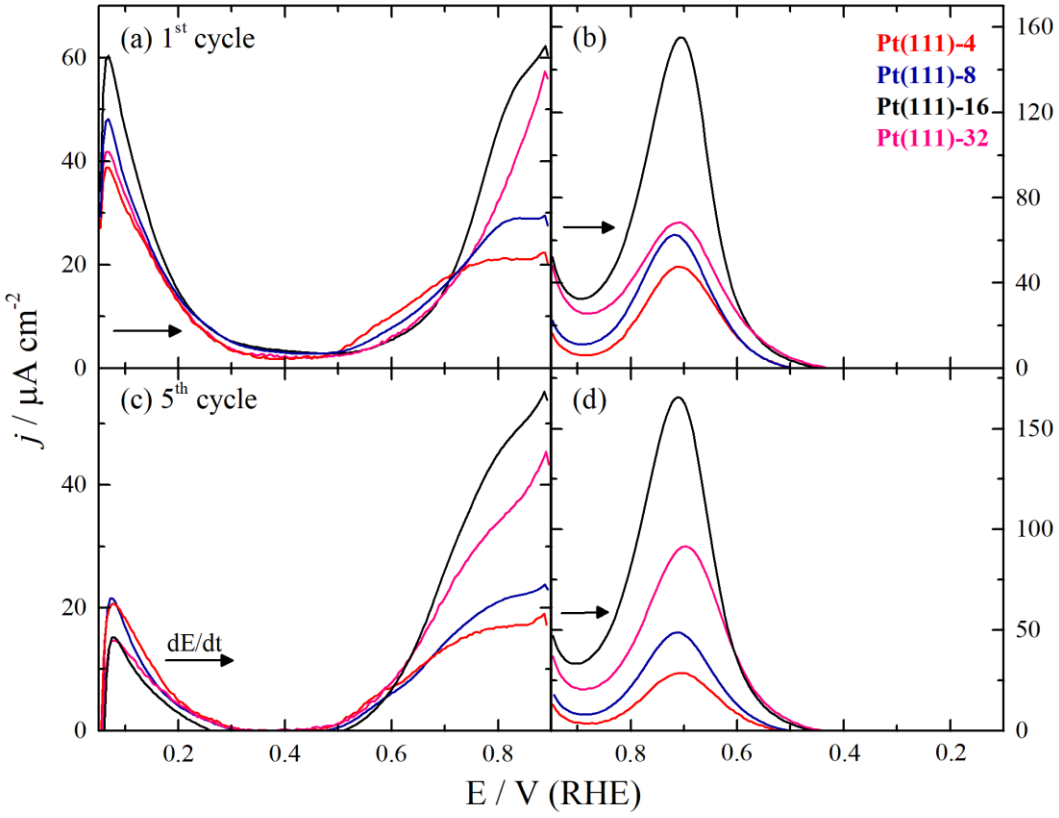

Figure A2.2. Current transients for acetaldehyde electrooxidation (0.1 M + 0.1 M $HClO_4$) on Pt(111), Pt(111)-16, Pt(554) and Pt(110).